# Dissecting the sensory roles of motility-associated ciliary genes in *Caenorhabditis elegans*

**by**

**Catrina Loucks**

M.Sc., University of Calgary, 2011
B.HSc. (Hons.), University of Calgary, 2009

Thesis Submitted in Partial Fulfillment of the
Requirements for the Degree of
Doctor of Philosophy

in the
Department of Molecular Biology and Biochemistry
Faculty of Science

**© Catrina Loucks 2016**

**SIMON FRASER UNIVERSITY**

**Fall 2016**

All rights reserved.
However, in accordance with the *Copyright Act of Canada*, this work may be reproduced, without authorization, under the conditions for "Fair Dealing." Therefore, limited reproduction of this work for the purposes of private study, research, criticism, review and news reporting is likely to be in accordance with the law, particularly if cited appropriately.

# Approval

**Name:** **Catrina Loucks**

**Degree:** **Doctor of Philosophy (Molecular Biology and Biochemistry)**

**Title:** ***Dissecting the sensory roles of motility-associated ciliary genes in Caenorhabditis elegans***

**Examining Committee:** **Chair:** Ryan Morin
Assistant Professor

**Michel Leroux**
Senior Supervisor
Professor

**Lynne Quarmby**
Supervisor
Professor

**Harald Hutter**
Supervisor
Professor

**Michael Silverman**
Internal Examiner
Associate Professor
Department of Biology

**Miriam Goodman**
External Examiner
Professor
Molecular and Cellular Physiology
Stanford University

Date Defended/Approved: August 30, 2016

## Abstract

Cilia are microtubules based organelles that emanate from the surface of most mammalian cell types. Motile cilia have well known roles in producing flow, while nons motile cilia play important sensory/signalling roles. Both forms are based on a similar axonemal structure, but ciliary motility requires additional components that conform to a regular arrangement along microtubules thought to be dictated by the protofilament ribbon (pfs ribbon). While pfs ribbon proteins have been implicated in ciliary motility, sensory/signalling functions in nons motile cilia have been less apparent.

Although the ciliated organism *Caenorhabditis elegans* lacks motile cilia, orthologues of several ciliary pfs ribbons associated proteins are present, including PACRG (Parkin cos regulated gene) and EFHC1 (EFs hand containing 1). In addition to their localisation to motile cilia, the pfs ribbon proteins show expression in neuronal cells of the brain where they may play important sensory roles. In particular, *EFHC1* is mutated in the most common form of inherited epilepsy in humans and has been shown to be important for proper neuronal communication. This work investigates these motilitys associated genes in *C. elegans* to dissect their sensory/signalling roles.

We find that both PCRGs 1 and EFHCs 1 localise to a small subset of nons motile cilia in *C. elegans*, suggesting that they have been adapted to mediate specific sensory/signalling functions. We show that PCRGs 1 influences a learning behaviour known as gustatory plasticity, where it is functionally coupled to heterotrimeric Gs protein signalling. We also demonstrate that PCRGs 1 promotes longevity in *C. elegans* by acting upstream of the lifespans promoting FOXO transcription factor DAFs 16 and likely upstream of insulin/IGF signalling, and that EFHCs 1 also promotes longevity, suggesting shared signalling functions for these proteins. In addition, EFHCs 1 modulates dopamine signalling where it is required for ciliary mechanosensation and regulating synaptic release of dopamine in cooperation with a voltages gated calcium channel.

Our findings establish previously unrecognised sensory/signalling functions for both PACRG and EFHC1 that may be important for neuronal communication in the human brain, where both proteins are known to be present. Furthermore, our work provides important clues for understanding and ultimately providing novel avenues for intervention of disorders such as epilepsy.

**Keywords**: cilia, signalling, sensory, motility, behaviour

## Dedication

*For my husband, Kevin*

## Acknowledgements

I would first like to thank my supervisor, Dr. Michel Leroux, for the opportunity to further explore the genetics of cilia during my PhD. Next, I would like to thank all the members of the Leroux lab who have helped me throughout my studies, including Chunmei Li, Christine Kondratev, Dr. Jacque-Lynne Johnson, Dr. Melissa Frédéric, Dr. Tiffany Timbers, Dr. Victor Jensen, Meghna Joshi, Kwangjin Park and Jerry Cai.

# Table of Contents

Approval ..... ii
Abstract ..... iii
Dedication ..... v
Acknowledgements ..... vi
Table of Contents ..... vii
List of Figures ..... ix
List of Acronyms ..... xi

**Chapter 1. Introduction ..... 1**
1.1. Cilia ..... 1
1.1.1. Ciliary structure ..... 4
1.1.2. Protofilament ribbon ..... 6
PACRG ..... 7
EFHC1 ..... 8
1.1.3. Relevant cilia-dependent phenotypes/behaviours in *C. elegans* ..... 11
ASE-mediated behaviours ..... 11
Cilia-mediated longevity control ..... 13
OLQ-mediated behaviours ..... 14
Behaviours dependent on dopaminergic neurons ..... 14
1.2. Research aims ..... 16

**Chapter 2. PACRG, a protein linked to ciliary motility, mediates cellular signalling ..... 17**
2.1. Introduction ..... 19
2.2. Methods ..... 19
2.2.1. Strains ..... 19
2.2.2. Construction of transgenic strains ..... 20
2.2.3. Gustatory plasticity assay ..... 21
2.2.4. Cilium length measurements ..... 21
2.2.5. Lifespan assays ..... 21
2.2.6. Microscopy and intraflagellar transport assays ..... 22
2.2.7. Transmission electron microscopy ..... 22
2.3. Results ..... 23
2.3.1. *C. elegans* PCRG-1 localises to cilia of ASE and OLQ neurons ..... 23
2.3.2. PCRG-1 is not essential for cilium biogenesis or intraflagellar transport ..... 25
2.3.3. *pcrg-1* is required for gustatory plasticity, a learning behaviour dependent on ASE neurons ..... 28
2.3.4. *pcrg-1* interacts genetically with G-proteins in gustatory plasticity ..... 30
2.3.5. PCRG-1 positively regulates longevity in *C. elegans*, potentially independently of G-proteins implicated in gustatory plasticity ..... 31
2.3.6. *C. elegans* EFHC-1 shows restricted, partially overlapping localisation to PCRG-1 ..... 38

2.3.7. EFHC-1 regulates lifespan likely through the same pathway as PCRG-1 ..... 40
2.3.8. OLQ cilia/neurons appear to be involved in longevity control in *C. elegans* ..... 41
2.4. Discussion ..... 45

**Chapter 3. EFHC1 links the primary cilium, synapse, epilepsy and dopamine signalling ..... 48**
3.1. Introduction ..... 50
3.2. Methods ..... 51
3.2.1. Strains ..... 51
3.2.2. Generation and visualisation of transgenic animals ..... 52
3.2.3. Behavioural assays ..... 53
Tap habituation ..... 53
Swimming-induced paralysis (SWIP) ..... 53
Basal slowing response ..... 54
Suppression of foraging ..... 54
Single-worm tracking ..... 54
3.2.4. Calcium imaging of CEP and OLQ neurons ..... 55
3.2.5. Transmission electron microscopy ..... 55
3.3. Results ..... 56
3.3.1. *C. elegans* EFHC-1 localises to cilia of two classes of mechanosensory neurons ..... 56
3.3.2. EFHC-1 modulates dopamine signalling in *C. elegans* ..... 61
3.3.3. *C. elegans* EFHC1 is required for mechanosensation in dopaminergic CEP ciliated neurons ..... 67
3.3.4. *C. elegans* EFHC1 mediates dopamine signalling downstream of cilia ..... 75
3.4. Discussion ..... 79

**Chapter 4. Conclusions and future directions ..... 82**

**References ..... 86**
Appendix. Statistical analysis of all lifespan experiments in Chapter 2 ..... 98

# List of Figures


Figure 1.1 General structure of a cilium. ..... 2

Figure 1.2 Non-motile and motile ciliary structural features. ..... 4

Figure 2.1 PCRG-1::GFP fusion protein localisation and *pcrg-1* mutant alleles. ..... 24

Figure 2.2 Analyses of *pcrg-1* mutant alleles. ..... 27

Figure 2.3 *pcrg-1* animals show a defect in behavioural plasticity. ..... 30

Figure 2.4 *C. elegans pcrg-1* animals show a significant decrease in lifespan compared to wild-type. ..... 33

Figure 2.5 PCRG-1 does not appear to interact with G-proteins to affect lifespan. ..... 34

Figure 2.6 PCRG-1 functions in a parallel pathway to ciliary proteins to regulate longevity. ..... 35

Figure 2.7. A second mutant allele of *pcrg-1* similarly affects lifespan in a parallel pathway to that of other ciliary proteins. ..... 36

Figure 2.8 PCRG-1 functions upstream of DAF-16 and likely the insulin signalling pathway to regulate longevity. ..... 37

Figure 2.9 *efhc-1* mutant alleles, localisation of EFHC-1::GFP and a reduction in lifespan in *efhc-1* mutants. ..... 39

Figure 2.10 EFHC-1::GFP localisation is independent of PCRG, and PCRG-1::GFP localisation is independent of EFHC-1. ..... 41

Figure 2.11 OLQ neurons and/or cilia appear to play a role in longevity. ..... 43

Figure 2.12 *pcrg-1* mutants show no defects in OLQ-related mechanosensory or behavioural responses. ..... 45

Figure 3.1 EFHC-1 localises to cilia and synapses of a subset of mechanosensory neurons. ..... 58

Figure 3.2 EFHC-1 also localises to the dopaminergic ray neurons in the male tail. ..... 61

Figure 3.3 Molecular components of dopamine signalling in *C. elegans*. ..... 62

Figure 3.4 EFHC-1 is not required for the dopamine-dependent basal slowing response. ..... 63

Figure 3.5 Neural circuit outlining how dopaminergic neurons influence touch receptor neuron activity. ..... 64

Figure 3.6 EFHC-1 influences habituation to a mechanical stimulus by modulating dopamine signalling. ..... 65

Figure 3.7 Loss of EFHC-1 results in increased dopamine signalling even in the absence of food. ..... 66
Figure 3.8 EFHC-1 influences also impacts the dopamine-dependent swimming-induced paralysis (SWIP) phenotype..... 67
Figure 3.9 Like TRP-4, EFHC-1 is required for mechanosensation in non-motile CEP cilia. ..... 68
Figure 3.10 Animals that respond to mechanical stimuli in the CEP neurons show similar patterns of calcium changes independent of strain. ..... 69
Figure 3.11 *efhc-1* mutants show no defects in OLQ-related mechanosensory or behavioural responses..... 71
Figure 3.12 General ciliary structure is retained in *efhc-1* mutants and EFHC-1::GFP is expressed in the absence of the conventional ciliary transcription factor, DAF-19. ..... 73
Figure 3.13 Axonemal structure of CEP and OLQ cilia appears wild-type in *efhc-1* mutants. ..... 73
Figure 3.14 The second DM10 domain is sufficient for ciliary localisation in *C. elegans.* ..... 75
Figure 3.15 EFHC-1 influences habituation to a mechanical stimulus by modulating dopamine signalling..... 77
Figure 3.16 A proposed model for how EFHC1 was adapted to function in motile and non-motile cilia as well as at synapses. ..... 79

## List of Acronyms

| | |
|---|---|
| CEP | Cephalic |
| Che | Chemotaxis |
| DS | Distal segment |
| EFHC1/EFHC-1 | EF-hand containing 1 |
| Egl | Egg-laying |
| FGF | Fibroblast growth factor |
| GF | Gain-of-function |
| Hh | Hedgehog |
| IGF | Insulin-like growth factor |
| IFT | Intraflagellar transport |
| IAA | Isoamyl alcohol |
| JME | Juvenile myoclonic epilepsy |
| MAP | Microtubule-associated protein |
| MS | Middle segment |
| MWT | Multi-worm tracker |
| NGM | Nematode growth medium |
| NDK | Nucleoside-diphosphate kinase |
| Osm | Osmotic avoidance |
| OLQ | Outer labial quadrant |
| PARK2 | Parkin |
| PACRG/PCRG-1 | Parkin co-regulated gene |
| PCMC | Periciliary membrane compartment |
| PDGF | Platelet-derived growth factor |
| PCD | Primary ciliary dyskinesia |
| Pf-ribbon | Protofilament ribbon |
| ROI | Region of interest |
| SWIP | Swimming-induced paralysis |
| SNB-1 | Synaptobrevin |
| TEM | Transmission electron microscopy |
| TAM | Tubule-associated material |
| VGCC | Voltage-gated calcium channel |

# Chapter 1. Introduction

## 1.1. Cilia

Cilia are microtubule-based organelles that emanate from the cell surfaces of most mammalian cell types and perform a diverse array of biological functions **(Figure 1.1)**. In humans, motile forms of cilia have well known roles in clearing mucus from the respiratory tract, propelling sperm along the fallopian tube and moving cerebrospinal fluid in the brain ventricles. Consequently, impairment of ciliary motility can result in human disorders such as primary ciliary dyskinesia (PCD) characterized by respiratory dysfunction, sterility, and hydrocephalus (Lee, 2011). Conversely, non-motile cilia have only been recognized as biomedically important in the past 15 years, on the basis that a group of genetic disorders with overlapping phenotypes are attributed to genes whose encoded proteins localise to this organelle. These clinical manifestations include renal cysts, liver disease, retinal degeneration, *situs inversus*, brain malformations and neurological abnormalities, skeletal bone defects, and obesity (Waters and Beales, 2011).

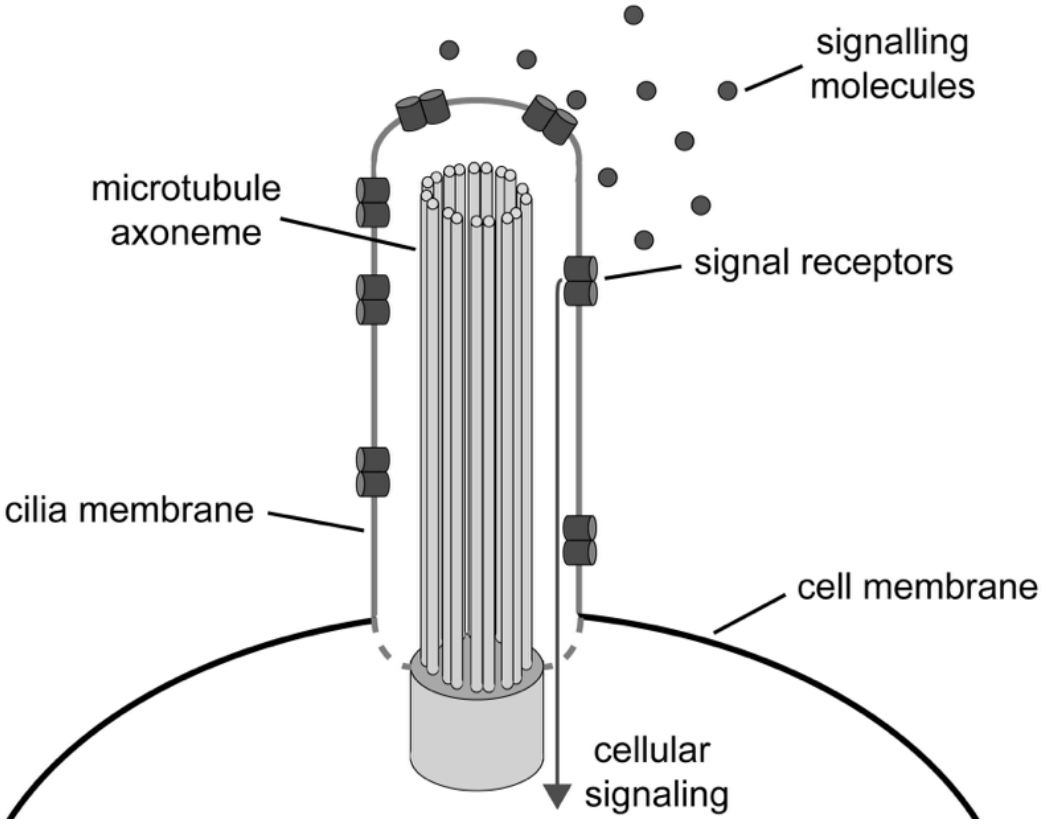


**Figure 1.1 General structure of a cilium.**
Both non-motile and motile cilia are microtubule-based organelles that emanate from the cell surface of most mammalian cell types. The microtubule-based axoneme of each cilium is surrounded by a membrane continuous with the cell membrane that is decorated with signal receptors responsible for responding to environmental cues. Figure adapted from Dr. Tiffany Timbers.

Single-celled organisms have a solitary cilium (often called a flagellum) that is responsible for both producing movement and responding to mechanosensory cues and other sensory signals to modulate its movement (Naitoh and Eckert, 1969; Ogura and Takahashi, 1976; Shah et al., 2009), and could thus represent the ancestral form of cilia. Non-motile cilia were adaptions in metazoans that took advantage of the sensory capabilities of motile cilia. These cilia have taken on a variety of shapes and sizes to mediate a diverse array of sensory processes, including mechanosensation, chemosensation, thermosensation and photosensation (Silverman and Leroux, 2009). Furthermore, the non-motile cilium functions as a cellular antenna to regulate several signalling pathways such as Hedgehog (Hh), platelet-derived growth factor (PDGF), fibroblast growth factor (FGF), cyclic nucleotide, and both canonical and non-canonical

Wnt cascades, and more recently, a link between primary cilia and insulin/IGF (insulin-like growth factor) signalling has begun to emerge (Apfeld and Kenyon, 1999; Yeh et al., 2013; Zhu et al., 2009).

This work uses the model organism, *Caenorhabditis elegans,* to study a specific subset of motility-associated ciliary proteins that may have important functions in non-motile cilia. *C. elegans* is unique among ciliated organisms in its lack of motile cilia. Nematode cilia are found exclusively in a subset of sensory neurons (60 neurons in total), where they are located at the ends of dendrites. Most ciliated sensory neurons are concentrated in the head of the animal, where they extend their dendrites, that terminate in cilia, toward the tip of the nose (Bae and Barr, 2008). Collectively, ciliated neurons in *C. elegans* modulate physiology, development, longevity, and most behaviors (reviewed in (Apfeld and Kenyon, 1999; Bae and Barr, 2008; Bargmann, 2006; de Bono et al., 2002; Inglis et al., 2007)).

Non-motile cilia in *C. elegans* demonstrate a high level of diversity in order to respond to various extracellular signals in the environment. For example, many sensory functions are performed by cilia located in the amphids, a pair of lateral sensilla in the head (Inglis et al., 2007; Perkins et al., 1986). Many amphid cilia (ASE, ASG, ASH, ASI, ASJ, ASK, ADL and ADF) are exposed to the external environment and perform important chemosensory functions. Other amphid cilia are not exposed to the external environment and respond to odorants (AWA, AWB and AWC) or temperature (AFD). In addition to the amphid ciliated neurons, there are inner/outer labial and cephalic ciliated neurons located in the head. The cilia of both glutamatergic OLQ (outer labial quadrant) and dopaminergic CEP (cephalic) neurons, that will be thoroughly investigated in this work, are embedded in the cuticle and are important for mechanosensation. Additional ciliated dopaminergic neurons are located in the anterior body (ADE) and in the posterior body (PDE) with cilia that are similarly embedded in the cuticle and important for mechanosensation (Bae and Barr, 2008). Finally, there are an additional 52 ciliated neurons that are only found in *C. elegans* males. These neurons are primarily located in the rays of the male tail where they perform diverse sensory functions primarily involved in mating behaviours (Inglis et al., 2007). Together, the non-motile ciliated neurons found

in *C. elegans* are able to mediate complex behaviours dependent on various sensory capabilities of different cilia.

### 1.1.1. Ciliary structure

Both motile and non-motile cilia are based on an axoneme composed of 9 outer doublet microtubules surrounded by a membrane continuous with the plasma membrane and nucleated from a centriolar structure termed basal body. Each doublet is composed of a complete 13 protofilament A-tubule and an incomplete 11 protofilament B-tubule (Figure 1.1; Linck and Stephens, 2007), and at the base of cilia, the nine outer doublet microtubules are attached to the ciliary membrane by Y-shaped connections (Y-links) in a region called the transition zone. For cilia to take on motility, additional structures are required, including a central microtubule pair, radial spokes, inner and outer dynein arms, interdoublet links and the protofilament ribbon **(Figure 1.2)**.

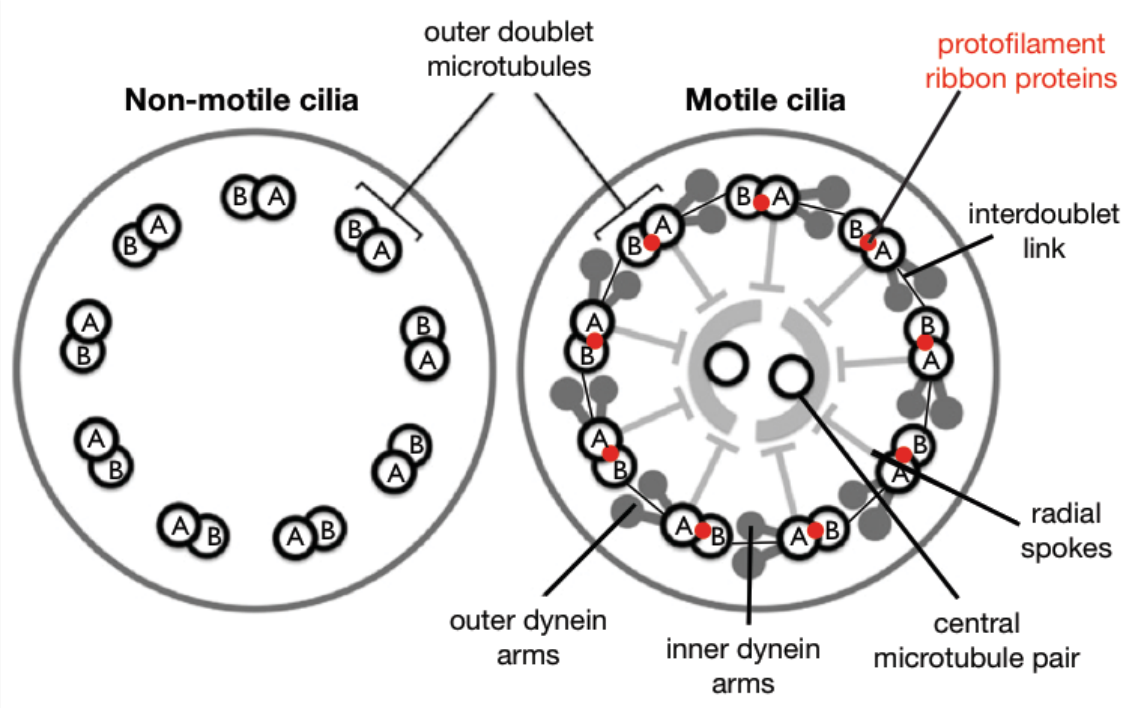


**Figure 1.2 Non-motile and motile ciliary structural features.**
Cross-sections of both non-motile and motile cilia show axonemes comprised of 9 outer microtubule doublets, where additional structures are present in motile cilia. Figure adapted from Takeda and Narita, 2012.

While large differences in axonemal structure exist between motile and non-motile cilia, dramatic differences also exist between different classes of non-motile cilia that perform diverse sensory functions. Typically, axonemal structure consists of 9 outer microtubule doublets that in many cilia transition to singlet microtubules in the distal segment. In some cases, cilia deviate from a canonical antenna or whip-like form. For example, the outer segment of vertebrate photoreceptor cilia is enlarged, and highly specialised for capturing light signals. This idea is further exemplified in *C. elegans* that boasts a diverse array of ciliary structures that contribute to the ability of these ciliated neurons to respond appropriately to different sensory signals. These structural differences manifest as both different shapes of distal segments and axonemal deviations.

For example, many amphid cilia responsible for chemosensation are shaped as single rods (ASE, ASG, ASH, ASI, ASJ, ASK) or pairs of rods (ADF, ADL). In contrast, other amphid cilia take on wing-like shapes (AWA, AWB, AWC) to facilitate olfaction or finger-like projections surrounding a single cilium (AFD) to mediate thermosensation (Bae and Barr, 2008; Inglis et al., 2007). Ciliary axonemes found in the mechanosensory OLQ and CEP neurons that will be a major focus of this work differ substantially from conventional non-motile cilia, where both forms of cilia show typical structures at their base (9 doublet microtubules and associated Y-links) yet diverge toward their distal ends. In OLQ cilia, four of the nine doublet microtubules become attached to each other in a square composed of thick cross-links and then to the centre of the axoneme with fine radial arms. Additionally, these doublet microtubules show a filled appearance not observed in most types of non-motile cilia (Doroquez et al., 2014; Perkins et al., 1986). CEP cilia also show unique axonemal structures, where the distal end shows enlargement due to the presence of over 30 supernumerary singlet microtubules interspersed with tubule-associated material. These singlet microtubules are composed of 14-15 protofilaments, in contrast to the 13 protofilaments that make up the A-tubule of ciliary doublet microtubules (Doroquez et al., 2014; Perkins et al., 1986). Given the diversity of axonemal structure in various classes of non-motile cilia, we suspected that motility-associated ciliary genes conserved in *C. elegans* may play specific roles in cilia responsible for specific sensory modalities such as mechanosensation that is also required for motile cilia.

### 1.1.2. Protofilament ribbon

Treatment of motile ciliary axonemes with the detergent Sarkosyl solubilizes the majority of microtubules and structures associated with them, leaving behind only a highly stable ribbon structure made up of three adjoining protofilaments (Linck and Norrander, 2003). This ribbon structure, known as the protofilament ribbon (pf-ribbon), is situated at the junction of the A- and B- tubules of the outer doublet microtubules and is composed of tubulin, tektin, and a small number of associated proteins (**Figure, 1.2**; Linck and Norrander, 2003). Motility-associated ciliary components conform to a regular arrangement along microtubules with 96 nm axial periodicity. Since tubulin dimers only show 8 nm axial periodicity, this complex pattern is thought to be dictated by the pf-ribbon (Pirner and Linck, 1994). Specifically, tektin filaments that make up the pf-ribbon show 8-, 16-, 24-, 32-, 40-, 48-, and 96-nm axial periodicities that align with tubulin periodicities and correspond to the axial repeats of dynein arms, radial spokes and interdoublet links (Norrander et al., 1996).

In motile cilia, pf-ribbon proteins are thought to tightly associate with the outer doublet microtubules to facilitate the attachment of proteins involved in producing movement. Mutations resulting in loss of these proteins can result in structural abnormalities of motile cilia, such as variable outer doublet microtubule loss (Dawe et al., 2005) and inner dynein arm loss (Tanaka et al., 2004). Not surprisingly, loss of pf-ribbon proteins can result in impaired motility in several organisms (Dawe et al., 2005; Lorenzetti et al., 2004; Suzuki et al., 2009; Tanaka et al., 2004; Wilson et al., 2010; Yanagisawa and Kamiya, 2004), but ciliary functions for these proteins apart from motility have been less apparent. In non-motile cilia, it is possible that pf-ribbon proteins also provide structural information that is important for sensory transduction and not for motility.

Interestingly, several orthologues of pf-ribbon-associated proteins are conserved in *C. elegans*, a ciliated organism with only non-motile cilia, including PACRG (Parkin co-regulated gene) and EFHC1 (EF-hand containing 1). Furthermore, in organisms

exhibiting both motile and non-motile cilia these pf-ribbon-associated proteins show expression in motile ciliated cells as well as in neuronal cells of the brain that project non-motile cilia, where they may play important sensory roles (Brody et al., 2008; Conte et al., 2009a; Léon et al., 2010; Norrander et al., 1998). In support of this, PACRG shares a common promoter with a gene implicated in inherited Parkinson's disorder and thus may have related neuronal functions (West et al., 2003). Additionally, EFHC1 is mutated in the most common form of inherited epilepsy in humans (Suzuki et al., 2004) and has been shown to be important for proper neuronal communication as discussed below (de Nijs et al., 2009a; Rossetto et al., 2011).

### *PACRG*

PACRG (Parkin co-regulated gene) was originally discovered as a gene that shares a bidirectional promoter with PARK2 (parkin), a gene associated with autosomal recessive, early-onset Parkinson's disease in humans (West et al., 2003). Parkinson's disease is a movement disorder resulting from progressive loss of dopaminergic neurons in the brain (Polymeropoulos et al., 1997). Given that bi-directional promoters are found in genes that share similar expression patterns and functions (Ito et al., 2000; Lennard et al., 1994; Orii et al., 1999), it was suspected that PACRG may contribute to the pathogenesis of Parkinson's disease. In support of this, both PACRG and PARK2 are co-expressed in several tissues, including the heart, brain, skeletal muscle, kidney and pancreas (West et al., 2003). Furthermore, PACRG is found in Lewy bodies, glial cytoplasmic inclusions and neurofibrillary tangles that are pathological features of Parkinson's disease (Imai et al., 2003; Taylor et al., 2012). Despite these lines of evidence, PACRG has not been found to be associated with early-onset Parkinsonism (Deng et al., 2005).

PACRG is also a highly conserved ciliary protein that was uncovered in several large-scale screens for cilium/basal body proteins (Avidor-Reiss et al., 2004; Keller et al., 2005; Li et al., 2004; Pazour et al., 2005; Stolc et al., 2005). Despite PACRG's expression in tissues with non-motile cilia such as the brain, discovered ciliary functions for PACRG have been restricted to motile cilia. For example, loss of *PACRG* in mice results in motility defects in ependymal cilia that line the brain ventricles, leading to abnormal cerebrospinal fluid flow and consequently hydrocephalus (Wilson et al., 2010).

In addition, RNAi knockdown of the two PACRG homologues in *Trypanosoma brucei* abolishes ciliary motility and leads to axonemal defects consisting of outer microtubule doublet loss worsening toward the distal end of cilia (Dawe et al., 2005). In *Chlamydomonas* cilia that are primarily motile, PACRG was discovered as a protein that may interact with Rib72 (homologue of EFHC1), and its axonemal localisation is only revealed in Sarkosyl-extracted axonemes where all but the pf-ribbon is solubilized, suggesting that PACRG is associated with the pf-ribbon (Ikeda et al., 2007). PACRG localises to basal bodies as well as along the entire length of *Chlamydomonas* cilia (Ikeda et al., 2007), and it was further demonstrated that PACRG specifically interacts with tubulin and microtubules (Ikeda, 2008).

### *EFHC1*

EFHC1 (EF-hand containing 1) was initially uncovered as a flagellar protein in *Chlamydomonas* where it was called Rib72 (or p72) (Ikeda et al., 2003; Patel-King et al., 2002). Rib72 was found to localise along the entire flagella apart from the ciliary transition zone (defined as the region immediately adjacent to the cell body) (Patel-King et al., 2002), and to specifically associate with the pf-ribbon (Ikeda et al., 2003). Furthermore, it has been proposed that Rib72 associates with interdoublet links that are required for ciliary motility and holding the 9 outer microtubule doublets together (Ikeda et al., 2003). A direct link between ciliary motility and EFHC1 function was seen in *Efhc-1*-deficient mice, where homozygous null mutants show enlarged brain ventricles due to defects in the ciliary beating frequency, while animals with heterozygous mutations did not show these features (Suzuki et al., 2009). Interestingly, both mice heterozygous and homozygous for EFHC1 mutations show spontaneous seizures, suggesting that the loss of ciliary motility in EFHC1-deficient mice is not responsible for epilepsy in these animals (Suzuki et al., 2009).

Rib72 is a unique protein composed of three DM10 domains of unknown function and a C-terminal EF-hand that is thought to bind calcium. Given its domain architecture, EFHC1 was originally proposed to function in the calcium-dependent regulation of flagellar motility (Patel-King et al., 2002). DM10 domains are found in only one other class of proteins: nucleoside-diphosphate kinases (NDKs), responsible for creating GTP from ATP and GDP. Flagellar microtubules are not static and are instead undergoing

constant turnover at their tips, requiring extensive GTP nucleotide hydrolysis. Given that *Chalmydomonas* flagella show NDK activity, it was suspected that Rib72 could influence NDK activity to regulate flagellar stability and motility (Patel-King et al., 2002).

In humans, EFHC1 came into the spotlight when several heterozygous missense mutations were identified that result in the most common form of idiopathic epilepsy: juvenile myoclonic epilepsy (JME) (Suzuki et al., 2004). Although many functions have since been attributed to EFHC1, how mutations influence epilepsy is not well understood. In humans, *EFHC1* is expressed in several tissues, including brain, and mouse Efhc1 localises to soma and dendrites of neurons (Suzuki et al., 2004), suggesting a conserved role of EFHC1 in neuronal function.

EFHC1 was originally proposed to be a pro-apoptotic protein because overexpression of EFHC1 results apoptotic cell death in mouse hippocampal primary culture neurons, while overexpression of EFHC1 containing human JME mutations reduces these defects (Suzuki et al., 2004). Given that EFHC1 contains a $Ca^{2+}$-binding EF-hand and that mutations in voltage-gated calcium channels (VGCCs) often result in epilepsy, it was suspected that EFHC1 may interact with a VGCC to execute its pro-apoptotic functions (Suzuki et al., 2004). Efhc1 expression largely overlaps with the expression pattern of $Ca_v2.3$, an R-type VGCC, in the adult mouse brain and treatment of EFHC1-positive neurons with VGCC antagonists revealed that impairment of R-type VGCCs increases neuronal survival rates. In addition, introduction of EFHC1 into baby hamster cells expressing $Ca_v2.3$ increased R-type $Ca^{2+}$ currents while introduction of EFHC1 harboring JME mutations reduces this effect. These results suggest that EFHC1 enhances $Ca^{2+}$ influx through $Ca_v2.3$ to promote cell death (Suzuki et al., 2004). The N-terminus of EFHC1 containing the first two DM10 domains (the location of the majority of JME mutations) was found to specifically interact with the C-terminus of $Ca_v2.3$, and given that VGCCs are often regulated by proteins interacting with their intracellular C terminus (Catterall, 2000), this again supports the idea that EFHC1 regulates calcium influx through $Ca_v2.3$. More recently, EFHC1 was found to interact and regulate the activity of the redox-sensitive TRPM2 calcium channel associated with cell death, again providing a potential link between EFHC1 and apoptosis (Katano et al., 2012). Thus, one hypothesis for how EFHC1 mutations contribute to epilepsy in humans is by preventing

the elimination of unnecessary neurons during development, resulting in hyperexcitable circuits (Suzuki et al., 2004).

It was later discovered that in addition to its ciliary localisation, EFHC1 associates with the mitotic spindle in dividing cells, while in non-dividing cells it specifically localises to the centrosome (de Nijs et al., 2006). Interestingly, the N-terminal region of EFHC1, not including its DM10 domains, is responsible for its association with the mitotic spindle (de Nijs et al., 2006). EFHC1 was then demonstrated as a microtubule-associated protein (MAP) that specifically interacts with α-tubulin through its N-terminal region (de Nijs et al., 2009a). Furthermore, disruption of EFHC1 results in mitotic spindle defects, microtubule bundling microtubule and apoptosis. The strong expression of EFHC1 in neuronal tissues during development along with a requirement of proper cell division in brain development prompted the investigation of EFHC1's roles in neurons. Brain development requires tight regulation of complex processes, including proliferation, cell cycle exit, cell migration and neuronal differentiation that are dependent on changes in cell shape mediated by cytoskeletal rearrangements (de Nijs et al., 2009a). In the developing brain of rats, loss of EFHC1 disrupts both cell division and cell cycle exit, as well as the organization of scaffolding glia and locomotion of neurons to their final destinations (de Nijs et al., 2009a). Furthermore, overexpression of EGFP-tagged EFHC1 constructs containing JME-associated mutations results in similar defects, suggesting that heterozygous EFHC1 mutations likely act in a dominant-negative manner to mediate their pro-epileptic effects (Nijs et al., 2012). More specifically, it has been hypothesized that abnormalities in brain development due to EFHC1 mutations may underlie epilepsy.

Further neuronal functions for EFHC1 were uncovered in *Drosophila* where *Defhc1.1* associates with synaptic microtubules and the loss of *Defhc1.1* results in increased spontaneous neurotransmitter release at the neuromuscular junction synapse due to overgrowth of neuronal processes (Rossetto et al., 2011). This led to the hypothesis that EFHC1 may be required to regulate microtubule dynamics and that the resulting increase in spontaneous neurotransmitter release could contribute to the excessive neuronal excitability seen in JME patients. Therefore, although it is clear

EFHC1 plays many roles in varied neuronal functions, it remains unclear how mutations in *EFHC1* contribute to epilepsy.

### 1.1.3. Relevant cilia-dependent phenotypes/behaviours in *C. elegans*

We find that the *C. elegans* orthologues of PACRG (PCRG-1) and EFHC1 (EFHC-1) localise to a small subset of non-motile ciliated cells. Specifically, PCRG-1 is found in the pair of ASE neurons **(Figure 2.1B)** that extend dendrites toward the tip of the nose in *C. elegans* and terminate in cilia that are exposed to the external environment, where they are able to respond to water-soluble chemicals such as NaCl (Bargmann and Horvitz, 1991). Additionally, both PCRG-1 and EFHC-1 are found in the four OLQ neurons **(Figures 2.1B** and **3.1A)** that similarly extend dendrites to the tip of the nose that terminate in cilia. These cilia are not exposed to the external environment, but are instead embedded in the cuticle, where they are able to respond to mechanical stimuli at the nose of the animal. EFHC-1 is found in one additional class of neurons: the mechanosensory dopaminergic neurons **(Figure 3.1A)**. Like OLQ neurons, these neurons terminate in cilia embedded in the cuticle at various locations to enable mechanosensation. The *C. elegans* dopaminergic neurons consist of four CEP neurons with cilia terminating in the nose, two ADE neurons with cilia in the anterior body and two PDE neurons with cilia in the posterior body (Inglis et al., 2007; Sulston et al., 1975; White et al., 1986). In this work, we wished to uncover the possible functions for both PCRG-1 and EFHC-1 in non-motile cilia by investigating *C. elegans* phenotypes and behaviours (outlined below) that are dependent on the non-motile ciliated cells to which these proteins localise.

#### *ASE-mediated behaviours*

The ASE neurons, to which PCRG-1 localises, project dendrites that terminate in cilia exposed to the external environment and are critical for chemotaxis toward water-soluble attractants such as $Na^+$, $Cl^-$, cAMP, biotin, lysine and serotonin (Bargmann and Horvitz, 1991). In this work, we investigated the attraction of *C. elegans* to low concentrations of NaCl, mediated primarily by the ASE neurons, but also in part by the ADF, ASG and ASI neurons (Bargmann and Horvitz, 1991). Animals also show

avoidance of high NaCl concentrations (above 200 mM) that is dependent on ASH neurons (Bargmann et al., 1990). The ASE neurons, along with the ASH, ADL, ASI and ADF neurons, are also implicated in a learning behaviour known as gustatory plasticity in which animals that are pre-exposed to a buffer containing 100 mM of NaCl show avoidance to normally attractive concentrations (25 mM) of NaCl (Jansen, 2002). It has been proposed that the ASH, ADF, ADL and ASI neurons are not activated (or weakly activated) by low NaCl concentrations, and that upon prolonged exposure to 100 mM NaCl an ASE-derived signal (acting through the body cavity neurons AQR, PQR and URX) sensitises these neurons to mediate avoidance of normally attractive NaCl concentrations (Hukema et al., 2006). It was later discovered that during gustatory plasticity *C. elegans* only avoid normally attractive salt concentrations if they are paired with a negative cue, such as the absence of food, during pre-exposure (Hukema et al., 2008).

Several mutants have been identified with defects in gustatory plasticity, with or without corresponding defects in chemotaxis to water-soluble chemicals like NaCl. Mutations in *che-1* and *ceh-36* result in the loss of functional ASE neurons and are consequently unable to chemotax toward attractive NaCl concentrations. These animals are also defective in gustatory plasticity where they show no response to normally attractive NaCl concentrations after pre-exposure in the absence of food (Hukema et al., 2006). Interestingly, mutants for several components of G-protein signalling components show no defects in chemotaxis, but display abnormal gustatory plasticity. G-protein-coupled receptors represent an important interface through which cells respond to sensory stimuli, and their activation results in the dissociation of heterotrimeric G-proteins into α and βγ subunits that regulate various downstream effectors. Mutants of the Gα subunits GPA-1 and ODR-3 and the Gγ subunit GPC-1 show wild-type chemotaxis to NaCl, but are defective in gustatory plasticity where *gpa-1* and *gpc-1* mutants show no response to NaCl after pre-exposure and *odr-3* mutants are always strongly attracted to NaCl (Jansen et al., 2002; Hukema et al., 2006). Interestingly, these G-protein components are not expressed in ASE neurons, but are instead expressed in one or more of the neurons that are thought to be sensitised by an ASE-derived signal upon prolonged exposure to NaCl (ADF, ADL, ASI and ASH) to promote avoidance of normally attractive salt concentrations.

### *Cilia-mediated longevity control*

Mutations that abrogate general ciliary function in *C. elegans* result in increased longevity, a phenotype that has been attributed to defects in sensory perception (Apfeld and Kenyon, 1999). The non-motile ciliated cells to which PCRG-1 and EFHC-1 localise have not previously been associated with longevity, but interestingly, while specific ciliated cells have been found to negatively regulate lifespan (ASI and ASG neurons), others promote longevity (ASJ and ASK neurons) (Alcedo and Kenyon, 2004). Furthermore, mutations in several G-proteins (GPA-1, GPC-1, ODR-3 and GPA-11) implicated in gustatory plasticity and expressed in a subset of non-motile ciliated cells (many of which had not previously been associated with longevity) also contribute to lifespan regulation (Lans and Jansen, 2007). Together, these data suggest that longevity control is dependent on the integration of various, and potentially additional, sensory signals.

Longevity control mediated by cilia in *C. elegans* is thought to function through the insulin/IGF-1 pathway, that when disrupted increases longevity (Apfeld and Kenyon, 1999). Activation of the insulin/IGF-1 receptor in *C. elegans* (DAF-2) by insulin-like peptides triggers a phosphorylation cascade starting with the phosphatidylinositol 3-kinase AGE-1/PI3K, followed by the serine/threonine kinases PDK-1, AKT-1 and AKT-2, that results in the phosphorylation of the forkhead box transcription factor (FOXO) DAF-16. The stimulated phosphorylation of DAF-16 prevents its entry into the nucleus and its ability to regulate genes important for longevity control (Kenyon, 2010). Interestingly, while the majority of lifespan regulation by cilia is thought to function through the insulin/IGF-1 signalling pathway, a fraction is expected to act independently of DAF-2/DAF-16 signalling, again suggesting an intricate integration of sensory cues that is required to modulate longevity (Apfeld and Kenyon, 1999; Lans and Jansen, 2007).

### *OLQ-mediated behaviours*

Both PCRG-1 and EFHC-1 localise to the four mechanosensory OLQ neurons that terminate in cilia that are embedded in the cuticle of the nose. OLQ cilia are positioned to play a minor role, in cooperation with the mechanosensory ASH and FLP neurons, to mediate reversals upon light touch to the nose (Kaplan and Horvitz, 1993). In addition, OLQ neurons work with the mechanosensory IL1 neurons to mediate an aversive head withdrawal response upon nose touch, the rate and bending angle of spontaneous foraging (side-to-side head movements), and the suppression of foraging upon nose touch or anterior touch to the body (Hart et al., 1995). Specifically, dysfunction of OLQ neurons results in an increased bending angle and decreased speed of foraging as well as the inability to suppress foraging movements upon nose touch or anterior touch to the body.

### *Behaviours dependent on dopaminergic neurons*

The ciliated dopaminergic neurons, to which EFHC-1 localises, are required for modulating many behaviours based on food availability. Dopaminergic neurons found in both hermaphrodite and male animals are mechanosensory and terminate in cilia embedded in the cuticle at various locations along the body. These include four CEP neurons with cilia in the nose, two ADE neurons with cilia in the anterior body and two PDE neurons with cilia in the posterior body (Inglis et al., 2007; Sulston et al., 1975; White et al., 1986). In response to mechanosensory activation of the dopaminergic neurons, released dopamine is able to act on various post-synaptic cells to modulate behaviours through the dopamine receptors DOP-1, DOP-3 and DOP-4. In this work, we took advantage of three dopamine-dependent behaviours (basal slowing response, tap habituation and swimming-induced paralysis) to understand how EFHC-1 contributes to dopamine signalling.

Dopamine signalling is required for the basal slowing response where the mechanosensory cilia of dopaminergic neurons mechanically sense food (bacteria) in the environment, resulting in the release of dopamine and the subsequent slowing of *C. elegans* locomotion (Sawin et al., 2000). Animals that are deficient in dopamine signalling due to mutations in the ciliary mechanosensory channel TRP-4, required for

the mechanical sensation of food (Li et al., 2006), or the rate-limiting enzyme for dopamine synthesis, CAT-2, are unable to slow in the presence of food (Sawin et al., 2000). To enable slowing in the presence of food, dopamine acts on DOP-1 receptors found on cholinergic ventral cord motor neurons and DOP-3 receptors found on both cholinergic and GABAergic ventral cord motor neurons (Chase et al., 2004).

Another behaviour mediated by the ciliated dopaminergic neurons is the rate of habituation to tap, a form of non-associative learning and memory (Rankin et al., 1990; Sanyal et al., 2004). When animals experience a non-localized tap stimulus to their petri dishes, the touch receptor neurons located along the length of *C. elegans* are mechanically stimulated, and worms execute an escape response, most often seen as reversals (Rankin et al., 1990). Upon repeated mechanical stimulation in the form of taps worms habituate in two ways: there is a decrease in the proportion of animals responding as well as the distance travelled in response to taps (Rankin et al., 1990). Interestingly, only the habituation in the proportion of animals responding is dependent on dopamine (Sanyal et al., 2004). Furthermore, the rate of habituation is dependent on food, where wild-type animals habituate faster in the absence of food, and this effect also seems to be mediated by dopamine (Kindt et al., 2007b). Several mutants associated with defective dopamine signalling habituate faster than wild-type animals, including *trp-4* mutants that cannot mechanically sense food (bacteria) due to a dysfunctional ciliary mechanosensory channel, *cat-2* mutants that are unable to synthesise dopamine and *dop-1* mutants that are defective in the post-synaptic dopamine receptor present on the touch receptor neurons (Rankin et al., 1990; Sanyal et al., 2004, Kindt et al., 2007b). In contrast, mutants that have excessive dopamine due to the absence of the dopamine reuptake transporter (DAT-1) habituate slower than wild-type animals (Kindt et al., 2007b). Consequently, investigating tap habituation can reveal mutants that show either decreased or increased dopamine signalling.

Excessive dopamine signalling also contributes to the swimming-induced paralysis (SWIP) behaviour. While stimulated dopamine release in the presence of food is known to slow locomotion (Sawin et al., 2000), and the addition of exogenous dopamine results in paralysis (Schafer and Kenyon, 1995), the increased dopamine signalling in *dat-1* mutants does not result in overt locomotion defects. When wild-type

animals are placed in a liquid environment (such as water or M9 buffer) they swim by exhibiting frequent C-shaped body bends or thrashes (McDonald et al., 2007). Wild-type animals can continuously thrash for over 30 minutes. In contrast, *dat-1* mutants show paralysis within 6 minutes, where the progressive paralysis of *dat-1* mutants is accompanied by a decrease in thrashing frequency (McDonald et al., 2007). The increased dopamine signalling attributed to *dat-1* mutants leads to swimming-induced paralysis through its action on DOP-3 receptors found on both cholinergic and GABAergic ventral cord motor neurons (Chase et al., 2004).

## 1.2. Research aims

Loss of pf-ribbon proteins results in impaired ciliary motility in several organisms, but ciliary functions for these proteins apart from motility have been less apparent. In addition to their localisation to motile cilia, the pf-ribbon proteins show expression in neuronal cells of the brain where they may play sensory roles (Brody et al., 2008; Conte et al., 2009a; Léon et al., 2010; West et al., 2003). In support of this, PCRG-1 shares a common promoter with a gene implicated in inherited Parkinson's disorder and thus may have related neuronal functions (West et al., 2003). Additionally, EFHC1 is mutated in the most common form of inherited epilepsy in humans (Suzuki et al., 2004) and has been shown to be important for proper neuronal communication (de Nijs et al., 2009a; Rossetto et al., 2011). Interestingly, although the ciliated organism *Caenorhabditis elegans* lacks motile cilia, orthologues of several ciliary pf-ribbon-associated proteins, including PCRG-1 (Parkin co-regulated gene) and EFHC-1 (EF-hand containing 1), are conserved. We wished to study these motility-associated genes in *C. elegans* to allow for the dissection of their potential sensory roles.

# Chapter 2. PACRG, a protein linked to ciliary motility, mediates cellular signalling

This chapter is a modified version of a paper that has been published in *Molecular Biology of the Cell* (Loucks et al., 2016). The authors and their affiliations are listed below:

Catrina M. Loucks[1,*], Nathan J. Bialas[1,*], Martijn P. J. Dekkers[2], Denise S. Walker[3], Laura J. Grundy[3], Chunmei Li[1], P. Nick Inglis[1], Katarzyna Kida[4], William R. Schafer[3], Oliver E. Blacque[4], Gert Jansen[2] and Michel R. Leroux[1]

[1]Department of Molecular Biology and Biochemistry, Simon Fraser University, Burnaby, BC, V5A 1S6, Canada

[2]Department of Cell Biology, Erasmus MC, P.O. Box 2040, 3000 CA, Rotterdam, The Netherlands

[3]Neurobiology Division, MRC Laboratory of Molecular Biology, Cambridge, United Kingdom

[4]School of Biomolecular and Biomedical Science, University College Dublin, Belfield, Dublin 4, Ireland

*co-first author

I am a co-first author of this manuscript. Dr. Nathan Bialas started this work under the supervision of Dr. Michel Leroux, and much of the work described in this chapter has been similarly reported in his PhD thesis. Dr. Nathan Bialas collected data for **Figures 2.1, 2.2** and **2.4-2.9**, interpreted results for these experiments and wrote a first draft of the manuscript. I collected data for **Figures 2.9** and **2.10** and performed the

longevity experiments in **Figure 2.11**. In addition, I extensively revised the eventual submitted manuscript. Dr. Martijn Dekkers collected data and interpreted results for **Figure 2.3** under the supervision of Dr. Gert Jansen. Chunmei Li generated the transgenic animals used in this chapter. Dr. Denise Walker collected the calcium imaging data presented in **Figure 2.12**, and Laura Grundy collected the foraging behaviour data presented in **Figure 2.12**. Nick Inglis performed the intraflagellar transport (IFT) assays in **Figure 2.2**. Katarzyna Kida performed the transmission electron microscopy analysis shown in **Figure 2.11**. I collected data for **Figures 2.10, 2.11** and **2.12**, interpreted results for all experiments and re-wrote/polished the submitted manuscript under the supervision of Dr. Michel Leroux. Dr. Gert Jansen and Dr. Michel Leroux contributed to the conception, design, interpretation and writing of the submitted manuscript.

## 2.1. Introduction

Here we investigate the non-motile ciliary/signalling roles of PACRG (parkin co-regulated gene), a protein linked to ciliary motility. PACRG is associated with the pf-ribbon and ciliary motility, yet roles for PACRG in non-motile cilia and cellular signalling have not been investigated. We show that PACRG localises to a small subset of non-motile cilia in *C. elegans*, suggesting that it has adapted to mediate specific sensory/signalling functions. We find that it influences a learning behaviour known as gustatory plasticity, where it is functionally coupled to heterotrimeric G-protein signalling. We also demonstrate that PACRG promotes longevity in *C. elegans* by acting upstream of the lifespan-promoting FOXO transcription factor DAF-16 and likely upstream of insulin/IGF signalling. Our findings establish previously unrecognized sensory/signalling functions for PACRG and point to a role for this protein in promoting longevity. Furthermore, our work suggests additional ciliary motility-signalling connections, since EFHC1 (EF-hand containing 1), a potential PACRG interaction partner similarly associated with the protofilament ribbon and ciliary motility, also positively regulates lifespan.

## 2.2. Methods

### 2.2.1. Strains

The *pcrg-1(tm2597) and efhc-1(tm6235)* strains used in this work were obtained from National Bioresource Project (http://shigen.lab.nig.ac.jp/c.elegans/index.jsp). The *pcrg-1(gk480)* strain was obtained from the *C. elegans* gene knockout consortium (http://celeganskoconsortium.omrf.org). *The efhc-1(gk424336)* strain was obtained from the Million Mutation Project (http://genome.sfu.ca/ mmp/). These strains were out crossed to wild-type (N2) worms at least six times.

Other strains used in this work:

*gpa-1(pk15)*

*gpa-11(pk349)*

*gpa-11XS(pkIs539)*

*gpc-1(pk298)*

*odr-3(n1605)*

*osm-5(p813)*

*che-11(e1810)*

*daf-16(mu86)*

*daf-2(e1370)*

*nphp-1(ok500)*

*nphp-4(tm925)*

*eat-2(ad465)*

*clk-1(e2519)*

*dpy-5(e907);Ex[gcy-5p::gfp + dpy5(+)]*

*dpy-5(e907);Ex[gcy-5p::osm-6::gfp) + dpy5(+)]*

AQ1490 *ljEx130[pocr-4::YCD3 OLQ]*

### 2.2.2. Construction of transgenic strains

Two translational PCRG-1::GFP constructs (A and B), and a translational EFHC-1::GFP construct were generated as described previously (Blacque et al., 2004). The 5' upstream sequence included in the PCRG-1::GFP constructs also contain the predicted mitochondrial RNA processing non-coding RNA mprp-1. The 5' upstream sequence of

PCRG-1::GFP (construct B) also contains the E04F6.6 gene which codes for a protein of unknown function. All constructs contain the entire genomic coding regions along with 2169 bp (PCRG-1::GFP construct A), 4360 bp (PCRG-1::GFP construct B) or 2036 bp (EFHC-1::GFP) of promoter sequence 5' of the start codon fused upstream of and in frame with the GFP coding sequence.

### 2.2.3. Gustatory plasticity assay

The response to 25 mM NaCl, with or without pre-exposure to 100 mM NaCl, was assessed as described before (Jansen, 2002; Wicks et al., 2000). A chemotaxis index was calculated: (A-C)/(A+C), where A is the number of animals at the quadrants with NaCl, and C is the number of animals at the quadrants without attractant. The behaviour of animals was always compared to controls performed on the same day(s). 100-200 animals were tested in each assay and assays were performed at least 4 times. Statistical significance was determined using an ANOVA, followed by a Bonferoni post hoc test. Error bars represent s.e.m.

### 2.2.4. Cilium length measurements

ASER amphid sensory neurons were visualized by expressing the transcriptional reporter gcy-5p::GFP (Blacque et al., 2006). In this construct GFP diffuses freely throughout the neuron to stain the cell bodies, axons, dendrites, transition zone and cilia. 50 animals were measured per assay. Assays were repeated at least twice with consistent results. Cilium length was measured from the distal tip of the dendrite (base of cilium) to the distal tip of the cilium.

### 2.2.5. Lifespan assays

Lifespan assays were performed similar to that described in Apfeld and Kenyon, 1999. Worms were grown at 20°C for one generation before the eggs were collected through treatment with sodium hypochlorite. At the L4 molt, the animals were transferred to NGM plates seeded with *E. coli* strain OP50 and containing 16μM FUDR to prevent progeny growth. The assay plates were kept at 20°C for the duration of the assay. 100

animals were picked for each of the indicated strains, with 10 worms on each individual plate. Plates were scored every 1-2 days for the presence of live and dead worms. Individual worms were considered dead once they no longer responded to harsh touch (prodding with a platinum wire). Worms that crawled off of the plate or exploded were censored. All assays were performed at least twice with consistent results. Lifespan analyses of many mutant strains, together with wild-type controls, were conducted in parallel; some of these results are split into separate graphs to simplify the data presented and more clearly show relevant comparisons.

### 2.2.6. Microscopy and intraflagellar transport assays

Transgenic animals harboring GFP-tagged proteins were mounted on 1% agarose pads and immobilized with 100 mM levamisole. Amphid and phasmid cilia were examined with a 100X, 1.35 NA objective and an ORCA AG CCD camera mounted on an Zeiss Axioskop 2 mot plus microscope, with time-lapse images being acquired at 300-500 msec/frame, depending on the specific marker used. Images and movies were obtained in Openlab version 5.02 (Improvision). Kymographs were generated using the MultipleKymograph ImageJ plug-in (http://www.embl-heidelberg.de/eamnet/html/body_kymograph.html). Rates from middle and distal segments were obtained essentially as described (Ou et al., 2005). For transgenic strains at least 50 animals were observed per strain with consistent results.

### 2.2.7. Transmission electron microscopy

Wild-type or mutant worms were washed directly into a primary fixative of 2.5% glutaraldehyde in 0.1M Sorensen phosphate buffer. To facilitate rapid ingress of fixative, worms were cut in half under a dissection microscope using a razor blade, transferred to Ependorf tubes and fixed for one hour at room temperature. Samples were then centrifuged at 3,000 rpm for two minutes, supernatant removed and washed for ten minutes in 0.1M Sorensen phosphate buffer. Worms were then post-fixed in 1% osmium tetroxide in 0.1M Sorensen phosphate buffer for one hour at room temperature. Following washing in buffer, specimens were processed for electron microscopy by standard methods; briefly, they were dehydrated in ascending grades of alcohol to

100%, infiltrated with Epon and placed in aluminum planchetes orientated in a longitudinal aspect and allowed to polymerize at 60°C for 24 hours. Using a Leica UC6 ultramicrotome, individual worms were sectioned in cross section, from anterior tip, at 1 µm until the area of interest was located as judged by examining by light microscopy the sections stained with toluidine blue. Thereafter, serial ultra-thin sections of 80 nm were taken for electron microscopical examination. These were picked up onto 100 mesh copper grids and stained with uranyl acetate and lead citrate. Using a Tecnai Twin (FEI) electron microscope, sections were examined to locate, in the first instance, the most distal region of the ciliary region and subsequently from that point to the more proximal regions of the ciliary apparatus. At each strategic point, distal segment, middle segment and transition zone/fiber regions were tilted using the Compustage of the Tecnai to ensure that the axonemal microtubules were imaged in an exact geometrical normalcy to the imaging system. All images were recorded, at an accelerating voltage (120kV) and objective aperture of 10 µm, using a MegaView 3 digital recording system

## 2.3. Results

### 2.3.1. *C. elegans* PCRG-1 localises to cilia of ASE and OLQ neurons

Given the established link between protist PACRG and motile cilia, we first sought to determine if the uncharacterized *C. elegans* PCRG-1 protein also associates with (non-motile) ciliary structures. We generated two constructs containing the complete *pcrg-1* gene along with 2169 bp and 4360 bp respectively of endogenous upstream promoter, fused in-frame to GFP (PCRG-1::GFP constructs A and B). Multiple transgenic lines were generated for each construct, and consistent localisation of PCRG-1::GFP to cilia was observed **(Figure 2.1B)**. Surprisingly, PCRG-1::GFP is only observed in a subset of ciliated neurons, namely 2 ASE neurons and 4 outer labial quadrant (OLQ) neurons. Expression of PCRG-1::GFP in these neurons overlaps with the similarly limited expression pattern of EFHC-1, a core ciliary protofilament ribbon protein, (see below), suggesting that the observed expression pattern reflects that of the endogenous protein. ASE cilia are exposed to the external environment via openings in the cuticle (Perkins et al., 1986), and are specifically implicated in salt (NaCl) chemotaxis

behaviours (Bargmann and Horvitz, 1991). Unlike ASE cilia, OLQ cilia are embedded in the cuticle and act as mechanosensors, modulating nose-touch avoidance and withdrawal responses, rate and bending angle of foraging, and suppression of foraging upon nose touch or anterior touch to the body (Hart et al., 1995; Kaplan and Horvitz, 1993; Perkins et al., 1986). The restricted localisation of *C. elegans* PCRG-1 to a subset of cilia provides evidence that the protein regulates specific sensory/signalling functions in non-motile cilia.

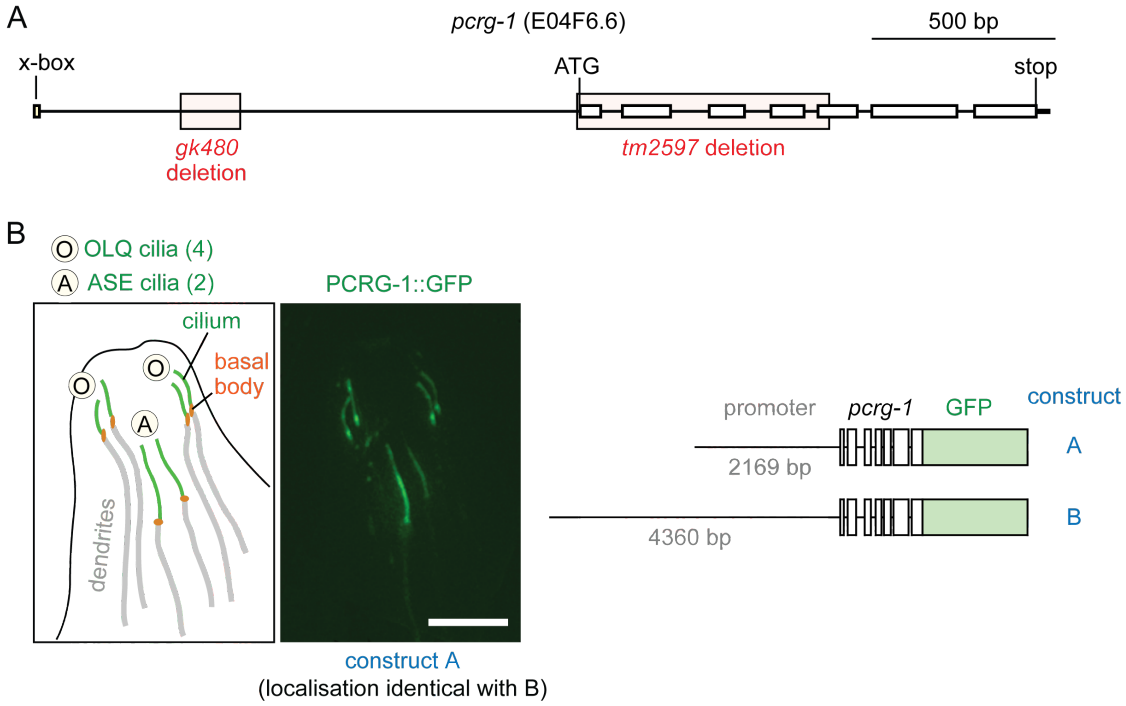


**Figure 2.1 PCRG-1::GFP fusion protein localisation and *pcrg-1* mutant alleles.** **(A)** Gene model for *E04F6.2* (*pcrg-1*) in the nematode. Positions and relative sizes of the two deletion alleles examined in this work (*gk480, tm2597*) as well as the position of the X-box sequence are shown. **(B)** Localisation of PCRG-1::GFP constructs A (991 bp promoter) and B (3182 bp promoter) to the 4 OLQ cilia and the 2 ASE cilia of *C. elegans*. On the left hand side is a schematic diagram outlining the fusion protein localisation in the nematode. The base of cilia (basal bodies) are indicated by orange ovals; cilia denoted by green lines; dendrites denoted by grey lines. Scale bar, 5 µm.

### 2.3.2. PCRG-1 is not essential for cilium biogenesis or intraflagellar transport

Based on the localisation of PCRG-1 to cilia, we examined what ciliary defects, if any, resulted from disrupting its function. We tested two *pcrg-1* mutant alleles, *gk480* and *tm2597* **(Figure 2.1A)**. The *gk480* allele disrupts part of the promoter region just downstream of a putative X-box transcriptional regulatory sequence commonly found in ciliary genes (Efimenko et al., 2005). The *tm2597* allele completely removes exons 1-4 and part of exon 5, and is likely a null. Based on the consistent phenotypes displayed with both alleles (see below), the *gk480* could prevent *pcrg-1* expression by disrupting binding of transcription factors that work in cooperation with the ciliary transcription factor DAF-19 to regulate its unique expression pattern.

To test ciliary integrity of *C. elegans* cilia in *pcrg-1* mutants, we conducted several standard assays for cilium structure and function. Notably, although most or all of GFP-tagged PCRG-1 appears to localise exclusively within ASE and OLQ cilia, we could not eliminate the possibility that it may be present (albeit at reduced levels) and function in other cilia. Many cilia in nematodes terminate at openings in the protective cuticle, exposing the sensory neurons to the external environment (reviewed in (Bae and Barr, 2008; Bargmann, 2006; Inglis et al., 2007)); this allows lipophilic dyes to permeate some ciliated sensory neurons, whereby a dye-filling assay detects differences between normal cilia and structurally impaired (e.g., truncated) cilia. Both *pcrg-1* alleles exhibit wild-type dye-filling **(Figure 2.2A)**. This may not be unexpected, since ASE and OLQ cilia do not normally dye-fill in wild-type animals (Perkins et al., 1986). *pcrg-1* mutants were also wild-type with respect to two other cilium-dependent behaviours, namely avoidance of high-osmolarity (Osm assay; **Figure 2.2B)** and chemotaxis towards the volatile attractants isoamyl alcohol and acetone (Che assays; **Figure 2.2B)**. Furthermore, *pcrg-1* mutants are wild-type with respect to development to adulthood **(Figure 2.2C)** and egg-laying behaviour **(Figure 2.2B)**, two physiological aspects regulated by sensory inputs (Fujiwara et al., 2002).

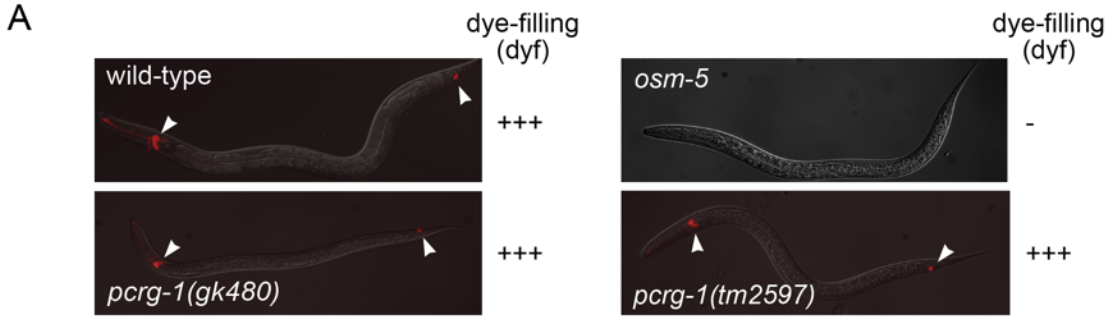


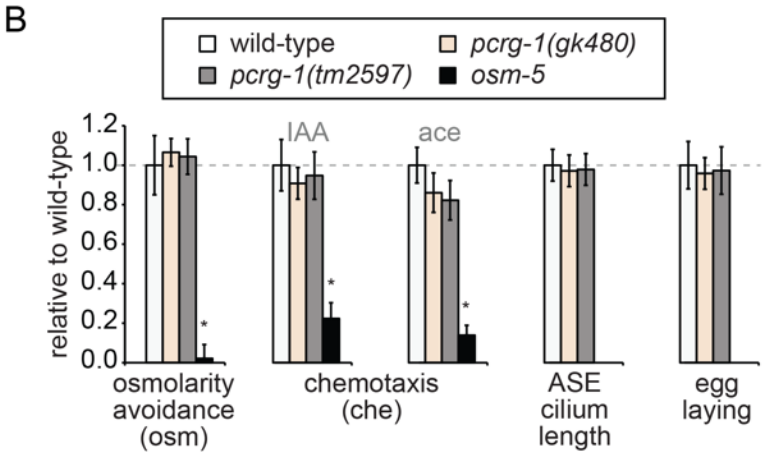


C

| | post-embryonic development (h) |
|---|---|
| wild-type | 45.1 +/- 1.5 |
| *daf-16* | 44.1 +/- 1.1 |
| *daf-2* | 49.4 +/- 2.6 |
| *osm-5* | 45.8 +/- 1.9 |
| *pcrg-1(gk480)* | 44.7 +/- 1.0 |
| *pcrg-1(tm2597)* | 44.8 +/- 1.2 |

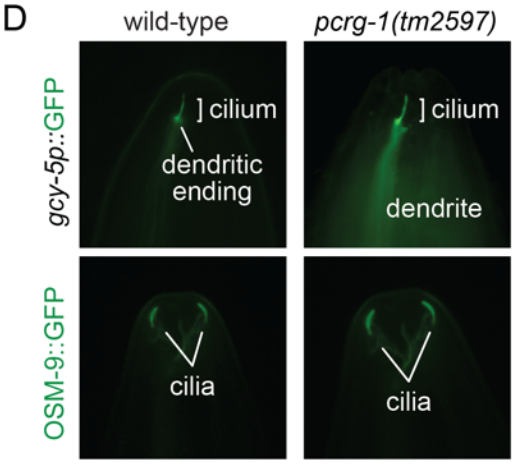


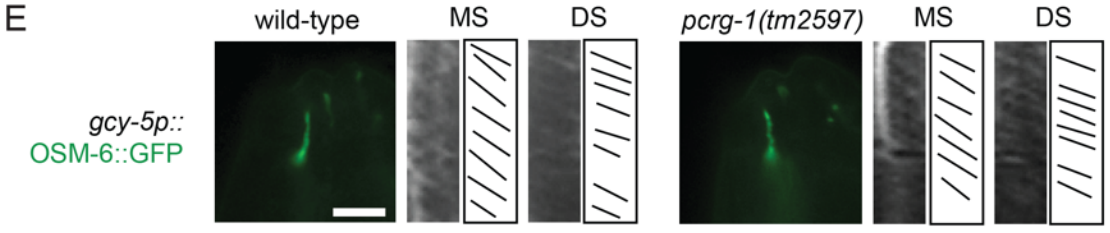


| | middle segment (MS) | | | | distal segment (DS) | | | |
|---|---|---|---|---|---|---|---|---|
| | n | vel. (µm/s) | error | p-value | n | vel. (µm/s) | error | p-value |
| wild-type | 101 | 0.6826 | 0.14 | | 86 | 1.0665 | 0.18 | |
| *pcrg-1(tm2597)* | 106 | 0.6377 | 0.11 | 0.011 | 97 | 0.9676 | 0.18 | 0.0055 |

**Figure 2.2 Analyses of *pcrg-1* mutant alleles.**
**(A)** Dye-filling analysis of *pcrg-1* mutant worms. Dye-filling in wild-type (N2), *osm-5* (dye-filling defective), *pcrg-1(gk480)* and *pcrg-1(tm2597)* worms is shown. Both amphid (head) and phasmid (tail) cell bod- ies of neurons that uptake dye (marked as '+++') are denoted by arrowheads. **(B)** Detailed char- acterization of the *pcrg-1* alleles. Results of several assays, including the osmotic avoidance (Osm) assay, chemotaxis (Che) to isoamyl alcohol (IAA) and acetone (Ace), lengths of ASER cilia (as visualized by *gcy-5p*::GFP), and egg-laying characteristics (Egl). Wild-type (N2) values are shown as white bars, *pcrg-1(gk480)* as light grey bars, *pcrg-1(tm2597)* as grey bars, and *osm- 5* as black bars. For each assay, wild-type values are plotted as 1, and the values of all other strains are shown as fractions of wild-type values. *, statistically significantly different compared to wild-type ($P<0.05$). **(C)** Results of developmental timing assays for wild-type (N2), *daf-16*, *daf-2*, *osm-5*, and both *pcrg-1* alleles (*gk480*, *tm2597*). Both pcrg-1 alleles show normal devel- opmental timing to the L4 stage. **(D)** Representative images examining ASER and OLQ cilium integrity in wild-type (N2) and *pcrg-1(tm2597)* mutant backgrounds. ASER cilium visualized by *gcy-5*::GFP; OLQ cilia visualized by OSM-9::GFP. Relative positions of cilia and dendritic end- ings are also denoted on each image. **(E)** Kymographic analyses of intraflagellar transport of the ASE-specific fusion protein (*gcy-5p*::OSM-6::GFP) in wild-type (*N2*) and *pcrg-1 (tm2597)* mu- tant animals. Top: representative still images for each strain, with representative kymographs and associated anterograde traces. Bottom: numerical scoring of velocities in both middle segments (MS) and distal segments (DS) of cilia. Scale bar, 5 μm.

Given the apparent cell-specific expression of *pcrg-1* in ASE and OLQ neurons, we specifically investigated cilia structure in these neurons, using gcy-5p::GFP to mark ASE cilia/neurons (Swoboda et al., 2000) and OSM-9::GFP to mark the OLQ cilia/neurons (Tobin et al., 2002). *pcrg-1* mutant ASE(R) cilium length is similar to wild-type **(Figure 2.2B and 2.2D)** and we observed no difference in the OSM-9::GFP localisation pattern between *pcrg-1* mutant and wild type animals **(Figure 2.2D)**. These data are consistent with PCRG-1 not playing a major role in cilium formation, even in neurons where it is clearly present.

Given the absence of gross structural ciliary defects in the *pcrg-1* mutant, we hypothesized that the intraflagellar transport (IFT) machinery, required for ciliary protein delivery, should still operate to build and maintain cilia. To test this, we monitored the behaviour of a GFP-tagged core IFT protein (OSM-6; ortholog of mammalian IFT52) expressed specifically in the ASE(R) neurons of *pcrg-1* mutant animals. In wild-type *C. elegans* cilia, OSM-6 displays transport velocities of ~0.7 μm/sec in the middle segment and ~1.1 μm/sec in the distal segment (Snow et al., 2004). In *pcrg-1* mutants, anterograde IFT is robust and largely normal, although velocities were minimally yet significantly slower than in wild-type animals (0.64 μm/s and 0.97 μm/s, respectively) **(Figure 2.2E)**. Together, these data show that PCRG-1 is not strictly required for general cilium structure/function, consistent with a largely normal axonemal ultrastructure

(unpublished observation) and a functioning IFT system. The absence of overt ciliary defects in *pcrg-1* mutants may point to a more specific role for *C. elegans* PACRG in sensory reception and signalling.

### 2.3.3. *pcrg-1* is required for gustatory plasticity, a learning behaviour dependent on ASE neurons

The expression of PCRG-1 in ASE neurons **(Figure 2.1B)** prompted us to analyze its potential role in chemotaxis to salts, which is critically dependent on these sensory neurons (Bargmann and Horvitz, 1991). We found that *pcrg-1* mutants display wild-type chemotactic behaviours to various NaCl concentrations **(Figure 2.3A)**. In addition to enabling chemotaxis, ASE neurons, along with ASI, ASH (Hukema et al., 2006) and possibly ADL and ADF neurons (Hukema et al., 2008), are essential for gustatory plasticity. This behaviour represents the reduced attraction or avoidance of *C. elegans* to NaCl after prolonged exposure to this salt in the absence of food (Bargmann, 2006; Jansen, 2002). We discovered that *pcrg-1* mutants show significant defects in gustatory plasticity, whereby animals remain attracted to NaCl even after prolonged exposure to NaCl in the absence of food **(Figure 2.3B)**. Notably, expression of PCRG-1::GFP in the *pcrg-1* mutant did not rescue the gustatory plasticity defect, as overexpression of PCRG-1::GFP itself in wild-type animals results in a similar gustatory plasticity defect **(Figure 2.3B)**. Together, these data provide evidence that correct PCRG-1 levels are needed for proper signalling associated with gustatory plasticity. Interestingly, overexpression of GPC-1, a G-protein implicated in gustatory plasticity with a mutant phenotype similar to *pcrg-1* mutants, also disrupts gustatory plasticity (Jansen, 2002). This observation led us to investigate a potential connection between PCRG-1 and G-proteins.

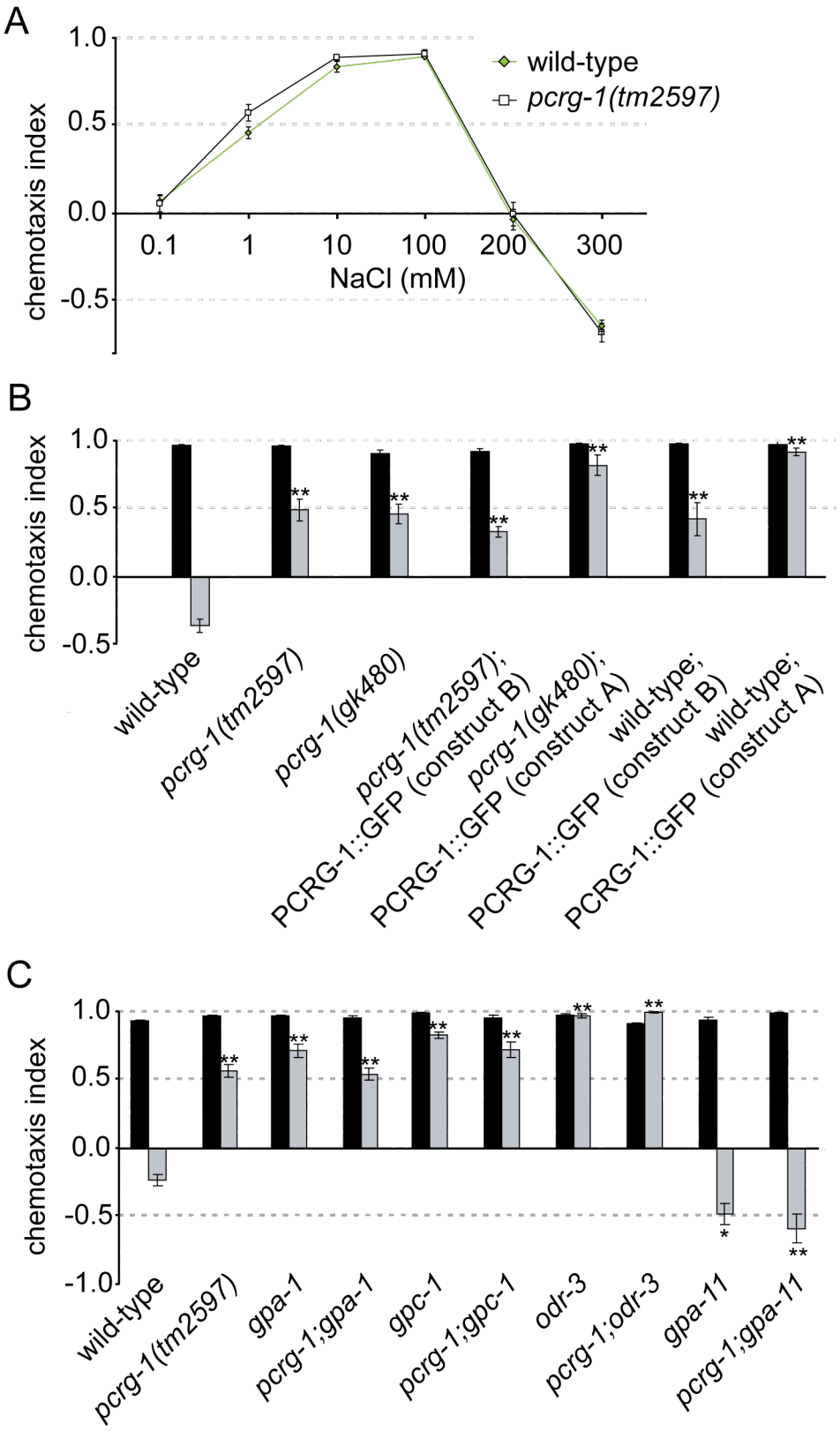
A
chemotaxis index
1.0
0.5
0.0
-0.5
0.1
1
10
100
200
300
NaCl (mM)
wild-type
pcrg-1(tm2597)
B
chemotaxis index
1.0
0.5
0.0
-0.5
wild-type
pcrg-1(tm2597)
pcrg-1(gk480)
pcrg-1(tm2597); PCRG-1::GFP (construct B)
pcrg-1(gk480); PCRG-1::GFP (construct A)
wild-type; PCRG-1::GFP (construct B)
wild-type; PCRG-1::GFP (construct A)
C
chemotaxis index
1.0
0.5
0.0
-0.5
-1.0
wild-type
pcrg-1(tm2597)
gpa-1
pcrg-1;gpa-1
gpc-1
pcrg-1;gpc-1
odr-3
pcrg-1;odr-3
gpa-11
pcrg-1;gpa-11

**Figure 2.3 *pcrg-1* animals show a defect in behavioural plasticity.**
**(A)** Naïve responses to NaCl are not affected in *pcrg-1* animals. Chemotaxis responses of *wild-type* (black line) and *pcrg-1(tm2597)* (green line) animals to various concentrations of NaCl. **(B)** Mutation of *pcrg-1* affects gustatory plasticity. Worms are washed for 15 min. in a low salt buffer (black bars) or a buffer containing 100 mM NaCl (grey bar) and tested for chemotaxis to 25 mM NaCl. Wild-type animals show avoidance of NaCl after pre-exposure, while the two *pcrg-1* mutants and the two transgenic strains carrying extra copies of *pcrg-1* remain attracted to NaCl. **, statistically significantly different compared to *wild-type* ($P<0.001$). **(C)** *pcrg-1* interacts with G protein signal transduction in gustatory plasticity. Worms are washed for 15 min. in a low salt buffer (black bars) or a buffer containing 100 mM NaCl (grey bar) and tested for chemotaxis to 25 mM NaCl. Shown are means + s.e.m.; $n > 100$ for all assays. *, statistically significantly different compared to *wild-type* ($P<0.05$). **, statistically significantly different compared to *wild-type* ($P<0.05$). Comparisons were also performed between double mutants and their corresponding single mutants. The only statistically significantly differences ($P<0.001$) were between *pcrg-1* and *odr-3, pcrg-1* and *pcrg-1;odr-3, pcrg-1* and *gpa-11,* and *pcrg-1* and *pcrg-1;gpa-11.*

## 2.3.4. *pcrg-1* interacts genetically with G-proteins in gustatory plasticity

G-protein-coupled receptors represent an important interface through which cells respond to sensory stimuli. Their activation results in the dissociation of heterotrimeric G-proteins into α and βγ subunits that regulate various downstream effectors. In *C. elegans,* at least 14 of the 21 known Gα subunits and one of the Gγ genes (*gpc-1*) are specifically expressed in sensory neurons (Jansen et al., 1999; Roayaie et al., 1998; Zwaal et al., 1996), making them promising candidates for contributing to the integration of several sensory cues in cooperation with PCRG-1 to enable gustatory plasticity. The *pcrg-1* mutant phenotype is reminiscent of two G-protein mutant phenotypes: mutants of the Gα subunit GPA-1 and the Gγ subunit GPC-1 (Hukema et al., 2006). Like *pcrg-1* mutants, these G-protein mutants show wild-type chemotaxis to NaCl, but display defects in gustatory plasticity with *gpa-1* and *gpc-1* working in the same pathway to modulate the behaviour.

To analyse if *pcrg-1* genetically interacts with these G-protein genes in gustatory plasticity, we examined the behaviour of double mutants. Mutant combinations of *pcrg-1* with either *gpc-1* or *gpa-1* do not exacerbate the phenotype, suggesting that all three genes function in the same pathway in gustatory plasticity **(Figure 2.3C)**. Mutants of another Gα subunit, ODR-3, also show gustatory defects in the absence of NaCl chemotaxis defects (Hukema et al., 2006). *odr-3* mutants display a stronger gustatory plasticity defect than *pcrg-1* mutants, whereby they are always strongly attracted to

NaCl. The *pcrg-1;odr-3* double mutant also displays this phenotype **(Figure 2.3C)**; but because *odr-3* mutants display the maximum attraction to NaCl, it is possible that the two genes function either in parallel genetic pathways or that *odr-3* functions downstream of *pcrg-1*. Interestingly, we also found that mutants of the Gα subunit GPA-11 show increased avoidance of NaCl after prolonged exposure to NaCl in the absence of food compared to wild-type animals, and fully suppress the plasticity defect of *pcrg-1* mutant animals **(Figure 2.3C)**. This latter finding suggests that *gpa-11* functions downstream of *pcrg-1* in gustatory plasticity. Together, our results provide evidence that PCRG-1 functionally interacts with several G-proteins to modulate the gustatory plasticity response.

### 2.3.5. PCRG-1 positively regulates longevity in *C. elegans*, potentially independently of G-proteins implicated in gustatory plasticity

Interestingly, the G-proteins thought to function in the same pathway as PCRG-1 in gustatory plasticity also modulate lifespan. Increased lifespan is seen in *gpa-1*, *gpc-1* and *odr-3* mutants and in animals with *gpa-11* overexpressed (Lans and Jansen, 2007). This prompted us to analyze longevity in *pcrg-1* mutants. Surprisingly, the two *pcrg-1* alleles show significantly reduced lifespan compared to wild-type **(Figure 2.4A and Table A.1)**, both of which are fully rescued by GFP-tagged PCRG-1 **(Figure 2.4B-C and Table A.1)**. This confirms that decreased longevity specifically arises from disrupting the *pcrg-1* gene, and that PCRG-1::GFP localisation to cilia is biologically relevant. Unlike previously identified longevity-promoting proteins, PCRG-1::GFP expression in wild-type animals does not increase lifespan **(Figure 2.4D** and **Table A.1)**. This is likely because many longevity- promoting proteins are kinases involved in signalling pathways like the insulin signalling pathway. Consequently, increased signalling via increased kinase activity may further extend longevity in a wild-type background. In contrast, PCRG-1 is thought to associate with the protofilament ribbon, a structural component of ciliary axonemes, where it is suspected to anchor signalling molecules. The amount of PACRG associated with the protofilament is likely fixed, so that an increase of PACRG may not lead to increased signalling in this context.

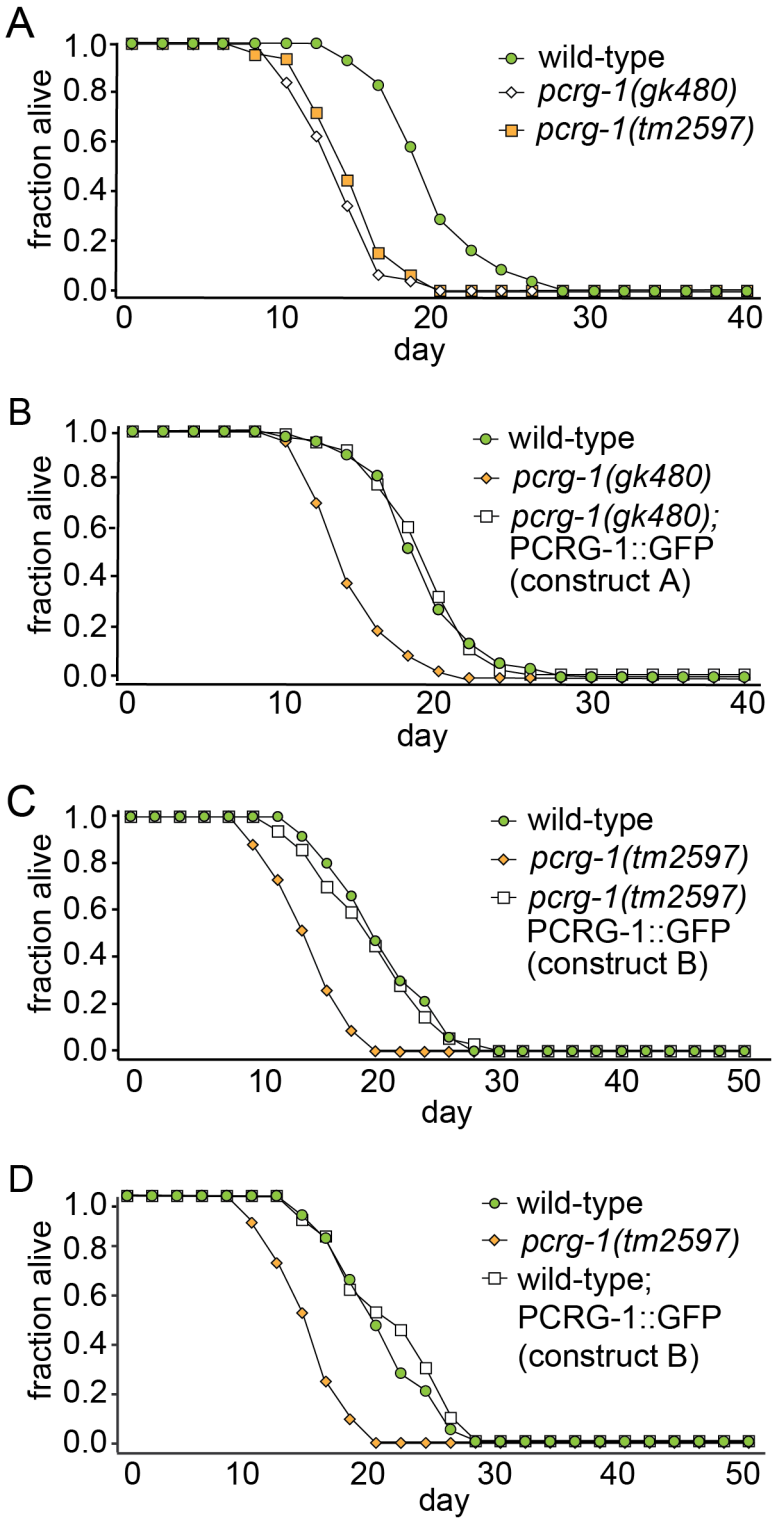
A
fraction alive
1.0
0.8
0.6
0.4
0.2
0.0
0
10
20
30
40
day
wild-type
pcrg-1(gk480)
pcrg-1(tm2597)
B
fraction alive
day
wild-type
pcrg-1(gk480)
pcrg-1(gk480);
PCRG-1::GFP
(construct A)
C
fraction alive
0
10
20
30
40
50
day
wild-type
pcrg-1(tm2597)
pcrg-1(tm2597)
PCRG-1::GFP
(construct B)
D
fraction alive
day
wild-type
pcrg-1(tm2597)
wild-type;
PCRG-1::GFP
(construct B)

**Figure 2.4 *C. elegans pcrg-1* animals show a significant decrease in lifespan compared to wild-type.**

**(A)** Both alleles of *pcrg-1* (*gk480*, *tm2597*) show a significant decrease in lifespan compared to the wild-type *N2* strain. **(B)** Expression of PCRG-1::GFP (construct A with 991 bp promoter) rescues the lifespan defect shown in the *gk480* allele. **(C)** Expression of PCRG-1::GFP (construct B with 3182 bp promoter) rescues the lifespan defect shown in the *tm2597* allele. **(D)** Expression of PCRG-1::GFP (construct B) in the wild-type (*N2*) background does not affect the lifespan of the worm. For experimental number of animals (n) and p values comparing differences between strains in lifespan experiments, see Table A.1.

We tested for genetic interactions between *pcrg-1* and these G-protein signalling mutants implicated in gustatory plasticity. Interestingly, mutant combinations of *pcrg-1* with *gpc-1* or *gpa-1* show lifespans more similar to the G-protein single mutants ($p>0.05$; **Figure 2.5A-B** and **Table A.1**). The statistical analyses are consistent with all three genes functioning in the same pathway, with PCRG-1 acting upstream of the two G-proteins (Lans and Jansen, 2007). However, since the p-value for the *pcrg-1; gpc-1* double mutant compared to the *gpc-1* single mutant is only slightly above the 0.05 cutoff for significance (0.0825), the possibility that *pcrg-1* functions in a parallel pathway to *gpc-1* could not be ruled out. In contrast, *pcrg-1* clearly acts in a pathway parallel to the two other G-protein genes tested, *gpa-11* and *odr-3*, as double mutants display a lifespan significantly different from either mutant alone **(Figures 2.5C** and **2.5E)**, and overexpression of *gpa-11* increases the short lifespan of the *pcrg-1* mutant **(Figure 2.5D** and **2.5F)**. These data, together with evidence that *gpa-1*, *gpc-1*, *gpa-11* and *odr-3* are thought to all act in the same genetic pathway to regulate longevity (Lans and Jansen, 2007), suggest that *pcrg-1* may promote longevity independently of these G-proteins. PCRG-1 regulates lifespan upstream of the longevity-promoting FOXO transcription factor, DAF-16.

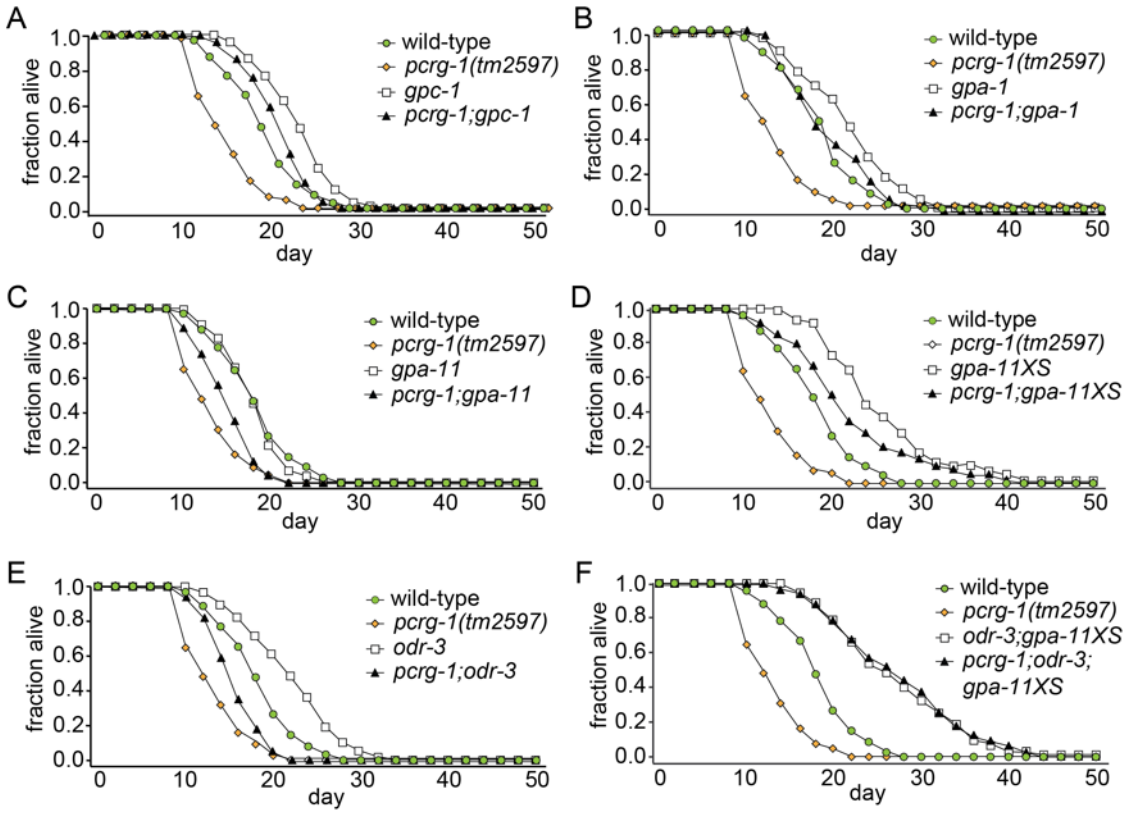


**Figure 2.5 PCRG-1 does not appear to interact with G-proteins to affect lifespan.**

**(A)** The lifespan of a *pcrg-1; gpc-1* double mutant is not statistically different from that of *gpc-1*. **(B)** The lifespan of a *pcrg-1; gpa-1* double mutant is not statistically different from that of *gpa-1*. **(C)** The lifespan of a *pcrg-1; gpa-11* double mutant is significantly different from that of either single mutant. **(D)** The lifespan of a *pcrg-1; gpa-11XS* mutant strain is significantly different from that of *gpa-11XS* and *pcrg-1* animals. **(E)** The lifespan of a *pcrg-1; odr-3* double mutant is significantly different from that of either single mutant. **(F)** The lifespan of a *pcrg-1; odr-3; gpa-11XS* mutant strain is indistinguishable from that of *odr-3; gpa-11XS*. For experimental number of animals (n) and p values comparing differences between strains in lifespan experiments see Table A.1.

Mutations in insulin signalling genes, including the insulin/IGF-1 receptor homolog *daf-2*, greatly extend lifespan (Kenyon et al., 1993). This lifespan extension depends on the FOXO family transcription factor DAF-16, which translocates to the nucleus to promote longevity in *daf-2* mutants (Lee et al., 2001). A seminal study by Apfeld and Kenyon (1999) established that loss of ciliogenic genes increased lifespan in *C. elegans*, where cilia are thought to influence longevity by controlling the insulin/IGF-1 pathway (Apfeld and Kenyon, 1999). It is notable that disruption of *pcrg-1* (confirmed in two mutants) results in decreased lifespan; in contrast, ablation of IFT (Apfeld and

Kenyon, 1999; Lans and Jansen, 2007; Schafer et al., 2006), the transition zone (membrane diffusion barrier at the ciliary base) (Bialas et al., 2009; Winkelbauer et al., 2005), or most sensory G-proteins (except GPA-2) (Lans and Jansen, 2007) all cause increased lifespan. To test for interactions between PCRG-1 and other ciliary proteins, we queried for genetic interactions between *pcrg-1* (both alleles) and IFT mutants (*osm-5* and *che-11*) or transition zone mutants (*nphp-1* and *nphp-4*), which exhibit increased lifespan to varying degrees (Apfeld and Kenyon, 1999; Winkelbauer et al., 2005; Wolf et al., 2005). In all cases, double mutants show intermediate lifespans compared to individual mutants **(Figure 2.6A-D, Figure 2.7A-D** and **Table A.1)**. This intermediate phenotype is interesting, as it suggests that PCRG-1 functions parallel to other ciliary (ciliogenic) proteins that affect lifespan. Hence, the opposite phenotypes of *pcrg-1* and ciliogenic (IFT/transition zone) mutants on lifespan are supported by these genetic epistasis results. Furthermore, the results may not be surprising, since PCRG-1 is restricted to a small number of ciliated neurons and likely contributes to specific ciliary signalling functions as opposed to affecting all cilia in the animal.

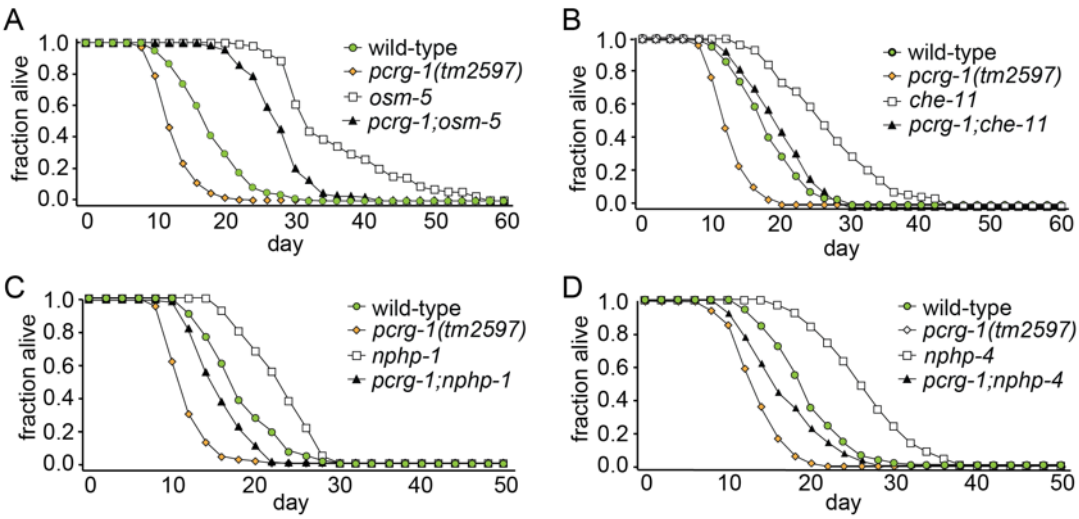


**Figure 2.6 PCRG-1 functions in a parallel pathway to ciliary proteins to regulate longevity.**

**(A)** The lifespan of a *pcrg-1;osm-5* double mutant is significantly different from that of either single mutant. **(B)** The lifespan of a *pcrg-1;che-11* double mutant is significantly different from that of either single mutant. **(C)** The lifespan of a *pcrg-1;nphp-1* double mutant is significantly different from that of either single mutant. **(D)** The lifespan of a *pcrg-1;nphp-4* double mutant is significantly different from that of either single mutant. For experimental number of animals (n) and p values comparing differences between strains in lifespan experiments see Table A.1.

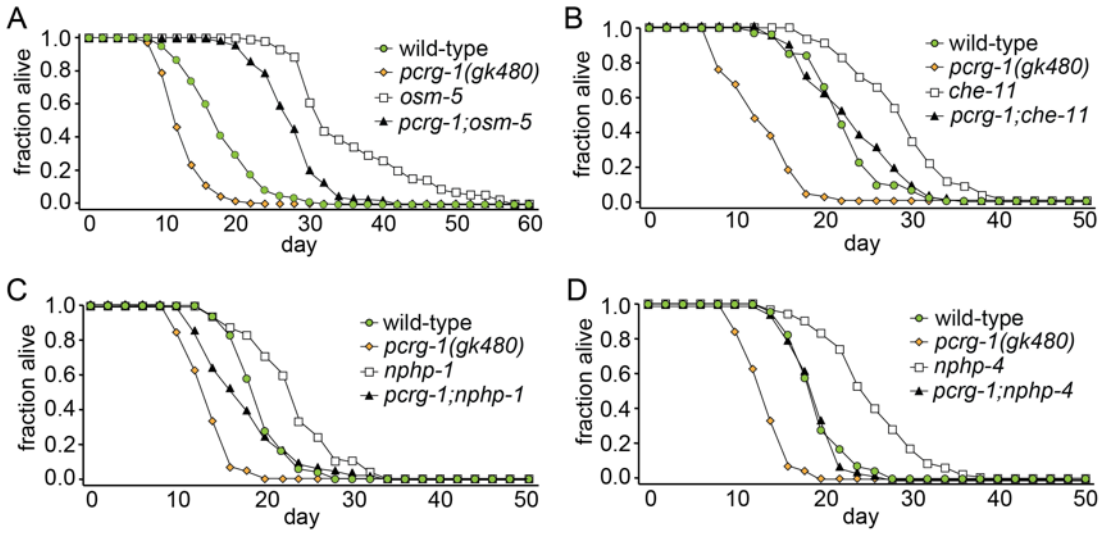


**Figure 2.7. A second mutant allele of *pcrg-1* similarly affects lifespan in a parallel pathway to that of other ciliary proteins.**

**(A)** The lifespan of a *pcrg-1;osm-5* double mutant is significantly different from that of either single mutant. **(B)** The lifespan of a *pcrg- 1;che-11* double mutant is significantly different from that of either single mutant. **(C)** The lifespan of a *pcrg-1;nphp-1* double mutant is significantly different from that of either single mutant. **(D)** The lifespan of a *pcrg-1;nphp-4* double mutant is significantly different from that of either single mutant. For experimental number of animals (n) and p values comparing differences between strains in lifespan experiments see Table A.1.

Many pathways that regulate longevity converge on the lifespan promoting transcription factor DAF-16, including the insulin signalling pathway. We tested double mutants with either *pcrg-1* allele and the short-lived *daf-16(mu86)* null allele. If PCRG-1 extends lifespan independently of DAF-16 function, double mutants would be predicted to show decreased lifespans compared to the two single mutants. For example, mutants of the AMP-activated protein kinase AAK-2 promote longevity independent of DAF-16 function, and double mutants show reduced lifespan compared to both *aak-2* and *daf-16* single mutants (Apfeld et al., 2004). In contrast, we find that loss of *pcrg-1* does not reduce the lifespan of *daf-16* mutants **(Figure 2.8A** and **Table A.1)**, indicating that *pcrg-1* modulates longevity in cooperation with *daf-16*. Next, we wanted to determine if *pcrg-1* and *daf-16* modulate longevity as part of the insulin signalling pathway. The hypomorphic, non-null nature of the *daf-2(e1370)* allele prevents definitive epistasis experiments, but the absence of *pcrg-1* activity does not reduce the lifespan of *daf-2* mutants; indeed, the *daf-2;pcrg-1* double mutant is as long-lived as the *daf-2* mutant **(Figures 2.8B** and **Table A.1)**. This finding strongly supports the notion that the *pcrg-1*

mutant is not simply 'sick', since it can live much longer than wild-type by simply reducing insulin signalling. Also, our data are consistent with both genes functioning in the same pathway, with PCRG-1 functioning upstream of DAF-2 as part of the insulin pathway and DAF-16 functioning downstream of both proteins.

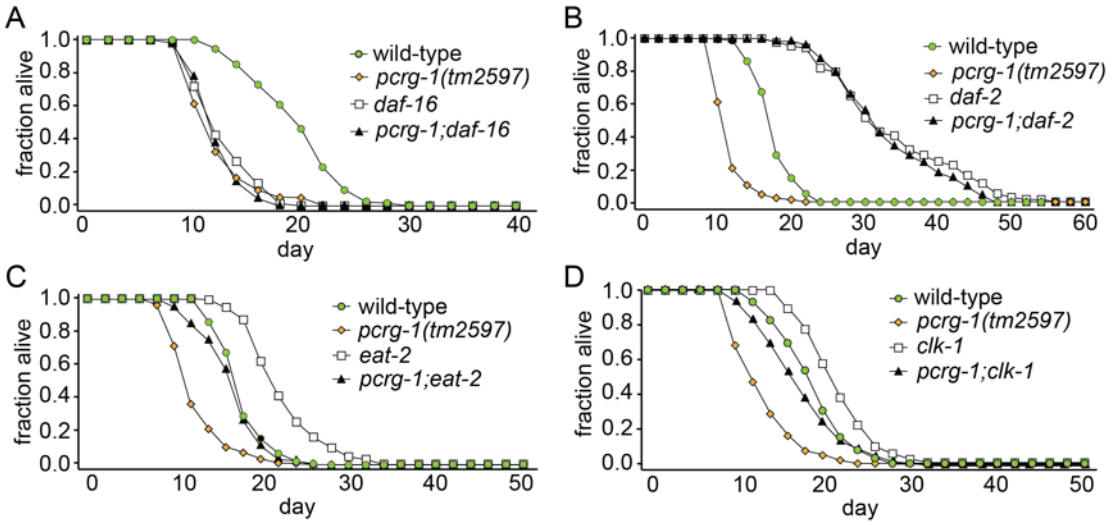


**Figure 2.8 PCRG-1 functions upstream of DAF-16 and likely the insulin signalling pathway to regulate longevity.**

**(A)** The lifespan of a *pcrg-1(tm2597);daf-16* double mutant is indistinguishable from that of either single mutant. **(B)** The lifespan of a *pcrg-1(tm2597);daf-2* double mutant is indistinguishable from that of *daf-2*. **(C)** The lifespan of a *pcrg-1;eat-2* double mutant is significantly different from that of either single mutant. **(D)** The lifespan of a *pcrg-1;clk-1* double mutant is significantly different from that of either single mutant. For experimental number of animals (n) and p values comparing differences between strains in lifespan experiments see Table A.1.

To provide further evidence that PCRG-1 functions in the insulin signalling pathway and not another longevity-related pathway we investigated dietary restriction and mitochondrial function (Ewbank et al., 1997; Klass, 1977). We tested for genetic interactions between the short-lived *pcrg-1* mutant and (i) long-lived *eat-2* mutant (impaired in feeding) and (ii) long-lived *clk-1* mutant (impaired in mitochondrial activity). In contrast to the extremely long-lived *pcrg-1;daf-2* double mutants, *pcrg-1;eat-2* and the *pcrg-1;clk-1* double mutants exhibit intermediate lifespans **(Figure 2.8C-D** and **Table A.1)**. These results suggest that PCRG-1 does not directly act within the diet restriction or mitochondrial pathways, but instead, functions in a parallel pathway, consistent with a specific role for PACRG in the insulin/IGF-1 pathway.

### 2.3.6. *C. elegans* EFHC-1 shows restricted, partially overlapping localisation to PCRG-1

*Chlamydomonas* PACRG is thought to interact with Rib72 (Ikeda et al., 2007), another highly conserved ciliary protein (Li et al., 2004; Ostrowski et al., 2002; Pazour et al., 2005; Smith et al., 2005; Stolc et al., 2005) orthologous to human EF-hand containing 1 (EFHC1) and commonly mutated in juvenile myoclonic epilepsy (JME) (Suzuki et al., 2004). In protist cilia, EFHC1 is a core component of the protofilament ribbon (Ikeda et al., 2003), and is also implicated in ciliary motility (Conte et al., 2009a; Ikeda et al., 2005; Suzuki et al., 2008, 2009). The localisation of PCRG-1 to a subset of cilia in *C. elegans* was surprising, given its high level of conservation in ciliated organisms. We wished to determine if EFHC1, thought to be functionally/physically linked to PACRG (Ikeda et al., 2007), showed a similar restricted localisation in a subset of ciliated neurons. We analyzed the unstudied *C. elegans* orthologue of EFHC1, encoded by *Y49A10A.1* (*efhc-1*). A construct with the complete *efhc-1* gene along with 2036 bp of endogenous upstream promoter fused in-frame to GFP (EFHC-1::GFP) was made. Several independent transgenic lines consistently reveal EFHC-1::GFP localisation to cilia **(Figure 2.9B)**. Like PCRG-1, the fusion protein is expressed in only a subset of ciliated neurons: the 4 outer labial quadrant (OLQ) neurons like PCRG-1, and the 4 cephalic (CEP) neurons **(Figure 2.9B)**. EFHC1::GFP appears to localise along the full length of each OLQ and CEP cilium **(Figure 2.9B)**. These data suggest that although both PACRG and EFHC1 play shared roles in motility in several organisms, in *C. elegans* they function in only a subset of non-motile cilia where they can modulate specific sensory modalities.

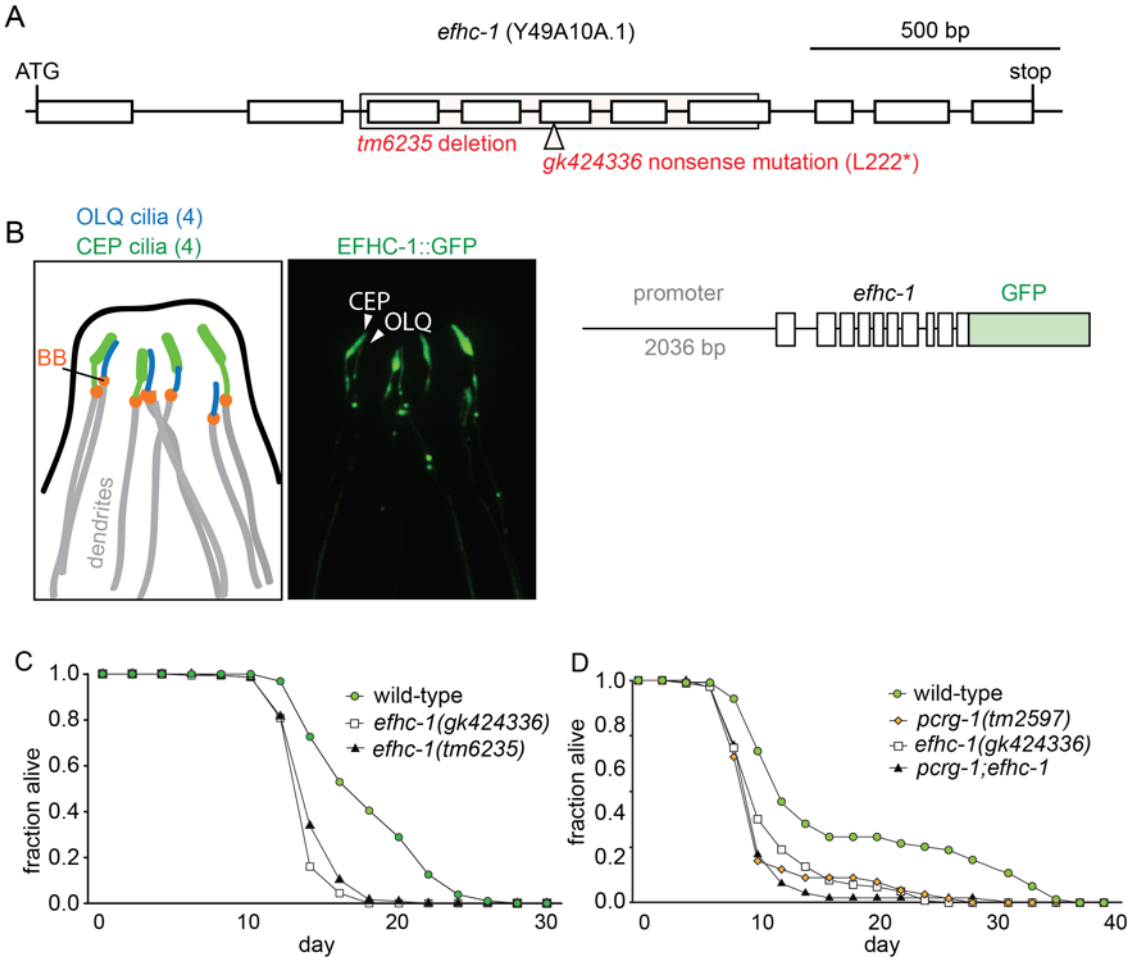


**Figure 2.9 *efhc-1* mutant alleles, localisation of EFHC-1::GFP and a reduction in lifespan in *efhc-1* mutants.**

**(A)** Gene model for the *Y49A10A.1* (*efhc-1*) gene in the nematode. Positions and size/nature of the two alleles examined in this study (*gk424336* and *tm6235*) are shown. **(B)** Localisation of EFHC-1::GFP to the 4 OLQ cilia and the 4 CEP cilia of *C. elegans*. Basal body regions (BB) are indicated by orange ovals; cilia denoted by green lines; dendrites denoted by grey lines. Scale bar, 5 µm. **(C)** Both *efhc-1(gk424336)* and *efhc-1(tm6235)* worms show significantly decreased lifespans compared to wild-type (*N2)*. **(D)** The reduced lifespan in *efhc-1* mutants is similar to the lifespan of *pcrg-1* mutants as well as double mutants, suggesting that the two genes work in the same genetic pathway to regulate lifespan. For experimental number of animals (n) and p values comparing differences between strains in lifespan experiments see Table A.1.

### 2.3.7. EFHC-1 regulates lifespan likely through the same pathway as PCRG-1

Given that most known ciliary mutants show increased lifespans, the decreased lifespan seen in *pcrg-1* mutants was unexpected. Considering the restricted localisation patterns of PCRG-1 and EFHC-1 to a small subset of ciliated neurons in *C. elegans*, we queried if disrupting EFHC-1 also influences lifespan. We tested two *efhc-1* alleles in aging assays. The *efhc-1(gk424336)* allele contains a nonsense mutation halfway through the gene, and *efhc-1(tm6235)* allele has an in-frame deletion of exons 3-7 **(Figure 2.9A)**. Remarkably, both mutants show significant decreases in lifespan, similar to *pcrg-1* mutants **(Figure 2.9C)**. The overlapping localisation of PCRG-1 and EFHC-1 in only OLQ neurons, in combination with their similar roles in lifespan extension, suggests that both proteins may act in OLQ (and perhaps not ASE or CEP) neurons to promote longevity.

The similarities between PCRG-1 and EFHC-1 also suggest a potential functional interaction between the two proteins, as was suspected but unconfirmed from Chlamydomonas studies (Ikeda et al., 2007). Indeed, *pcrg-1;efhc-1* double mutants did not show a further decrease in lifespan compared to the single mutants **(Figure 2.9D)**, consistent with both genes functioning in the same genetic pathway to regulate nematode lifespan. Given their co-localisation to OLQ cilia, we queried if the proteins depend on each other for ciliary localisation, as implied by work in *Chlamydomonas* (Ikeda et al., 2007). Interestingly, our results show that PCRG-1 is dispensable for EFHC-1 ciliary localisation, and vice versa **(Figure 2.10)**. Our findings suggest that although both proteins likely function together to exert their shared effect on lifespan, their association with the ciliary axoneme is independent.

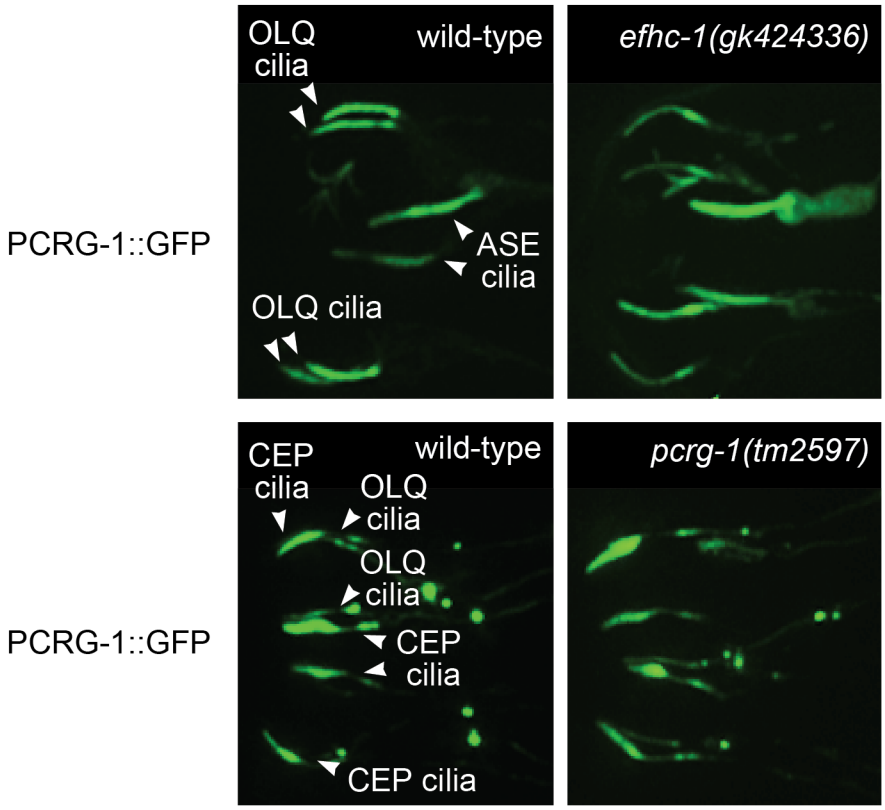


**Figure 2.10 EFHC-1::GFP localisation is independent of PCRG, and PCRG-1::GFP localisation is independent of EFHC-1.**
Ciliary localisation of EFHC-1 is un- changed in *pcrg-1(tm2597)* mutants compared to wild-type animals, and ciliary localisation of PCRG-1 is unchanged in *efhc-1(gk424336)* mutants compared to wild-type animals.

### 2.3.8. OLQ cilia/neurons appear to be involved in longevity control in *C. elegans*

To investigate a possible role of OLQ cilia in longevity control, we first looked for structural defects in OLQ cilia of *pcrg-1* mutants via transmission electron microscopy (TEM). The majority of *C. elegans* cilia possess at their very base transition fibers that stem from a degenerate basal body, a transition zone characterized by the presence of Y-shaped axoneme-membrane linkers, a 'middle segment' consisting of microtubule doublets and a 'distal segment' consisting of microtubule singlets (Perkins et al., 1986). The OLQ axoneme deviates from this, displaying nine doublet microtubules of which four are joined together into a square by thick cross-bridges and attached at the centre of the

axoneme with fine radial arms (Perkins et al., 1986). Our TEM analysis revealed that *pcrg-1* mutant animals show variable loss of microtubule doublets and a disrupted microtubule square that frequently results in three microtubule doublets connected as a triangle **(Figure 2.11A)**. These defects show parallels to axonemal defects in motile cilia of *Trypanosoma brucei* consisting of outer microtubule doublet loss toward the tip of the cilium (Dawe et al., 2005). These data are also consistent with the idea that PCRG-1 is important for attachments such as the thick cross-links between outer microtubule doublets and fine radial arms between the outer microtubule doublets and the center of the axoneme in the non-motile OLQ cilium **(Figure 2.11A)**. Finally, these results suggest that defects in OLQ ciliary structure in *pcrg-1* mutants may lead to signalling defects that disrupt longevity control. We next investigated if expressing PCRG-1::GFP specifically in the OLQ neurons using the *ocr-4* promoter in *pcrg-1* mutants increases their longevity, and indeed we found that *pcrg-1* mutants carrying the *pocr-4::PCRG-1::GFP* construct live longer than their non-transgenic siblings **(Figure 2.11B)**. To directly interrogate the involvement of OLQ neurons in longevity in *C. elegans*, we genetically ablated OLQ neurons using a *pocr-4::egl-1(d)* construct. Interestingly, animals carrying the ablation construct show increased longevity compared to non-transgenic, wild-type siblings **(Figure 2.11C)**. This suggests that the ciliated OLQ neurons may play an important role in longevity control in *C. elegans,* and that PCRG-1 and EFHC-1 may exert their longevity-promoting activities through their functions in OLQ.

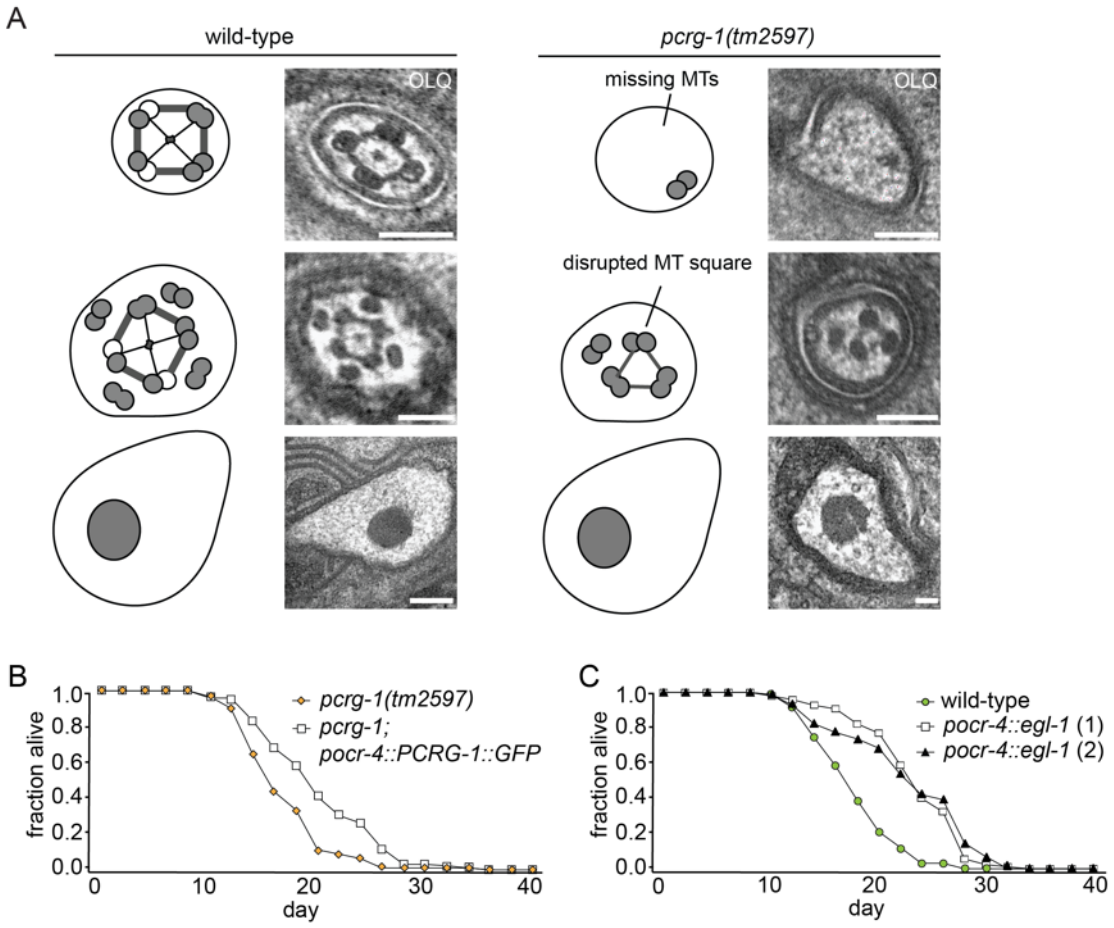


**Figure 2.11 OLQ neurons and/or cilia appear to play a role in longevity.**
**(A)** Ultrastructure of OLQ cilia in *pcrg-1* mutants is shown by representative TEM images from serial cross-sections. The bottom row shows the striated rootlet at the base of OLQ cilia that is unaltered in *pcrg-1* mutants. The middle row shows the proximal region of the OLQ cilia. In wild-type cilia, four outer doublets are connected in a square by thick cross-bridges, and to the centre with fine radial arms surrounded by additional microtubule doublets. In *pcrg-1* mutants microtubule doublets no longer form a square, but frequently form a triangle instead, and radial arms are missing. The top row shows the distal region of OLQ cilia where wild-type animals retain microtubule doublets connected in a square but lose additional doublets. pcrg-1 mutants completely lose connections between doublets and retain a small number of doublets. The scale bars represent 200 nm. **(B)** *pcrg-1* animals with PCRG-1 fused to GFP and driven by the *ocr-4* promoter specifically in OLQ neurons show increased longevity compared to non-transgenic, *pcrg-1* siblings. **(C)** Genetic ablations of OLQ neurons show increased longevity compared to non-transgenic, wild-type siblings.

Given that OLQ cilia are known to function in mechanosensation at the nose of *C. elegans* (Hart et al., 1995; Kaplan and Horvitz, 1993), we investigated the consequences of the loss of PCRG-1 on mechanosensory responses and OLQ-related behaviours. Interestingly, we find that *pcrg-1* mutants retain mechanosensory responses

to both light (buzz stimulus) and strong (press stimulus) stimulation to the nose **(Figure 2.12A-B)**. In addition, we find that foraging behaviours mediated by OLQ neurons are similarly unaffected in *pcrg-1* mutants **(Figure 2.12C-D)**. Together, these data show that PCRG-1, and likely EFHC-1, function in OLQ to mediate signalling functions/molecules specific to longevity and not implicated in the forms of mechanosensation and foraging behaviours tested for.

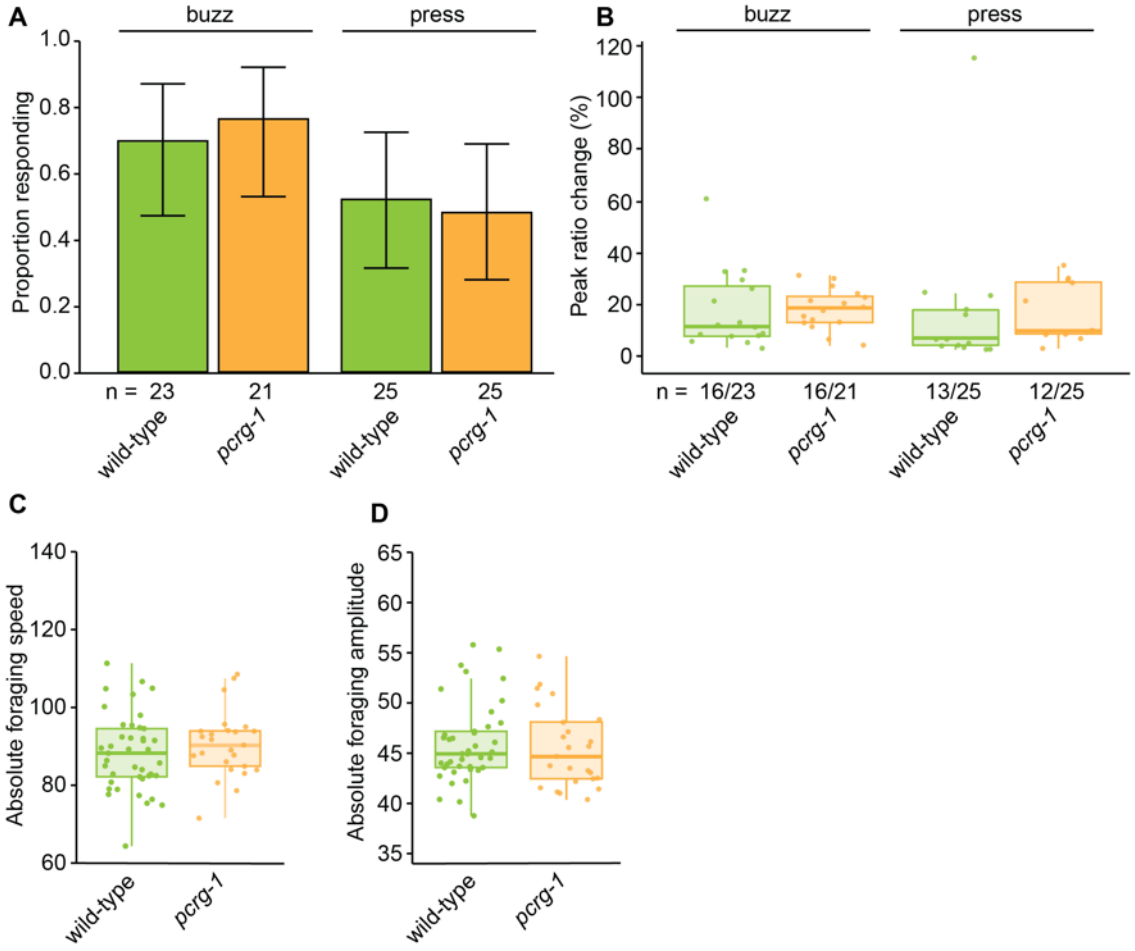

**Figure 2.12 *pcrg-1* mutants show no defects in OLQ-related mechanosensory or behavioural responses.**

**(A)** Loss of PCRG-1 has no effect on the activation of OLQ neurons upon gentle mechanical stimulation (buzz) or a stronger stimulation (press). In this panel, n represents the total number of animals assessed. Each bar represents the number of worms responding to mechanical stimulation over the total number of worms assessed per strain, and the error bars represent the binomial confidence intervals. Binomial logistic regression followed by Tukey's HSD (honest significant difference) test was used to determine significance for each pair of strains. Differences between all strains are not significant. **(B)** The peak ratio change (%) representing the amplitude of the neuronal response, is similar between strains for animals responding to each stimulus. In this panel, n represents the number of animals responding to the stimulus over the total number of animals assessed. **(C)** *pcrg-1* mutants showed similar foraging speeds and **(D)** foraging amplitudes, two behaviours mediated by the OLQ neurons. Here the absolute values of the forward foraging speed/amplitude are depicted.

## 2.4. Discussion

A distinction between motile and non-motile (sensory) cilia is often made, owing to their well-established roles in motility, and sensory transduction, respectively. Nevertheless, sensory functions have been ascribed to motile cilia (Bloodgood, 2010; Shah et al., 2009). Both forms of cilia require the same evolutionarily conserved intraflagellar transport (IFT) machinery for their formation; and both possess similar ultrastructures, with the exception of various appendages associated with the motile axoneme, such as the central microtubule pair, radial spokes, inner and outer dynein arms and interdoublet links. The protofilament ribbon, located at the junction of the A and B tubules of outer doublet microtubules, has long been suspected of being a major attachment point for structures/proteins involved in producing movement (Amos, 2008; Linck and Norrander, 2003; Setter et al., 2006; Tanaka et al., 2004). Consistent with this, PACRG, which is specifically associated with the protofilament ribbon (Ikeda et al., 2007), functions in ciliary motility (Brody et al., 2008; Dawe et al., 2005; Lorenzetti et al., 2004; Wilson et al., 2010). Given the presence of a PACRG ortholog in *C. elegans*, which lacks motile cilia, we hypothesized that this protofilament ribbon protein may provide a scaffold important for sensory transduction; similar functions may also exist in motile cilia, but could be masked by prominent motility phenotypes in mutants.

Our results demonstrate that *C. elegans* PACRG localises specifically to cilia; however, rather than being a ubiquitous ciliary component, it appears to have been adopted for specific functions in a restricted number of ciliated sensory neurons. In

particular, while *pcrg-1* mutants show wild-type chemotaxis to NaCl they display defects in the learning behaviour known as gustatory plasticity in which wild-type animals avoid normally attractive NaCl concentrations when pre-exposed to the salt in the absence of food. *pcrg-1* mutants remain attracted to NaCl after pre-exposure in the absence of food, a phenotype similar to that seen in mutants for the Gα subunits GPA-1 and the Gγ subunit GPC-1. All three genes were found to function in the same pathway, supporting a highly intricate integration of sensory cues in the modulation of gustatory plasticity. It has been proposed that ASE neurons (which express *pcrg-1*) provide a signal to sensitise ADF, ADL, ASI and ASH (many of which express *gpa-1* and/or *gpc-1*) neurons in gustatory plasticity to increase avoidance of normally attractive NaCl concentrations after prolonged exposure (Hukema et al., 2006). An appealing possibility is that *pcrg-1* plays a role in the production of this signal.

In this work, we also find that *pcrg-1* mutants display marked decreases in lifespan compared to wild-type animals. Nematode cilia collectively represent the sensory apparatus of the animal (reviewed in (Inglis et al., 2007)), and decreased sensation is associated with increased longevity (Kenyon, 2010). In *C. elegans*, mutations affecting the insulin/IGF receptor DAF-2 result in lifespan extension that depends on the FOXO transcription factor DAF-16. All investigated proteins that influence cilium formation (e.g., IFT and transition zone components) negatively regulate insulin/IGF signalling, and thus, reduce longevity (i.e., mutants have increased lifespans). It is therefore surprising that PCRG-1 has the opposite effect, positively regulating insulin/IGF signalling. Yet, our genetic interaction studies reveal that PCRG-1 functions in a parallel pathway to the previously-studied IFT and transition zone proteins, supporting the notion that its role at the cilium in modulating signalling is unique. Remarkably, EFHC1, an integral component of the protofilament ribbon also localises to cilia within a small, partially overlapping, subset of neurons and positively regulates longevity, likely through the same pathway as PACRG. Hence, both protofilament ribbon proteins carry out distinct roles in ciliary signalling compared to ciliogenic proteins.

Our genetic epistasis studies reveal that PCRG-1 modulates lifespan upstream of the longevity- promoting FOXO transcription factor, DAF-16; this is like other ciliary (IFT, transition zone) proteins, but PCRG-1 exerts an opposite effect on lifespan compared to

other ciliary proteins. Although ciliary mutants most often display increased longevity, the ablation of specific gustatory neurons, and likely other ciliated sensory neurons, can either inhibit or promote longevity (Alcedo and Kenyon, 2004). The longevity-promoting nature of both PCRG-1 and EFHC-1 and the overlapping localisation of the two proteins in OLQ neurons suggests the existence of a lifespan-modulating signal derived from OLQ neurons. This putative signal is independent of the G-protein signalling network implicated in gustatory plasticity. A role for OLQ cilia/neurons in longevity control is further supported by the discovery that ciliary structure is abrogated in *pcrg-1* mutants that could lead to impairment of signalling pathways that rely on intact cilia. Furthermore, we find that expression of PCRG-1::GFP specifically in OLQ neurons results in lifespan extension of *pcrg-1* mutants. Interestingly, genetic ablations of OLQ neurons result in increased longevity, suggesting that OLQ is responsible for producing a lifespan-reducing signal, and that ciliary dysfunction in *pcrg-1* mutants may increase the production of this signal and reduce lifespan.

In conclusion, our work has identified roles for the *C. elegans* PACRG ortholog in regulating signalling functions associated with non-motile, sensory cilia. It is possible that the proteins have comparable roles in signalling within motile cilia—which have known sensory-signalling functions (Bloodgood, 2010; Shah et al., 2009). Uncovering such signalling functions may be difficult, given the prominent roles for PACRG in maintaining axonemal structure integrity and motility. The other possibility is that the signalling roles of PACRG are innovations in metazoans; the protein was adopted by non-motile cilia to regulate sensory signal transduction. Furthermore, in this work we show that additional ciliary motility-signalling connections may exist, since EFHC1 (a core protofilament ribbon protein associated with ciliary motility) also positively regulates lifespan. Future studies aimed at dissecting the roles of mammalian PACRG and EFHC1 in primary cilia-mediated sensory processes and insulin/IGF (and potentially other) signalling pathways should prove to be valuable, as they may provide insights into lifespan control as well as other physiological and developmental processes.

# Chapter 3. EFHC1 links the primary cilium, synapse, epilepsy and dopamine signalling

A modified version of this chapter is being submitted to *Nature.* The authors and their affiliations are listed below:

Catrina M. Loucks[1], Denise S. Walker[2], Andrea H. McEwan[3], Tiffany A. Timbers[1], Evan A. Ardiel[3], Laura J. Grundy[2], Julie Kennedy[4], Chunmei M. Li[1], Jacque-Lynne Johnson[1], Oliver E. Blacque[4], William R. Schafer[2], Catharine H. Rankin[3,5] and Michel R. Leroux[1]

[1]Department of Molecular Biology and Biochemistry, Simon Fraser University, Burnaby, BC, leroux@sfu.ca

[2]Cell Biology Division, MRC Laboratory of Molecular Biology, Cambridge, UK

[3]Brain Research Centre, University of British Columbia, Vancouver, BC

[4]School of Biomolecular and Biomedical Science, University College Dublin, Belfield, Dublin 4, Ireland

[5]Department of Psychology, University of British Columbia, Vancouver, BC

I am the first author of this submitted manuscript. I conceived/designed all experiments, collected data for most experiments (exceptions below), interpreted results for all experiments and wrote the submitted manuscript under the supervision of Dr. Michel Leroux. Andrea McEwan ran many of the preliminary tap habituation assays shown in **Figures 3.6, 3.7** and **3.15**. Dr. Denise Walker collected data for the calcium imaging experiments in **Figures 3.9, 3.10** and **3.11**. Laura Grundy collected data for the foraging behaviour assayed using the single-worm tracker in **Figure 3.11**. Dr. Evan Ardiel helped in the preliminary analysis of swimming-induced paralysis (SWIP) assays

in **Figures 3.8** and **3.15**. Julie Kennedy performed the transmission electron microscopy analysis in **Figures 3.12** and **3.13**. Dr. Jacque-Lynne Johnson injected some of the constructs to create transgenic strains. Dr. Tiffany Timbers contributed through valuable discussions. Dr. Michel Leroux created the model in **Figure 3.16**. Drs. Oliver Blacque, William Schafer, Catharine Rankin and Michel Leroux contributed to the conception, design, interpretation and writing of the submitted manuscript.

## 3.1. Introduction

The cilia of multicellular organisms are typically classified as either motile, to enable fluid flow, or non-motile, to allow for sensory and signalling functions. Single-celled organisms possess one or more cilia responsible for both producing movement and responding to mechanosensory cues to modulate movement, and could thus represent the ancestral form of cilia. EFHC1, one of several proteins linked to juvenile myoclonic epilepsy (Suzuki et al., 2004), is an evolutionarily conserved protein specifically associated with ciliary motility (Conte et al., 2009a; Suzuki et al., 2008, 2009), and whose potential function in non-motile cilia remains unclear (Zhao et al., 2016). Here, we demonstrate that instead of being a core component of ciliary motility-associated machinery, the *C. elegans* orthologue of EFHC1 is required for mechanosensation in specialised non-motile cilia, where it regulates neuronal activation and dopamine signalling. EFHC1 also localises to the synapse, where it further regulates dopamine signalling in cooperation with a known EFHC1-interaction partner (Suzuki et al., 2004), an R-type voltage-gated calcium channel. Our work therefore highlights the importance of exaptation (functional adaptation) of a cilium motility protein in non-motile sensory cilia. Moreover, our findings reveal a previously undescribed dual-regulation of neuronal excitability at the site of sensory neuron input (cilium) and sensory neuron output (synapse), and suggest an important correspondence between dopamine neurotransmission and epilepsy.

Mutations in *EFHC1* frequently underlie cases of juvenile myoclonic epilepsy (JME), the most common form of idiopathic epilepsy in humans (Delgado-Escueta, 2007; Delgado-Escueta and Enrile-Bacsal, 1984), yet it remains unclear how disruption of this gene contributes to epilepsy. EFHC1 is a highly conserved ciliary protein and a core component of the protofilament ribbon, a structure thought to dictate the ordered attachment/arrangement of proteins required for ciliary motility (Ikeda et al., 2003, 2007). To date, most known ciliary functions for EFHC1 are restricted to enabling motility (Conte et al., 2009a; Suzuki et al., 2008, 2009). Yet, motile cilia dysfunction in ependymal cells of the brain does not correlate with epilepsy in mice (Suzuki et al., 2009). Intriguingly, non-motile cilia are ubiquitous in the mammalian brain and EFHC1 is expressed in many brain regions (Conte et al., 2009b; Ikeda et al., 2005; Léon et al.,

2010; Nijs et al., 2012; de Nijs et al., 2009a; Suzuki et al., 2004), leading to the possibility that EFHC1 functions in non-motile cilia and plays important sensory roles in neurons to regulate neuronal excitability.

## 3.2. Methods

### 3.2.1. Strains

The following strains were used in this work:

MX081 *N2;nxEx[Y49A10A.1::gfp + xbx-1::tdTomato + rol-6(su1006)]*

C1112 cat-2(e1112)

RM2702 dat-1(ok157)

AQ2044 *ljIs20[cat-1::YC2.1]*

AQ1427 *trp-4(gk341);ljIs19[cat-1::YC2.1]*

AQ2829 *ljEx130[pocr-4::YCD3(cameleon)]*

VC818 *trp-4(gk341)*

TQ420 *trp-4(sy695);xuEx542[trp-4::yfp + Podr-1::RFP]*

DR86 *daf-19(m86)*

OW47 *unc-2(zf35gf)*

MT10661 *tdc-1(3420)*

The following strains were created in this work:

MX2195 *Ex[pefhc-1::EFHC-1::GFP*, *pefhc-1::XBX-1::tdTomato + cc::GFP*]

MX2194 *N2;nxEx[SNB-1::tdTomato + Y49A10A.1::gfp +ccgfp]*

MX2132 *efhc-1(gk424336);cat-2(e1112)*

MX2137 *efhc-1(gk424336);ljIs20[cat-1::YC2.1]*

MX2317 *efhc-1(gk424336);trp-4(sy695);xuEx542[trp-4::yfp + Podr-1::RFP]*

MX2129 *efhc-1(gk424336);trp-4(gk341)*

MX2316 *efhc-1(gk424336);daf-19(m86)*

MX1973 *daf-19(m86) II;daf-12(sa204);nxEx[Y49A10A.1::GFP + cc::GFP]*

MX2185 *dpy-5(e907);nxEx[unc-2(zf35) + cc::GFP + dpy-5(+)]*

MX2341 *efhc-1(gk424336);dpy-5(e907);nxEx[unc-2(zf35) + cc::GFP + dpy-5(+)]*

MX2317 *efhc-1(gk424336);trp-4(sy695);xuEx542[trp-4::yfp + Podr-1::RFP]*

MX2137 *efhc-1(gk424336);ljEx130[pocr-4::YCD3(cameleon)]*

### 3.2.2. Generation and visualisation of transgenic animals

Both the *pefhc-1*::XBX-1::tdTomato and *pefhc-1*::SNB-1::tdTomato constructs were created using 2036 bp of *efhc-1*'s endogenous upstream promoter fused to all the exons/introns of *xbx-1* or *snb-1* and then fused in-frame to tdTomato. The pefhc-1::unc-2(gf) construct was again created using 2036 bp of *efhc-1*'s endogenous upstream promoter fused to the cDNA of *unc-2* containing a gain-of-function mutation and a synthetic intron. Fluorescently-tagged proteins were visualised by first immobilising animals using 0.5µl of 10mM levamisole and 0.5µL of 0.1µm diameter polystyrene microspheres (Polysciences 00876-15, 2.5% w/v suspension) on 5% agarose pads. Z-stack images were collected using a spinning disc confocal microscope (WaveFX;

Quorum Technologies), a Hammamatsu 9100 EMCCD camera and Volocity software (PerkinElmer).

### 3.2.3. Behavioural assays

#### *Tap habituation*

Worms were age synchronised by allowing five gravid adults to lay eggs for 3–4 hours on individual NGM plates seeded with *E. coli* OP50 bacteria and testing the worms after 4 days. At least one hour before testing, 20–30 worms were transferred to fresh NGM plates, with or without food. Plates with food were seeded with 50 µl of liquid culture OP50 bacteria in lysogeny broth (LB) 24 hours beforehand, while plates without food were seeded with 50 µl LB. Plates with worms were then placed into the Multi-Worm Tracker (MWT) (Swierczek et al., 2011), and after a 300 or 600 second acclimatization period, 30 taps were administered at 10-second interstimulus intervals (ISI). All experiments were done at 20°C, and in most experiments strains were cultured at 20°C. In the habituation experiment involving *daf-19(m86)*, all strains were cultured at 15°C for four days then moved to 20°C for two days to enrich for non-dauer worms in *daf-19* and *daf-19;efhc-1* worms. Script for analysis available at: https://github.com/cloucks/dopamine_habituation).

#### *Swimming-induced paralysis (SWIP)*

Worms were age synchronized by allowing 10 gravid adults to lay eggs for 3 hours on individual NGM plates seeded with OP50 bacteria. L4 worms were tested after 2 days at 20°C. Two different SWIP assays were performed: one manual and one automated. For both assays, ten L4 animals were placed in 30 µL of tap water in a single well of a Pyrex Spot Plate (Fisher). For the manual assay, animals were assessed for paralysis after 10 minutes, defined as no C-shaped bends for at least 5 seconds. For the automated assay, the plate was analysed using the Multi-worm tracker (MWT) to assess thrashing frequency of animals over 11 minutes (script available at: https://github.com/cloucks/dopamine_swimming).

### *Basal slowing response*

Worms were age synchronised by allowing five gravid adults to lay eggs for 3–4 hours on individual NGM plates seeded with OP50 bacteria and testing the worms after 3 days. On the day of testing, worms were washed off their individual plates with M9 buffer and transferred to individual NGM with or without food. Plates with food were seeded with 100 µL HB101 24 hours beforehand, while plates without food were seeded with 100 µL LB. Plates with worms were then placed into the Multi-Worm Tracker (MWT) (Swierczek et al., 2011), and 600 seconds. Body bends were counted for animals persisting from 60-120 seconds.

### *Suppression of foraging*

Worms were age synchronized by allowing five gravid adults to lay eggs for 3–4 hours on individual NGM plates seeded with OP50 bacteria and testing young adult worms after 3 days. On the day of testing, worms were transferred to an NGM plate without bacteria for 10 minutes then transferred to NGM plates seeded with 50 µL OP50 4 hours beforehand. After waiting at least one minute after transfer, individual forward-moving worms were touched in their anterior body with a hair pick. Suppression of foraging upon reversal was defined as at least two consecutive body bends without foraging (Kindt et al., 2007a). The *tdc-1(n3420)* mutant, defective in the suppression of foraging, was used as a positive control (Alkema et al., 2005).

### *Single-worm tracking*

Single-worm tracking was essentially as described previously (Yemini et al., 2013). Worms were maintained under strictly controlled conditions up until the point of tracking. Animals were staged by picking late L4 animals the evening before tracking. On the day of tracking, animals were transferred to 3.5 cm plates with low peptone nematode growth medium (NGM) and seeded with 20 µL of *E. coli* OP50 that was allowed to dry for at least 30 minutes. A 30-minute wait was implemented before tracking to allow worms to habituate after being picked and moved to their tracking plate. To ensure sufficient phenotypic sampling, at least 20 young-adult hermaphrodites per strain were filmed for 15 minutes. The camera magnification was to set between 3.5–4.5 microns/pixel (a corresponding FOV of, approximately, 2.5×2mm at 640×480 resolution)

and the frame rate to 20–30 frames/second to ensure a high-resolution analysis. To avoid potential room conditions that may bias measurement, recording was randomized, across multiple trackers. Strains were matched to all wild-type animals (N2) recorded alongside the mutants.

### 3.2.4. Calcium imaging of CEP and OLQ neurons

Calcium imaging of nose touch stimulation of glued animals was essentially as described previously, using a 1 second “press” or 3.7 second “buzz” stimulus (Kindt et al., 2007a, 2007b). Images were recorded at 10 Hz using an iXon EM camera (Andor Technology), captured using IQ1.9 software (Andor Technology) and analysed using a Matlab (MathWorks) program custom written by Ithai Rabinowitch. A rectangular region of interest (ROI) was drawn around the cell body and for every frame the ROI was shifted according to the new position of the centre of mass. Fluorescence intensity, F, was computed as the difference between the sum of pixel intensities and the faintest 10% pixels (background) within the ROI. Fluorescence ratio $R=F_{yellow}/F_{cyan}$ (after correcting for bleed through) was used for computing ratio change, expressed as a percentage of $R_0$ (the average R within the first 3 sec of recording).

### 3.2.5. Transmission electron microscopy

Wild-type or mutant worms were washed directly into a primary fixative of 2.5% glutaraldehyde in 0.1M Sorensen phosphate buffer. To facilitate rapid ingress of fixative, worms were cut in half under a dissection microscope using a razor blade, transferred to Ependorf tubes and fixed for one hour at room temperature. Samples were then centrifuged at 3,000 rpm for two minutes, supernatant removed and washed for ten minutes in 0.1M Sorensen phosphate buffer. Worms were then post-fixed in 1% osmium tetroxide in 0.1M Sorensen phosphate buffer for one hour at room temperature. Following washing in buffer, specimens were processed for electron microscopy by standard methods; briefly, they were dehydrated in ascending grades of alcohol to 100%, infiltrated with Epon and placed in aluminum planchetes orientated in a longitudinal aspect and allowed to polymerize at 60°C for 24 hours. Using a Leica UC6 ultramicrotome, individual worms were sectioned in cross section, from anterior tip, at 1

μm until the area of interest was located as judged by examining by light microscopy the sections stained with toluidine blue. Thereafter, serial ultra-thin sections of 80 nm were taken for electron microscopical examination. These were picked up onto 100 mesh copper grids and stained with uranyl acetate and lead citrate. Using a Tecnai Twin (FEI) electron microscope, sections were examined to locate, in the first instance, the most distal region of the ciliary region and subsequently from that point to the more proximal regions of the ciliary apparatus. At each strategic point, distal segment, middle segment and transition zone/fiber regions were tilted using the Compustage of the Tecnai to ensure that the axonemal microtubules were imaged in an exact geometrical normalcy to the imaging system. All images were recorded, at an accelerating voltage (120kV) and objective aperture of 10 μm, using a MegaView 3 digital recording system

## 3.3. Results

### 3.3.1. *C. elegans* EFHC-1 localises to cilia of two classes of mechanosensory neurons

To isolate non-motile ciliary functions of EFHC1, we took advantage of *Caenorhabditis elegans*, a nematode which lacks motile cilia. We generated a translational fusion of *C. elegans* EFHC-1 driven by its own promoter and found that EFHC-1::GFP is specifically expressed in a small subset of ciliated mechanosensory neurons: the dopaminergic CEP, ADE and PDE neurons, and the glutamatergic OLQ neurons **(Figure 3.1A)**. Both classes of neurons terminate in cilia embedded in the cuticle, ideally positioned to mediate mechanosensation at various locations along the body: four CEP neurons paired with four OLQ neurons project cilia in the nose, two ADE neurons position cilia in the anterior body and two PDE neurons localise cilia to the posterior body (Inglis et al., 2007; Sulston et al., 1975; White et al., 1986). Additionally, EFHC-1::GFP is expressed in the distal regions of sex-specific dopaminergic ray neurons in the male tail that promote efficient mating (Correa et al., 2012) **(Figure 3.1B)**. Interestingly, in ciliated OLQ and dopaminergic neurons, EFHC-1 localisation is enriched both in cilia, alongside the intraflagellar transport protein XBX-1 which marks basal bodies and the axoneme **(Figure 3.1C)**, and presynaptic regions, partially overlapping

with the synaptic protein, synaptobrevin (SNB-1) **(Figure 3.1D)**; this suggests that EFHC-1 may play important roles in both sensation and regulation of neuronal output.

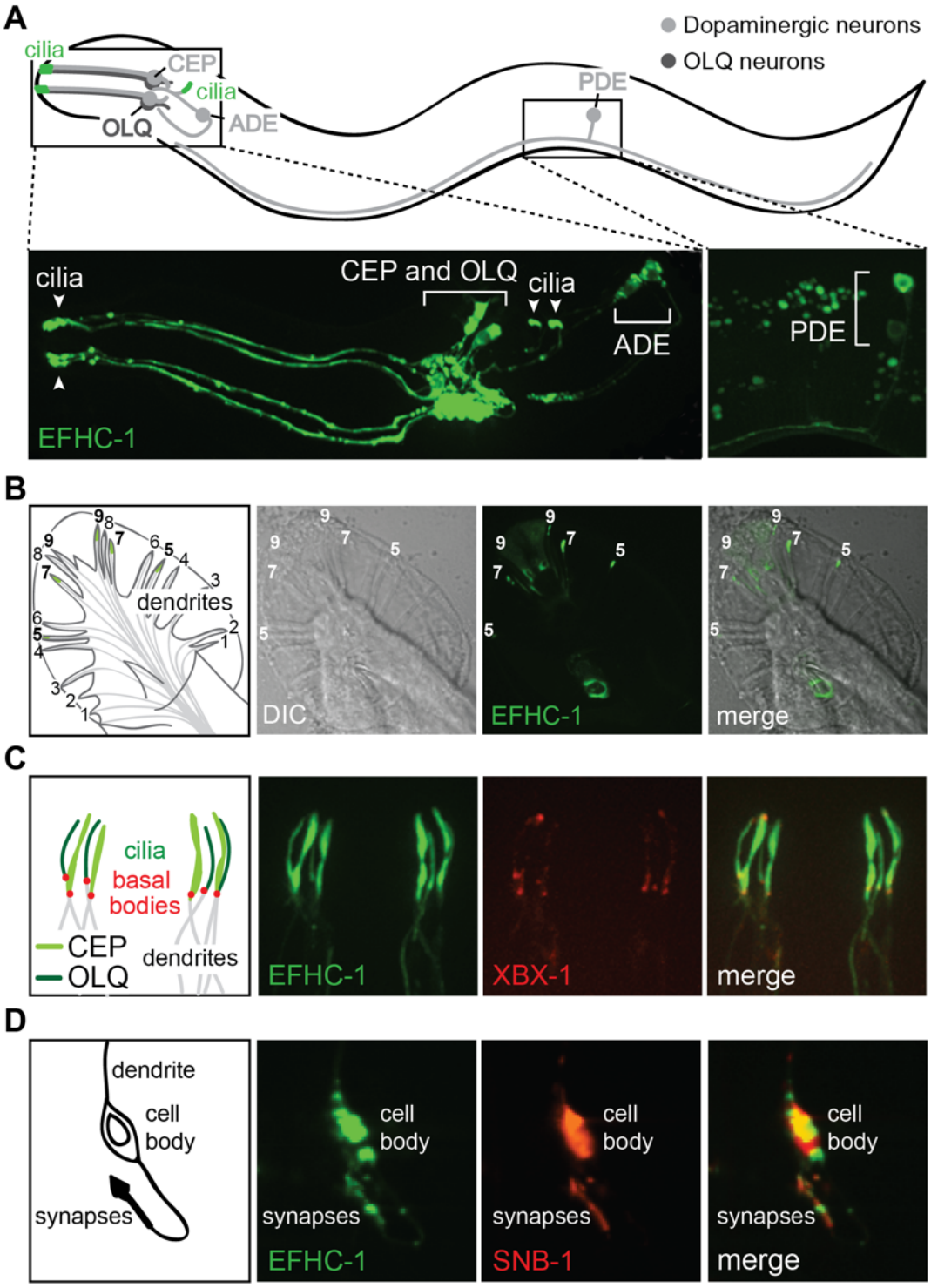

**Figure 3.1 EFHC-1 localises to cilia and synapses of a subset of mechanosensory neurons.**

**(A)** EFHC-1::GFP is expressed in all classes of dopaminergic neurons shared by both hermaphrodites and males: CEP, ADE and PDE, as well as in the the mechanosensory OLQ neurons. Localisation is enriched in cilia (arrowheads). **(B)** EFHC-1::GFP is also expressed in dopaminergic ray RnA neurons in the male tail (rays 5, 7 and 9) distal to dendrites. **(C)** In CEP cilia, EFHC-1::GFP localisation surrounds the axoneme marked by the intraflagellar transport protein XBX-1::tdTomato. **(D)** EFHC-1::GFP also localises to synaptic regions in CEP neurons in close proximity to the synaptic protein, SNB-1::tdTomato.

The OLQ neuron, along with ASH and FLP, is required for reversal upon light touch to the nose (Kaplan and Horvitz, 1993). In addition, OLQ functions, in cooperation with IL1, to mediate an aversive head withdrawal response upon nose touch, the rate and bending angle of spontaneous foraging (side-to-side head movements), and the suppression of foraging upon nose touch or anterior touch to the body (Hart et al., 1995). In contrast, dopaminergic neurons (CEP, ADE and PDE) modulate behaviours based on food availability (Ezcurra et al., 2011; Kindt et al., 2007b; Sawin et al., 2000) by mechanically activating in response to food (bacteria) and releasing dopamine. In *C. elegans,* dopamine impacts several behaviours, including inhibition of locomotion and egg laying (Schafer and Kenyon, 1995), the basal slowing response, a behaviour where animals slow their locomotion in the presence of food (Sawin et al., 2000), and a foraging strategy that controls turning frequency to maximize the time spent in food-rich areas called area-restricted search (Hills et al., 2004). In addition, dopamine modulates a form of non-associative learning called tap habituation where animals learn to ignore mechanical stimuli (Rankin et al., 1990; Sanyal et al., 2004). Furthermore, excessive dopamine signalling results in swimming-induced paralysis (SWIP) (McDonald et al., 2007), a behaviour that shows parallels to the paralysis of animals in the presence of high concentrations of exogenous dopamine (Schafer and Kenyon, 1995).

EFHC-1 localisation is enriched in cilia of both OLQ and dopaminergic neurons. OLQ cilia resemble conventional cilia at their transition zones, where 9 outer microtubule doublets are attached to the ciliary membrane through ciliary Y-links, but unlike conventional cilia, these doublet microtubules appear filled with four of the nine attached to each other in a square composed of thick cross-links and then to the center of the axoneme with fine radial arms (Perkins et al., 1986). Despite these unique features, OLQ cilia display a morphologically rod-like appearance. The intraflagellar transport

protein XBX-1::tdTomato driven by *efhc-1*'s promoter was used to mark the ciliary axonemes of cells expressing EFHC-1, where it shows localisation both along the axonemal length as well as the ciliary base (basal body) **(Figure 3.1C)**. It has previously been reported that EFHC1 in *Chlamydomonas* (Rib72) localises along the entire ciliary length except for at the transition zone (reported as the ciliary base) (Ikeda et al., 2003). We also find that EFHC-1::GFP localises uniformly along the length of OLQ cilia and is excluded from the base of cilia **(Figure 3.1C)**, but using XBX-1::tdTomato to mark the cilia revealed that EFHC-1::GFP is not excluded from the transition zone but instead from the basal body.

The axonemes of CEP cilia also show 9 outer microtubule doublets at their base, but interestingly the middle segment contains approximately 5 doublet microtubules. The distal region is enlarged to accommodate numerous (>30) singlet microtubules that do not appear to arise from the axonemal doublet microtubules (Doroquez et al., 2014; Perkins et al., 1986). These singlets make fine attachments to each other and the ciliary membrane and are surrounded by amorphous, tubule-associated material commonly seen in mechanosensory neurons/cilia. In addition, unlike the axonemal doublet microtubules made up of 13 (A-tubule) or 10 (B-tubule) protofilaments, they are composed of 14-15 protofilaments (Doroquez et al., 2014; Perkins et al., 1986), also commonly found in non-ciliated mechanosensory (touch receptor neuron or TRN) *C. elegans* cells. EFHC-1::GFP appears to be enriched at the distal region of CEP cilia where it appears to envelop XBX-1::tdTomato localisation **(Figure 3.1C)**. This suggests that while XBX-1::tdTomato only marks the ciliary axoneme, EFHC-1 may also associate with the singlet microtubules, microtubule attachments or the ciliary membrane in the distal region of the cilium where it may play important roles in anchoring microtubule attachments or sensory molecules to appropriate positions along the axoneme to enable mechanosensation.

In addition to EFHC1's known roles at cilia, EFHC1 has also been found to function at the synapse, where loss of EFHC1 in *Drosophila* results in synaptic overgrowth and spontaneous neurotransmitter release occurs (Rossetto et al., 2011). To determine the possibility of EFHC-1 functioning at the synapse in *C. elegans,* EFHC-1::GFP localisation was compared to that of the synaptic vesicle protein, synaptobrevin

(SNB-1::tdTomato) **(Figure 3.1C)**. EFHC-1::GFP localisation shows partial overlap with that of SNB-1::tdTomato at synaptic regions, suggesting that EFHC-1 may play an important role in the regulation of neuronal output at the synapse.

In addition to EFHC-1's localisation in select hermaphrodite cilia, it localises to male dopaminergic ray neurons. Two neurons make up each male ray: RnA and RnB. RnB neurons terminate in cilia exposed to the external environment. In contrast, RnA neurons lack classic cilia, and instead have long striated rootlets and broad tips filled with material (Sulston et al., 1975) that may be analogous to the tubule-associated material of CEP cilia. In both RnA and RnB neurons, the retrograde IFT protein XBX-1::tdTomato appears to localise at the end of the dendrites where it stops in RnA neurons at the basal body but continues along the axoneme of RnB cilia **(Figure 3.2)**. Surprisingly, EFHC-1::GFP does not localise with XBX-1::tdTomato in the ciliary axoneme of RnB neurons. Instead, it localises distal to the end of dendrites of RnA neurons in rays 5, 7 an 9 that are known to be dopaminergic **(Figure 3.2)**. This distal region is where the electron-dense material resides in RnA neurons, and it is possible that since this region has not been extensively studied that it may contain singlet microtubules similar to those seen in CEP cilia with which EFHC-1 may interact. In addition, it is important to note that as in CEP cilia, EFHC-1::GFP localsation is not seen in the basal body marked by XBX-1::tdTomato.

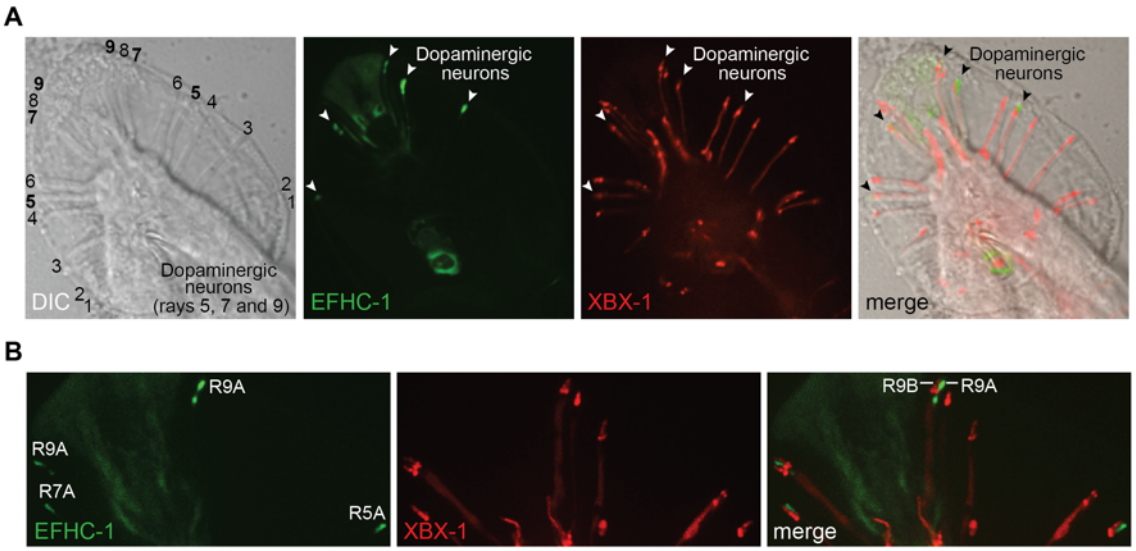

**Figure 3.2 EFHC-1 also localises to the dopaminergic ray neurons in the male tail.**

**(A)** EFHC-1::GFP localises to regions distal to the dendrites of dopaminergic ray RnA neurons in the male tail (rays 5, 7 and 9). In contrast, XBX-1::tdTomato driven in ciliated cells by the *bbs-8* promoter, that represents the ciliary axoneme, is found in all ray neurons of the male tail. **(B)** XBX-1::tdTomato only localises to the ciliary axonemes of RnB neurons but localises to dendrites and basal bodies of both RnA and RnB neurons. EFHC-1::GFP is found distal to the basal body in dopaminergic RnA neurons.

### 3.3.2. EFHC-1 modulates dopamine signalling in *C. elegans*

The localisation of EFHC-1 in dopaminergic neurons prompted the investigation of *efhc-1* mutants in dopamine-associated behaviours. In the presence of food, ciliary TRP-4 channels (orthologous to TRPN/NOMPC) localised to dopaminergic neurons are mechanically activated, resulting in the release of dopamine that modulates several behaviours through dopamine receptors (DOP-1, DOP-3 and DOP-4) on various post-synaptic cells **(Figure 3.3**, pictured are the post-synaptic touch receptor neurons**)**. Another protein required for dopamine signalling is CAT-2 (tyrosine hydroxylase), the rate-limiting enzyme for dopamine synthesis that catalyses the first step of dopamine synthesis. Dopamine release at the synapse is mediated by UNC-2, the $\alpha$ subunit of a voltage-gated calcium channel most closely related to P/Q/R/N-type voltage-gated calcium channels in vertebrates. UNC-2 is required for $Ca^{2+}$ influx at synaptic terminals upon neuronal activation that results in subsequent vesicle fusion and release of vesicular contents (Richmond et al., 2001; Schafer and Kenyon, 1995). Finally, DAT-1 is a plasma membrane dopamine transporter that is responsible for the reuptake of dopamine into presynaptic neurons and consequently prevents excessive dopamine signalling **(Figure 3.3)**.

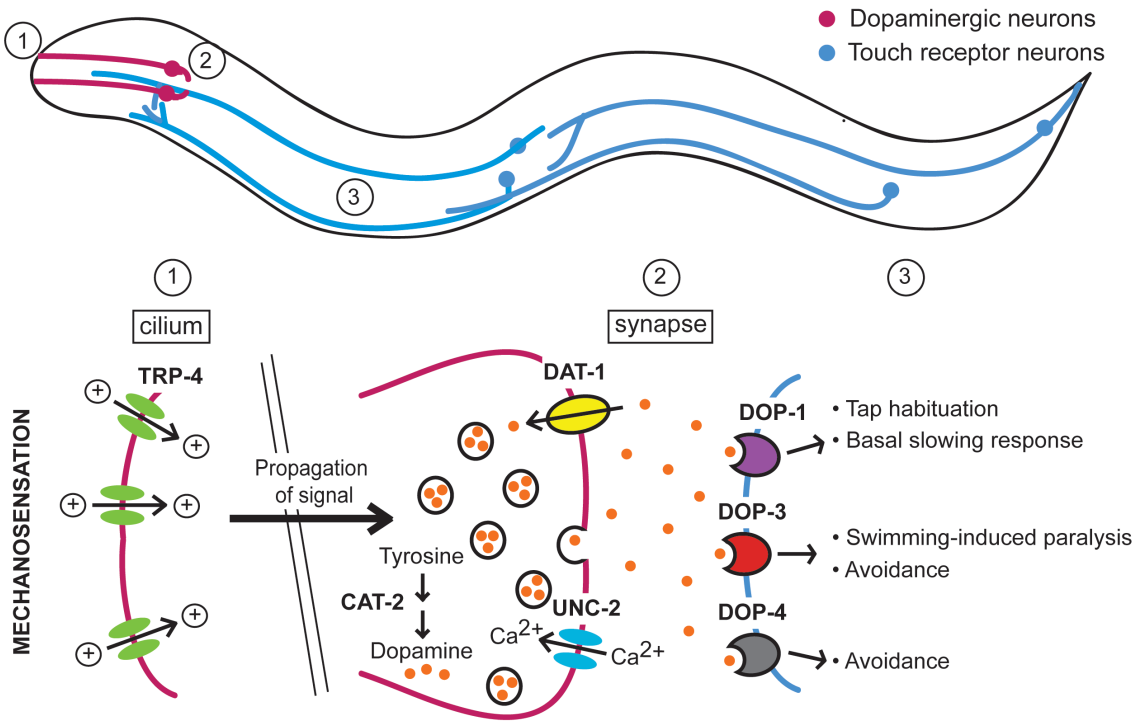


**Figure 3.3 Molecular components of dopamine signalling in *C. elegans*.**
A worm with the dopaminergic CEP neurons that project cilia into the tip of the nose in dark pink and post-synaptic touch receptor neurons in blue are depicted at the top of this image. At the cilium of these dopaminergic neurons (again shown in dark pink at the bottom, left of this image). TRP-4 channels are mechanically activated in the presence of food (bacteria) (1). Mechanosensation results in the propagation of neuronal activation along the neuron until it reaches the synapse of the dopaminergic neurons (2). In the dopaminergic neurons, CAT-2 (tyrosine hydroxylase) is required for the synthesis of dopamine from tyrosine. UNC-2 is crucial at the synapse to regulate vesicular release of dopamine. When neuronal activation reaches the synapse, the voltage-gated UNC-2 calcium channels are activated, leading to a rise in calcium and a consequent fusion and release of vesicles containing dopamine. DAT-1 is also required at the synapse to re-uptake dopamine and allow for a cessation of signalling. Various dopamine receptors are present on post-synaptic cells (3), such as the touch receptor neurons again depicted in blue, to mediate various behaviours based on food availability, including tap habituation, the basal slowing response, swimming-induced paralysis and avoidance.

To determine if *efhc-1* mutants show defects in dopamine signalling, we first investigated the basal slowing response, a dopamine-regulated behaviour where wild-type animals slow in the presence of food. Impairing dopamine signalling by disrupting either CAT-2 or TRP-4 prevents slowing in the presence of food (Sawin et al., 2000) **(Figure 3.4)**. In contrast, loss-of-function *efhc-1(gk424336)* mutants are able to slow in the presence of food **(Figure 3.4)**, suggesting that they can release dopamine in the

presence of food, but does not rule out the possibility of elevated dopamine signalling in *efhc-1* mutants.

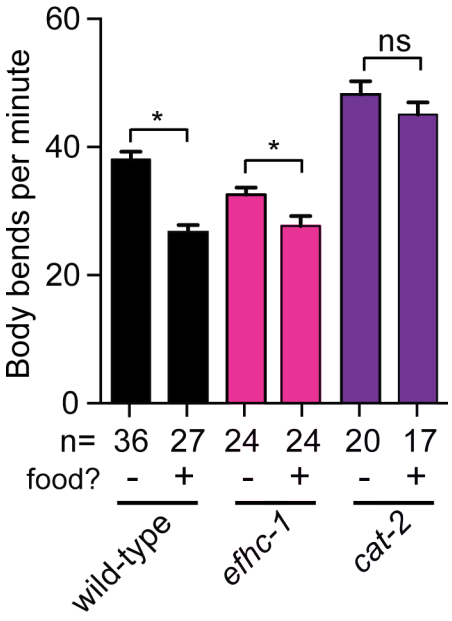


**Figure 3.4 EFHC-1 is not required for the dopamine-dependent basal slowing response.**

Wild-type animals are able to slow their locomotion in the presence of food (bacteria – HB101). In contrast, *cat-2* mutants that have diminished dopamine signalling are unable to slow in the presence of food. Like wild-type animals, *efhc-1* mutants are able to slow in the presence of food, suggesting that they are able to release dopamine in the presence of food. Bars represent the mean number or body bends counted per strain and error bars represent SEM.

To investigate the possibility that dopamine signalling may be increased in *efhc-1* mutants, we assessed their behaviour in tap habituation, a form of non-associative learning and memory modulated by dopamine (Kindt et al., 2007b; Rankin and Broster, 1992; Rankin et al., 1990; Sanyal et al., 2004) **(Figure 3.5)**. When animals experience a non-localised tap stimulus to their petri dishes, the touch receptor neurons are mechanically stimulated, and worms execute an escape response, most often seen as reversals (Rankin et al., 1990). The proportion of animals responding decreases with repeated taps (Rankin et al., 1990), and dopamine modulates this habituation (Kindt et al., 2007b). Both the proportion of animals responding and the distance travelled in response decrease, or habituate, with repeated taps (Rankin et al., 1990). Interestingly, only habituation of the proportion of worms responding is dependent on dopamine (Sanyal et al., 2004).

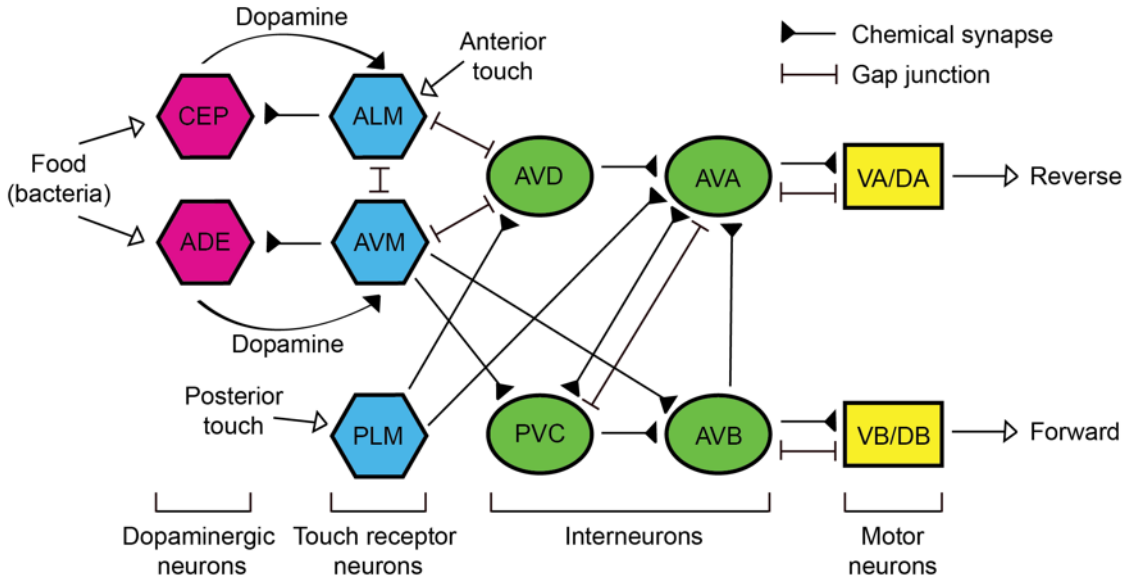


**Figure 3.5 Neural circuit outlining how dopaminergic neurons influence touch receptor neuron activity.**

Food (bacteria) mechanically stimulates the dopaminergic CEP and ADE neurons to release dopamine. This dopamine acts extra-synaptically to modulate the sensitivity of the anterior touch receptor neurons (ALM and AVM) to touch. ALM and AVM neurons are activated by anterior touch to promote backward movement, while the posterior touch receptor neuron PLM is activated by posterior touch to promote forward movement.

Decreased dopamine signalling in *cat-2* mutants results in fast habituation, while increased dopamine signalling in mutants that lack the dopamine re-uptake transporter DAT-1 results in slow habituation (Kindt et al., 2007b; Sanyal et al., 2004) **(Figure 3.6A)**. Habituation in *efhc-1* mutants closely resembles that of *dat-1* mutants, suggesting that abrogating EFHC-1 increases dopamine signalling **(Figure 3.6A)**. A second *efhc-1* allele (*tm6235*) lacking most of the gene also presents a slow habituation phenotype **(Figure 3.6B)**, confirming that slow habituation is a result of EFHC-1 dysfunction. Furthermore, introducing by genetic crossing the *cat-2* mutation into the *efhc-1* strain completely abolishes the slow habituation phenotype **(Figure 3.6C)**, indicating that the phenotype stems from increased dopamine signalling.

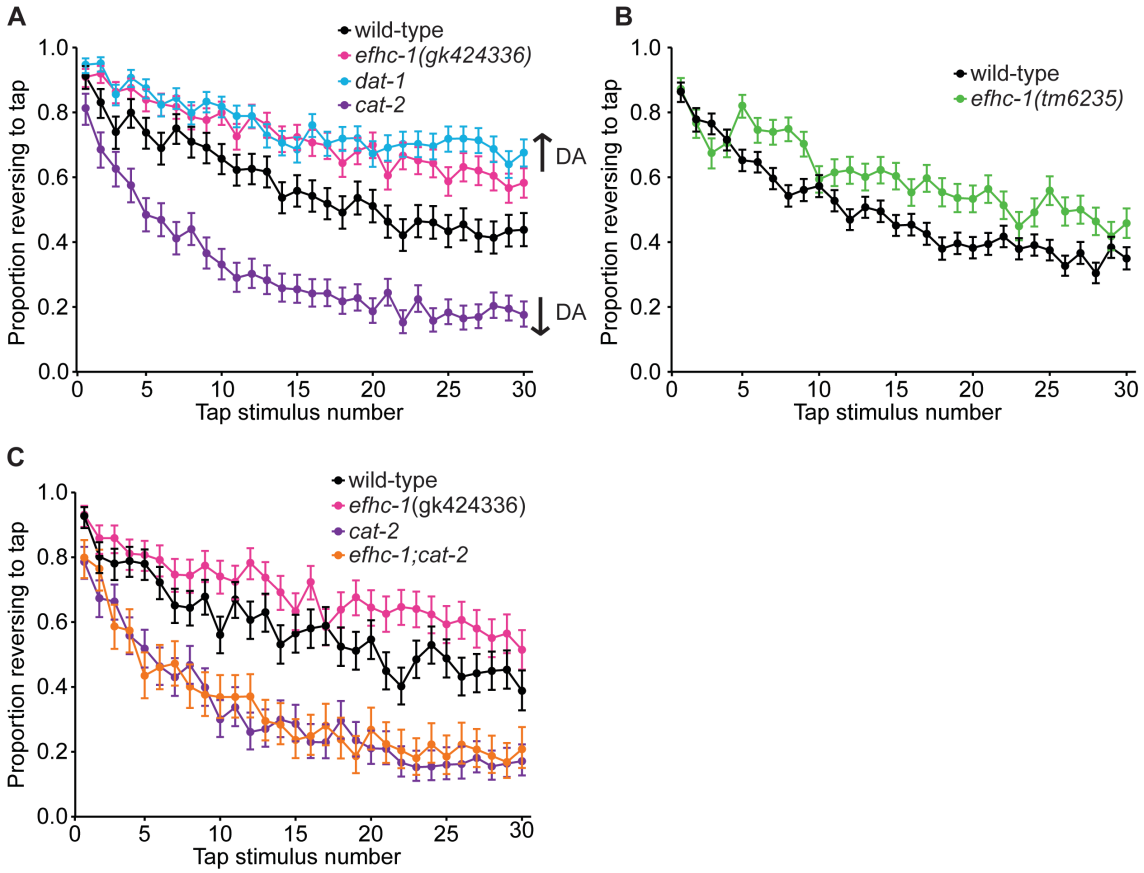


**Figure 3.6 EFHC-1 influences habituation to a mechanical stimulus by modulating dopamine signalling.**

**(A)** In the presence of food, *efhc-1* mutants habituate slower than wild-type animals and similar to *dat-1* mutants that have increased dopamine signalling (DA: dopamine). At each tap, the points represent the number of worms reversing over the total number of worms tracked per strain, and the error bars represent the binomial confidence intervals. Binomial logistic regression followed by Tukey's HSD (honest significant difference) test was used to determine significance of the habituated level (proportion reversing at tap 30) for each pair of strains. All strains are statistically different from each other. **(B)** A second allele of *efhc-1* leads to a similar slow habituation phenotype that is statistically different from wild-type. **(C)** The habituation phenotype seen in *efhc-1* mutants is abolished in *efhc-1;cat-2* double mutants, suggesting that the effect is dependent on dopamine. All strains are statistically different than each other except for *cat-1* and *efhc-1;cat-2.*

To further investigate the dopamine signalling defect in *efhc-1* mutants, we analysed their behaviour in the absence of food. Tap habituation represents a behaviour that is modulated by food, and the slower habituation seen in the presence of food is due to the stimulated release of dopamine by the mechanosensation of food (Kindt et al., 2007b). As expected, *efhc-1* mutants also show slow habituation compared to wild-type animals in the absence of food, suggesting that *efhc-1* mutants are able to release

dopamine even in the absence of food **(Figure 3.7A)**. Interestingly, *dat-1* mutants show even slower habituation compared to *efhc-1* mutants. Similarly, *efhc-1* mutants off food mimic the habituation phenotype of wild-type animals on food, while *dat-1* mutants habituate slightly slower than *efhc-1* mutants off food **(Figure 3.7B)**, suggesting that while both mutants increase dopamine signalling, they likely increase dopamine signalling in different ways and to different extents. We further confirm this possibility by exploiting the dopamine-dependent swimming-induced paralysis (SWIP) phenotype seen in *dat-1* mutants, which is attributed to excessive dopamine signalling (McDonald et al., 2007). While most wild-type animals continue swimming at 10 minutes, most *dat-1* animals are paralysed **(Figure 3.8A)** and show an average thrashing frequency consistently lower than wild-type animals **(Figure 3.8B)**. Interestingly, both *efhc-1* alleles show intermediate levels of paralysis at 10 minutes compared to wild-type animals and *dat-1* mutants **(Figure 3.8A)** and corresponding intermediate thrashing frequencies **(Figure 3.8B)**. Together, our data are consistent with *efhc-1* mutants having increased dopamine signalling compared to wild-type animals, but less than *dat-1* mutants.

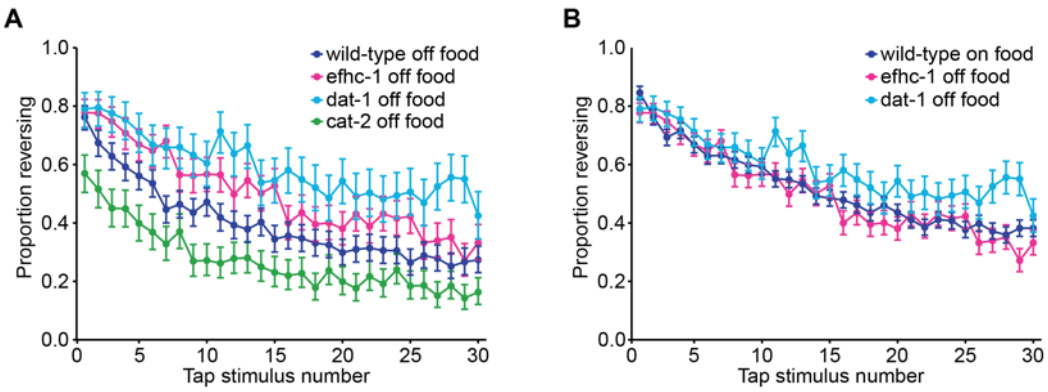


**Figure 3.7 Loss of EFHC-1 results in increased dopamine signalling even in the absence of food.**

**(A)** In the absence of food, *efhc-1* mutants also habituate slower than wild-type animals but faster than *dat-1* mutants that have increased dopamine signalling due to defects in dopamine re-uptake. At each tap, the points represent the number of worms reversing over the total number of worms tracked per strain, and the error bars represent the binomial confidence intervals. Binomial logistic regression followed by Tukey's HSD (honest significant difference) test was used to determine significance of the habituated level (proportion reversing at tap 30) for each pair of strains. All strains are statistically different from each other. **(B)** *Efhc-1* mutants off food mimic the habituation seen in wild-type animals on food. All strains are statistically different except for wild-type animals on food and *efhc-1* mutants off food.

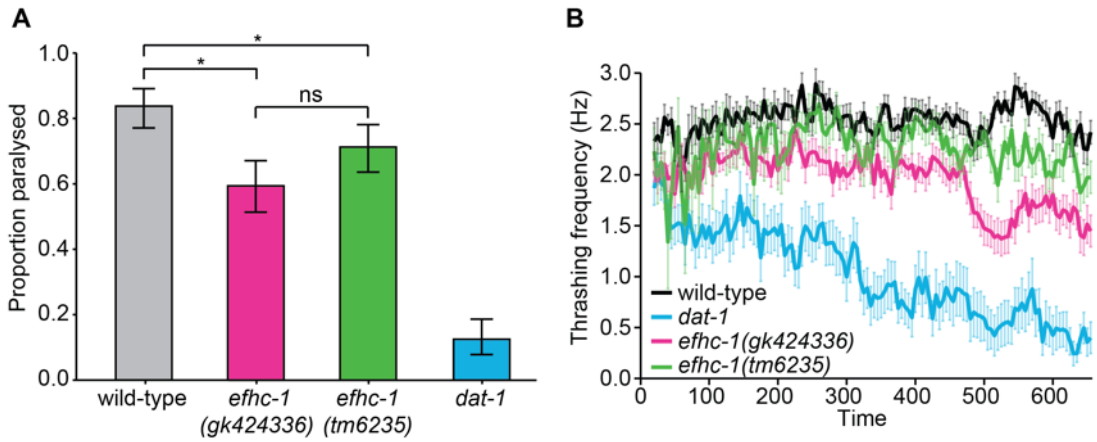


**Figure 3.8 EFHC-1 influences also impacts the dopamine-dependent swimming-induced paralysis (SWIP) phenotype.**

**(A)** *efhc-1* mutants also show defects in the dopamine-dependent swimming-induced paralysis phenotype with an intermediate level of paralysis after 10 minutes compared to wild-type and *dat-1* mutants. Each bar represents the number of paralysed worms over the total number of worms per strain, and the error bars represent the binomial confidence intervals. Binomial logistic regression followed by Tukey's HSD (honest significant difference) test was used to determine significance for each pair of strains. All strains are statistically different than each other except for the two *efhc-1* strains. **(B)** An automated swimming-induced paralysis (SWIP) assay shows intermediate thrashing frequencies for the two *efhc-1* compared to *dat-1* and wild-type animals. Each point represents the mean of thrashes counted over 5 seconds (divided by 5), and the error bars represent SEM.

### 3.3.3. *C. elegans* EFHC1 is required for mechanosensation in dopaminergic CEP ciliated neurons

A possible explanation for the increased dopamine signalling in *efhc-1* mutants is increased ciliary activation, even in the absence of food. To directly interrogate mechanosensory activation in *efhc-1* mutants, we used a genetically encoded calcium indicator that is specifically expressed in dopaminergic neurons (Kindt et al., 2007b). Two different mechanical stimuli to the nose were applied: a gentle buzz, designed to mimic the presence of food, and a stronger stimulus (press). Wild-type animals respond to each stimulus ~50% of the time, due to technical challenges associated with recording calcium transients at the cell body that can move during mechanical stimulation **(Figure 3.9A)**. In contrast, *efhc-1(gk424336)* mutants rarely respond upon gentle stimulation but respond at wild-type levels to the stronger stimulation **(Figure 3.9A)**. Interestingly, when *efhc-1* mutants exhibit calcium responses to either stimulus, they are of a comparable amplitude and shape as wild-type responses **(Figure 3.9b** and **Figure 3.10)**. This

behaviour is remarkably similar to that seen in animals lacking the cilium-localised mechanosensitive TRP-4 channel **(Figure 3.9B** and **Figure 3.10)**, which is required for food sensation (Kang et al., 2010; Kindt et al., 2007b). This suggests that like TRP-4, EFHC-1 has a specific role in mediating the likelihood of mechanosensory transduction upon gentle stimulation like that seen when an animal encounters food.

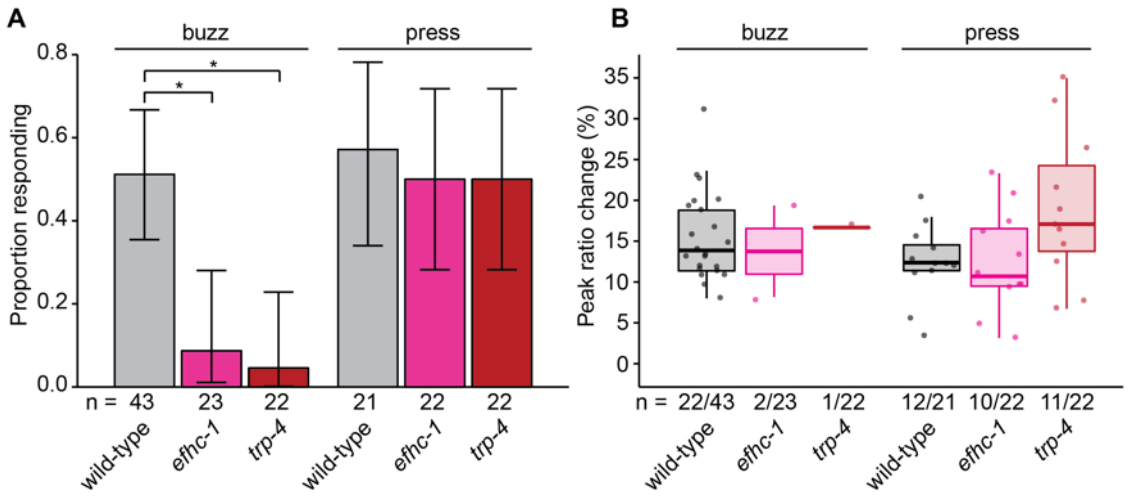


**Figure 3.9 Like TRP-4, EFHC-1 is required for mechanosensation in non-motile CEP cilia.**

**(A)** Loss of EFHC-1 or TRP-4 impairs activation of CEP neurons upon gentle mechanical stimulation (buzz) resulting in less animals responding to the stimulus. In contrast, *efhc-1* or *trp-4* mutants are able to respond to stronger stimulation (press). In this panel, n represents the total number of animals assessed. Each bar represents the number of worms responding to mechanical stimulation over the total number of worms assessed per strain, and the error bars represent the binomial confidence intervals. Binomial logistic regression followed by Tukey's HSD (honest significant difference) test was used to determine significance for each pair of strains. Differences between all strains subjected the the press stimulus are not significant, but differences between wild-type and *efhc-1* or *trp-4* mutants are significant. **(B)** The peak ratio change (%) representing the amplitude of the neuronal response is similar between strains for animals responding to each stimulus. In this panel, n represents the number of animals responding to the stimulus over the total number of animals assessed.

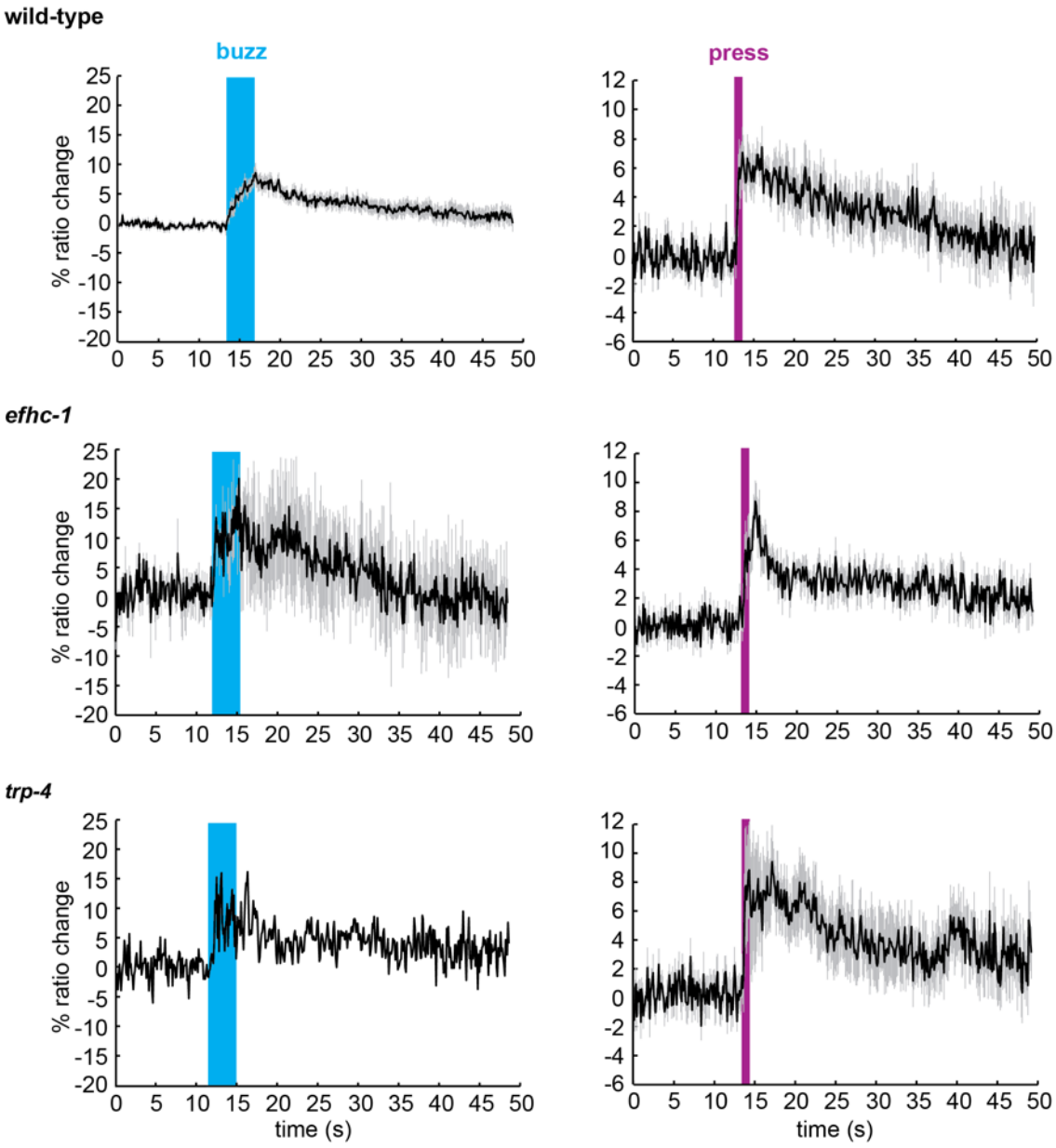


**Figure 3.10 Animals that respond to mechanical stimuli in the CEP neurons show similar patterns of calcium changes independent of strain.**
Average traces of calcium responses in CEP neurons upon the mechanical buzz or press stimuli (black), and SEM values associated with the calcium traces (grey). The duration of the mechanical stimulus is shown in blue (buzz) or purple (press). Here, % ratio change represents the YFP/CFP ratio change of the cameleon calcium indicator.

Interestingly, mechanosensory transduction is not impaired in *efhc-1* mutants expressing a genetically encoded calcium indicator in the OLQ neurons driven by the *ocr-4* promoter **(Figure 3.11A-B)**, indicating a specific mechanosensory function for EFHC-1 in CEP neurons. Similarly, no defects in OLQ-mediated behaviours were detected **(Figure 3.11C-E)**. Specifically, worms were individually tracked using the single-worm tracker to extract subtle worm movements mediated in part by the OLQ neurons, including foraging behaviour (side-to-side head movements) and the speed of foraging. No defects in foraging speed or foraging amplitude were observed in *efhc-1* mutants compared to wild-type animals **(Figure 3.11C-D)**. Similarly, *efhc-1* mutants show a wild-type ability to suppress foraging movements in the presence of a mechanosensory stimulus, a behaviour that is abrogated in mutants (such as *tdc-1* animals) that affect OLQ function (Alkema et al., 2005) **(Figure 3.11E)**.

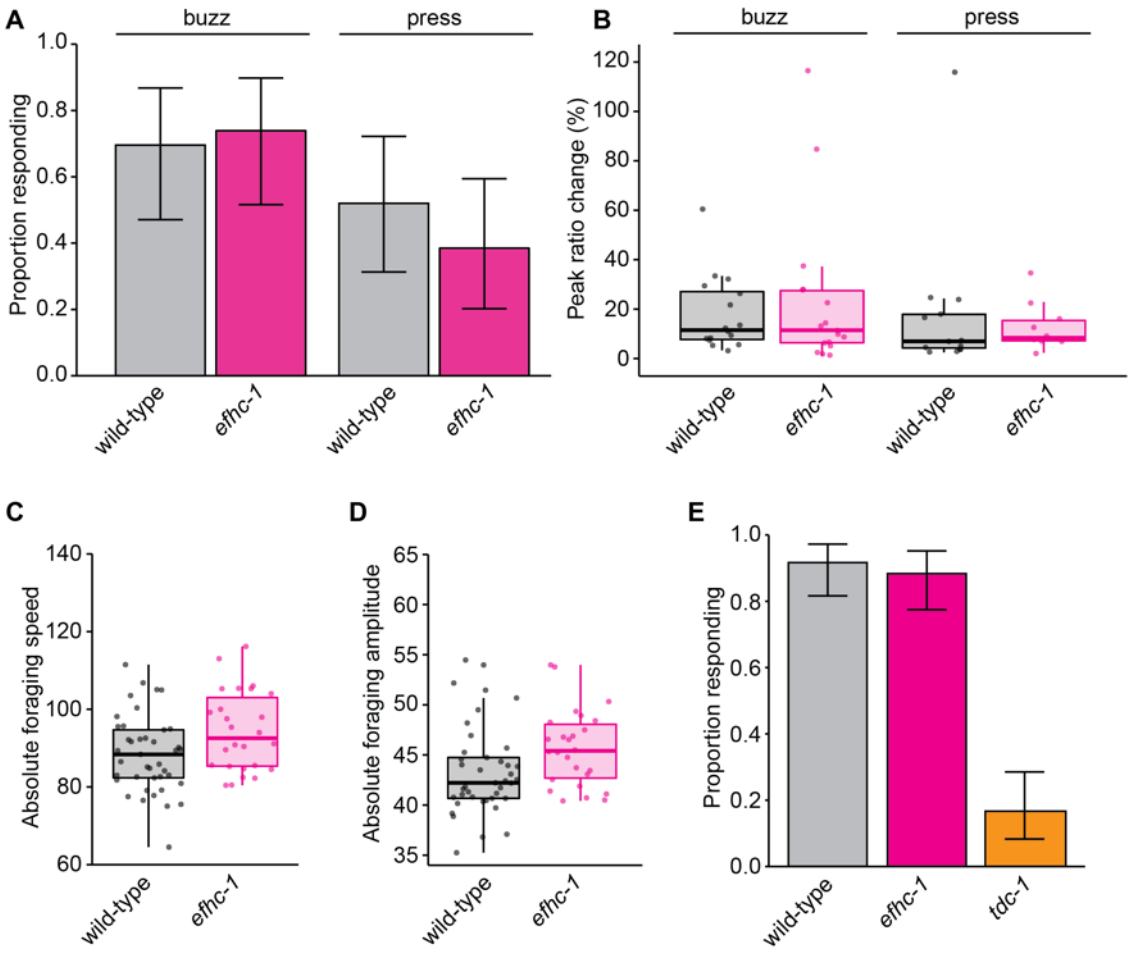

**Figure 3.11 *efhc-1* mutants show no defects in OLQ-related mechanosensory or behavioural responses.**

**(A)** Loss of EFHC-1 has no effect on the activation of OLQ neurons upon gentle mechanical stimulation (buzz) or a stronger stimulation (press). In this panel, n represents the total number of animals assessed. Each bar represents the number of worms responding to mechanical stimulation over the total number of worms assessed per strain, and the error bars represent the binomial confidence intervals. Binomial logistic regression followed by Tukey's HSD (honest significant difference) test was used to determine significance for each pair of strains. Differences between all strains are not significant. **(B)** The peak ratio change (%) representing the amplitude of the neuronal response is similar between strains for animals responding to each stimulus. In this panel, n represents the number of animals responding to the stimulus over the total number of animals assessed. **(C)** *efhc-1* mutants showed similar foraging speeds and **(D)** foraging amplitudes, two behaviours mediated by the OLQ neurons. Here the absolute values of the forward foraging speed/amplitude are depicted. **(E)** EFHC-1 is also not involved in the suppression of foraging, a behaviour in which worms subjected to mechanical stimulation of the anterior body suppress their foraging movements. OLQ neurons play a role in regulating this behaviour and mutants like *tmc-1* are unable to suppress their foraging movements when reversing. Each bar represents the number of worms that suppressed foraging over the total number of worms assessed per strain, and the error bars represent the binomial confidence intervals. Binomial logistic regression followed by Tukey's HSD (honest significant difference) test was used to determine significance for each pair of strains, and *efhc-1* mutants are not statistically different than wild-type animals.

Given the likely hypothesis that EFHC-1, as a protofilament ribbon protein, helps to anchor/arrange/regulate ciliary proteins along the ciliary axoneme in motile cilia (Ikeda et al., 2003; Linck and Norrander, 2003), it is possible that it has been adapted in non-motile cilia to anchor sensory proteins, such as TRP-4. We first confirmed by transmission electron microscopy (TEM) that 'conventional' cilia not harbouring EFHC-1::GFP are structurally normal in *efhc-1* mutants, displaying 9 outer doublet microtubules that become singlets in more distal regions **(Figure 3.12)**. Interestingly, EFHC-1-containing CEP and OLQ cilia—which have supernumerary singlet microtubules interspersed with tubule-associated material or unique arrangement of doublets in their distal regions, respectively—also appear structurally normal **(Figures 3.13A** and **3.13C)**. Hence, EFHC-1 does not play an essential role in specifying or maintaining non-motile cilia ultrastructure in a metazoan. Furthermore, TRP-4::YFP localisation along the axoneme of CEP cilia is retained in *efhc-1* mutants **(Figure 3.13B)**, suggesting that in the absence of EFHC-1, ciliary localisation of TRP-4 still occurs, but its function might be perturbed. For example, EFHC-1 may be required for the regulation or anchoring of TRP-4 channels or other signalling molecules required for mechanosensory transduction.

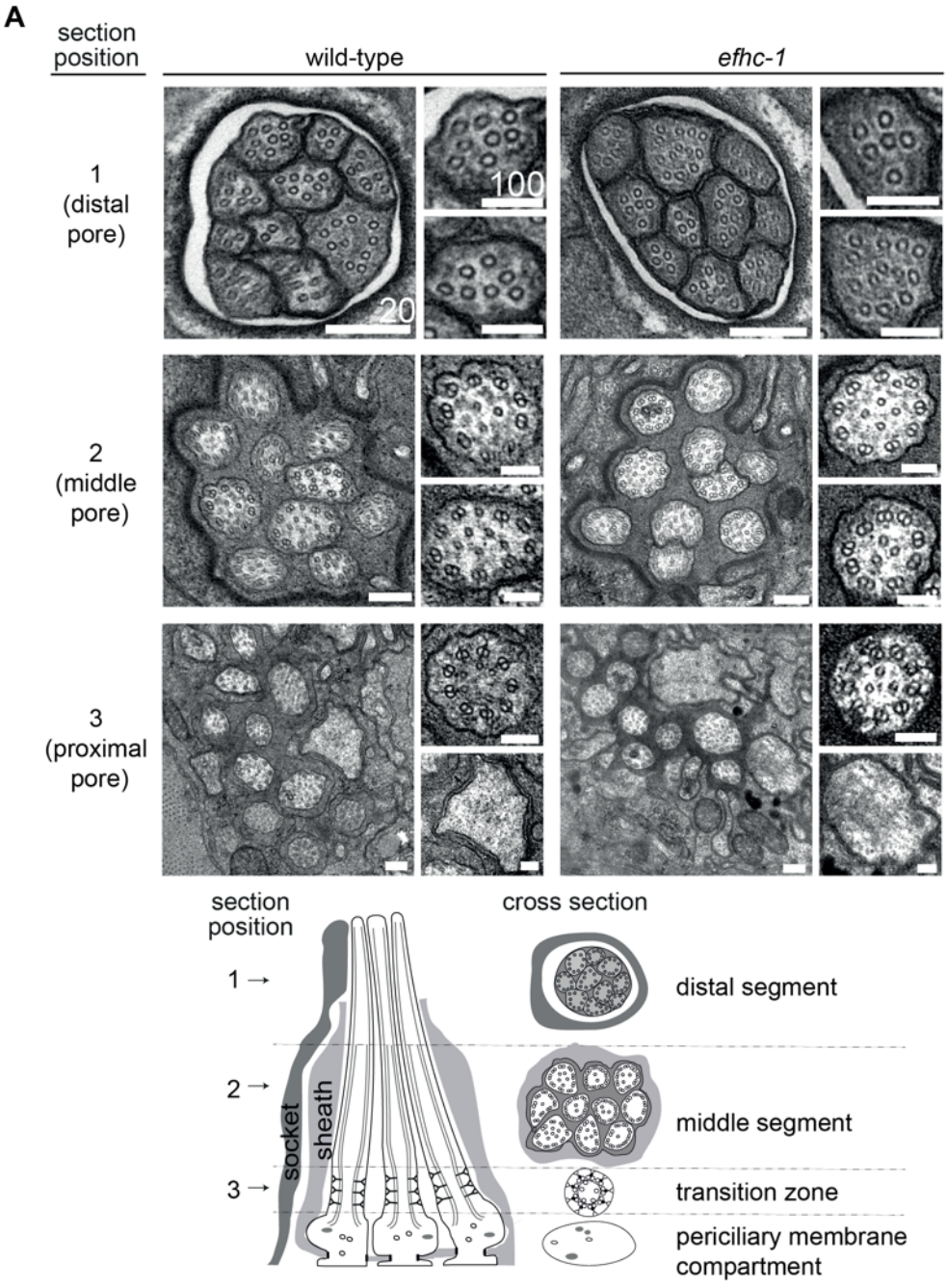
A
section position
wild-type
efhc-1
1 (distal pore)
2 (middle pore)
3 (proximal pore)
100
20
section position
cross section
1 →
2 →
3 →
socket
sheath
distal segment
middle segment
transition zone
periciliary membrane compartment
B
wild-type
daf-19;daf-12
CEP cilia
disrupted cilia
EFHC-1::GFP

**Figure 3.12 General ciliary structure is retained in *efhc-1* mutants and EFHC-1::GFP is expressed in the absence of the conventional ciliary transcription factor, DAF-19.**

**(A)** Transmission electron microscopy (TEM) serial cross-section images of amphid channel cilia in wild-type animals and *efhc-1* mutants shows that axonemal structure of conventional cilia is unaffected in *efhc-1* mutants. Each amphid channel contains 10 cilia composed of singlet microtubules in the distal pore, doublet microtubules and inner singlet microtubules in the middle pore and a transition zone with Y-link connectors between the microtubules and the membrane in the proximal pore. Scale bars: 200 nm (low-magnification images); 100 nm (high-magnification images). **(B)** While CEP cilia are disrupted in the absence of the ciliary DAF-19 transcription factor, EFHC-1::GFP is still expressed.

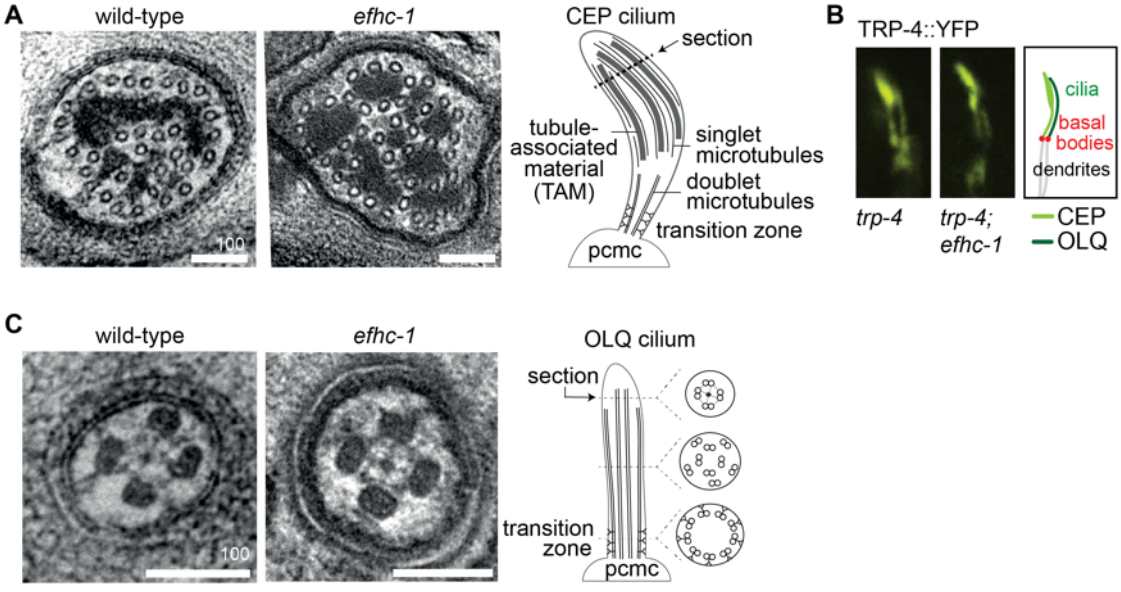


**Figure 3.13 Axonemal structure of CEP and OLQ cilia appears wild-type in *efhc-1* mutants.**

**(A)** Transmission electron microscopy (TEM) serial cross-section image of CEP cilia at the location where wild-type axonemal structure consists of many microtubule singlets interspersed with tubule-associated material. *efhc-1* mutants show no structural defects. **(B)** The mechanosensory channel, TRP-4, appears to localise to both CEP and OLQ cilia, and this localisation is unaffected in *efhc-1* mutants. **(C)** Transmission electron microscopy (TEM) serial cross-section image of OLQ cilia at the location where wild-type axonemal structure is composed of four doublet microtubules with a filled appearance connected to each other by thick cross bridges and to a central hub *via* fine radial arms. OLQ ciliary structure remains intact in *efhc-1* mutants.

In humans, EFHC1 is composed of three DM10 domains of unknown function and a C-terminal EF-hand domain that is thought to bind calcium (Suzuki et al., 2004). In *C. elegans,* only the first two DM10 domains are conserved and the EF-hand domain is

missing, but interestingly, mutations associated with juvenile myoclonic epilepsy cluster within the first two domains, suggesting that they play important roles in epilepsy **(Figure 3.14A)**. Given EFHC1's known role as a microtubule-associated protein (MAP) (de Nijs et al., 2009a), and the strong localisation of EFHC-1::GFP to non-motile cilia of OLQ and dopaminergic neurons in *C. elegans,* we suspected that one or both of the DM10 domains is involved in ciliary localisation. To begin to assess this, we generated two truncation constructs fused in-frame to GFP **(Figure 3.14A)**, each containing one of the two DM10 domains. Wild-type EFHC-1::GFP specifically localises to the ciliary axonemes of both OLQ and CEP neurons. Interestingly, while the truncation construct containing the second DM10 domain (fragment 2) shows specific ciliary localisation similar to that seen for the wild-type construct, the truncation construct containing only the first DM10 domain (fragment 1) shows non-specific localisation throughout all neuronal processes of OLQ and CEP neurons, and it is unclear if localisation is enriched in cilia. From these experiments, we can conclude that the second DM10 domain is sufficient for ciliary localisation, but it is unclear if the first DM10 domain also plays a role in ciliary localisation. Surprisingly, a recent publication (Zhao et al., 2016) reported conflicting results, where they found that truncations missing the N-terminal domain were unable to localise to cilia, whereas truncations containing only the N-terminus of the protein and no DM10 domains, or truncations missing either the second or the third DM10 domain were able to localise to cilia.

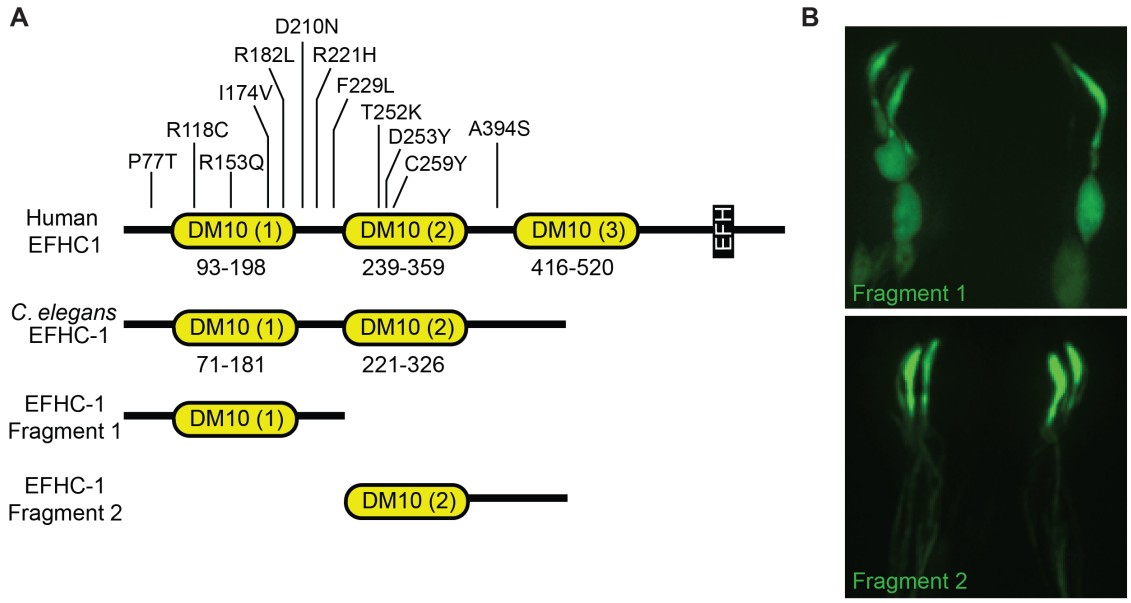


**Figure 3.14 The second DM10 domain is sufficient for ciliary localisation in *C. elegans.***

**(A)** Human EFHC1 is composed of three DM10 domains of unknown function and a C-terminal EF-hand domain that is thought to bind calcium. Mutations associated with juvenile myoclonic epilepsy cluster within the first two DM10 domains of human EFHC1. In *C. elegans,* only the first two DM10 domains are conserved. An EFHC-1 truncations containing either DM10 domain are able to localise to cilia. **(B)** Loss of the second DM10 domain in fragment 1 results in non-specific localisation, while loss of the first DM10 domain in fragment 2 does not disrupt ciliary localisation in OLQ and CEP cila.

### 3.3.4. *C. elegans* EFHC1 mediates dopamine signalling downstream of cilia

Given that mechanical activation by food is required for dopamine release and that EFHC-1 is required for mechanosensation, the increased dopamine signalling in *efhc-1* mutants is counterintuitive and suggests that EFHC-1 may regulate dopamine release at the synapse independent of ciliary-based signal transduction. To assess this, *trp-4* mutants that show fast habituation due to their inability to mechanically sense bacteria and subsequently release dopamine (Kindt et al., 2007b) **(Figure 3.15A)**, were crossed with *efhc-1* mutants. The resulting *efhc-1;trp-4* double mutants show slower habituation **(Figure 3.15A)** consistent with a rise in dopamine signalling independent of cilium-associated mechanosensation. To confirm this, *efhc-1* was combined with a *daf-19* mutant lacking cilia in dopaminergic neurons (*daf-19* encodes a transcription factor required for the expression of many ciliary genes, but not *efhc-1* - see **Figure 3.12B**).

Interestingly, *daf-19* mutants respond weakly to tap stimuli and habituate rapidly, likely due to loss or misregulation of many cilium-dependent sensory inputs required to fine-tune mechanosensation and habituation; however, *efhc-1;daf-19* double mutants show a shift toward wild-type levels of responsiveness and habituation **(Figure 3.15B)**. These data, along with the localisation of EFHC-1 at synaptic regions, are consistent with EFHC-1 preventing spontaneous release of dopamine at synapses in the absence of mechanical stimulation by food.

The release of dopamine at the synapse requires the activation of voltage-gated calcium channels at presynaptic termini, which allows for calcium influx and subsequent dopamine-bearing vesicle fusion (Fig. 2a). In humans, EFHC1 physically interacts with and modulates the alpha subunit of the R-type voltage-gated calcium channel (Suzuki et al., 2004) which is most closely related to UNC-2 in *C. elegans*. We therefore hypothesised that EFHC-1 prevents spontaneous activity of UNC-2 in *C. elegans* dopaminergic neurons, such that loss of *efhc-1* would stimulate UNC-2 activity even in the absence of mechanosensation and result in increased dopamine release. Since *unc-2* mutants are uncoordinated and cannot be tested for habituation defects, we took advantage of a gain-of-function (gf) allele that shows slow habituation compared to both wild-type animals and *efhc-1* mutants **(Figure 3.15C)**. Also, because *unc-2* expression is found in many neurons apart from the dopaminergic neurons that may modulate tap habituation, a construct was made with UNC-2(gf) under the control of the *efhc-1* promoter. Remarkably, expressing overactive UNC-2 specifically in *efhc-1*-expressing cells results in a slow habituation phenotype similar but not identical that that seen in *efhc-1* mutants, and crossing the UNC-2(gf) construct into *efhc-1* mutants did not result in slower habituation but instead phenocopied animals with UNC-2 specifically in *efhc-1*-expressing cells **(Figure 3.15C)**. Similarly, these trends were replicated in SWIP assays **(Figure 3.15D)**. Our findings provide evidence that independent of its sensory/activation role at the cilium, EFHC-1 negatively regulates UNC-2, such that loss of EFHC-1 results in maximum activation of the voltage-gated channel at the synapse.

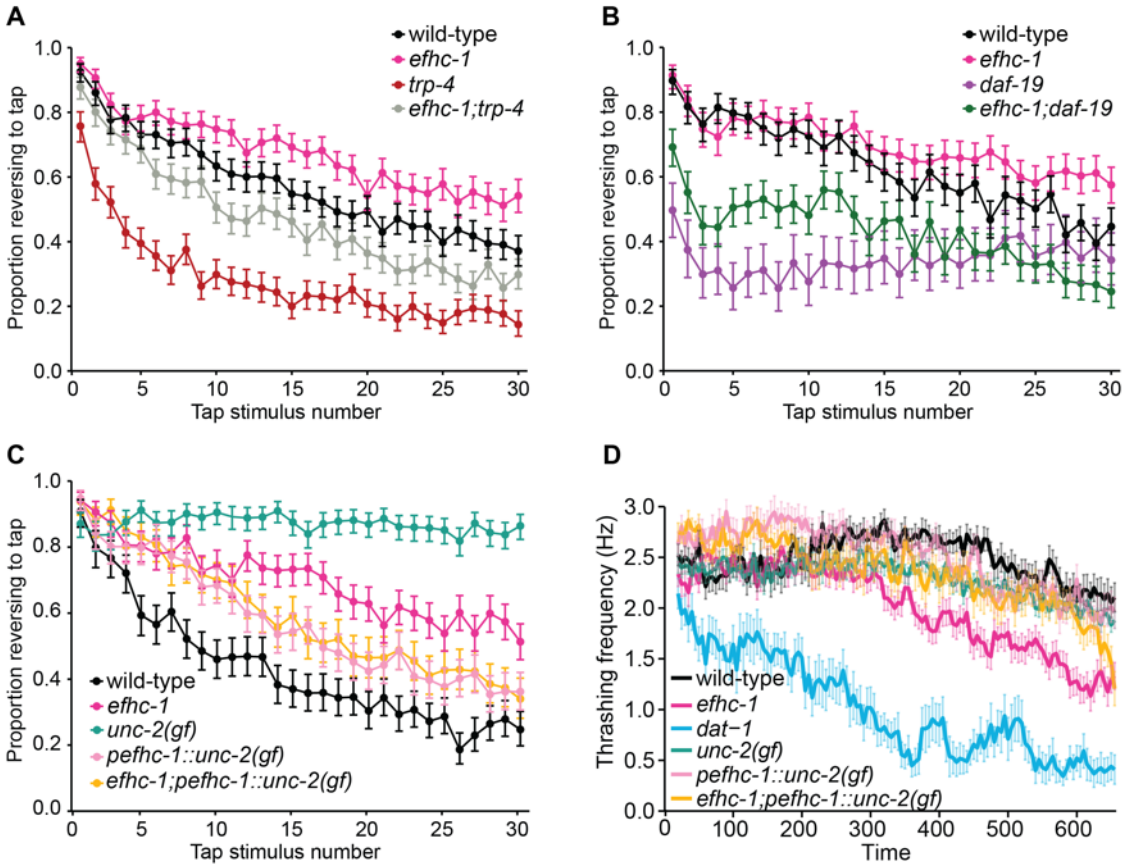


**Figure 3.15 EFHC-1 influences habituation to a mechanical stimulus by modulating dopamine signalling.**

**(A)** Double mutants of *efhc-1* and *trp-4* show intermediate habituation compared to the *trp-4* and *efhc-1* single mutants. At each tap, the points represent the number of worms reversing over the total number of worms tracked per strain, and the error bars represent the binomial confidence intervals. Binomial logistic regression followed by Tukey's HSD (honest significant difference) test was used to determine significance of the habituated level (proportion reversing at tap 30) for each pair of strains. All strains are statistically different from each other. **(B)** *efhc-1* mutants with absent cilia due to a *daf-19* mutation show intermediate habituation compared to *daf-19* and *efhc-1* single mutants. All strains are statistically different from each other. **(C)** An *unc-2(gain-of-function)* mutation driven in EFHC-1-expressing cells shows slow habituation like *efhc-1* mutants but faster than habituation seen in animals with the *unc-2(gain-of-function)* mutation expressed throughout. Furthermore, *efhc-1* mutants with the addition of an *unc-2(gain-of-function)* mutation driven in EFHC-1-expressing cells does not exacerbate the habituation phenotype. All strains are statistically different from each other except for *pefhc-1::unc-2(gf)* and *efhc-1; pefhc-1::unc-2(gf).* **(D)** *efhc-1* mutants show an intermediate thrashing frequency compared to wild-type and *dat-1* mutants. An *unc-2(gain-of-function)* mutation expressed throughout the animals, an *unc-2(gain-of-function)* mutation driven in EFHC-1-expressing cells, and *efhc-1* mutants with the addition of the *unc-2(gain-of-function)* mutation driven in EFHC-1-expressing cells all show an increased thrashing frequency compared to *efhc-1* animals but decreased compared to wild-type animals.

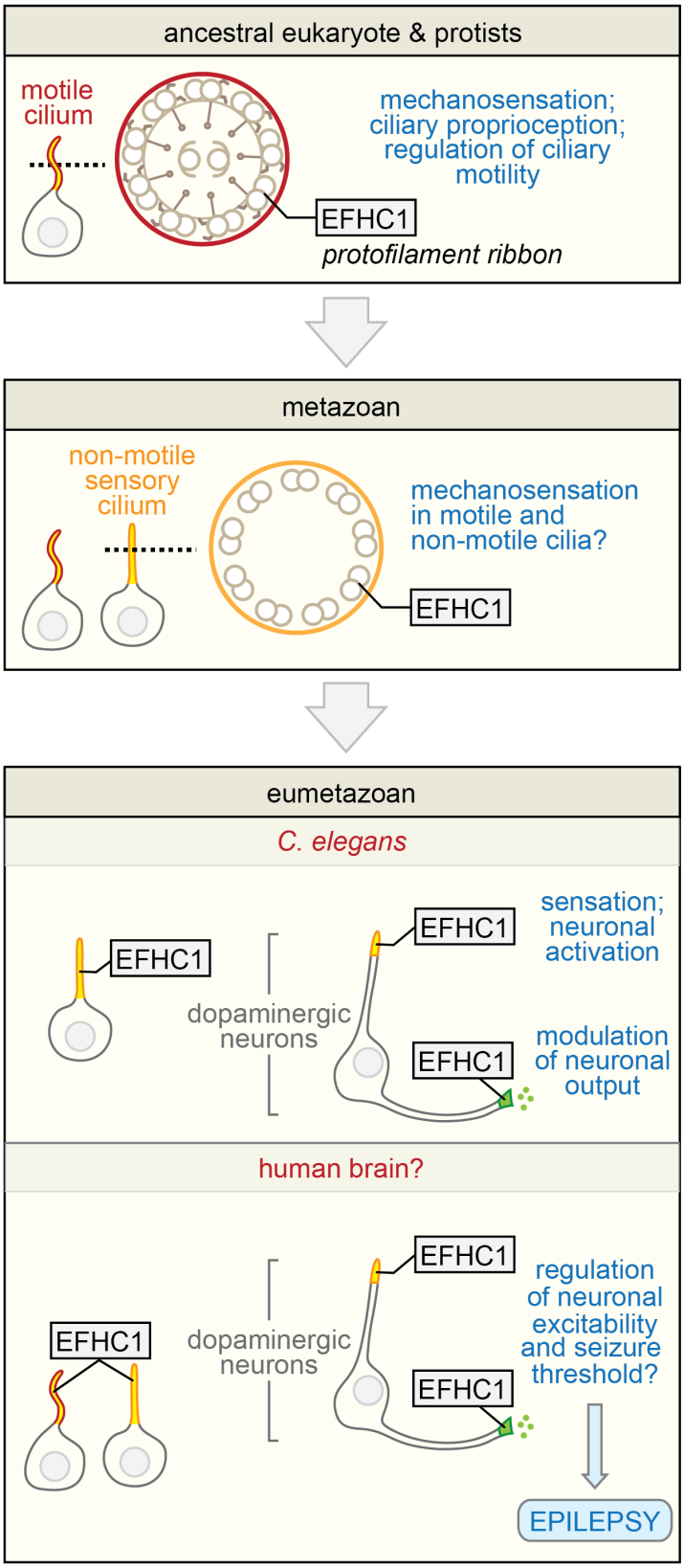
ancestral eukaryote & protists
motile cilium
mechanosensation; ciliary proprioception; regulation of ciliary motility
EFHC1
protofilament ribbon
metazoan
non-motile sensory cilium
mechanosensation in motile and non-motile cilia?
EFHC1
eumetazoan
C. elegans
EFHC1
dopaminergic neurons
EFHC1
sensation; neuronal activation
EFHC1
modulation of neuronal output
human brain?
EFHC1
dopaminergic neurons
EFHC1
regulation of neuronal excitability and seizure threshold?
EFHC1
EPILEPSY

**Figure 3.16 A proposed model for how EFHC1 was adapted to function in motile and non-motile cilia as well as at synapses.**

In ancestral eukaryotes and protists, before the appearance of non-motile cilia, EFHC1 played a role in motile cilia. It was then adapted to function in both motile and non-motile cilia in metazoans, and finally adapted to function in both non-motile cilia and at synapses in the representative eumetazoan, *C. elegans.* Its potential role in non-motile cilium-mediated sensation, and modulation of synaptic neuronal output, remains speculative for other animals, but may have implications for dopamine neuronal excitability and hence epilepsy in humans.

## 3.4. Discussion

In multicellular organisms (metazoans), cilia are often thought of as either motile or non-motile (sensory); yet, there is evidence that motile cilia possess sensory functions (Bloodgood, 2010; Shah et al., 2009). Given that the ancestral form of cilia was motile, to enable movement of ancestral eukaryotes and protists, these cilia were also required to provide sensory feedback to regulate motility, likely in the form of mechanosensation and proprioception **(Figure 3.16)**. The emergence of non-motile cilia in metazoans set the stage for exaptation (functional adaptation) of previosusly motility-associated ciliary proteins in non-motile cilia. Free from the requirement to enable ciliary motility, these proteins could be adapted to facilitate signalling functions for specialised non-motile cilia.

Although EFHC1 has been shown to be important for ciliary motility, no gross structural defects have been observed in EFHC1-deficient motile ependymal cilia of mice (Suzuki et al., 2009), raising the possibility that EFHC1 plays a role in regulating motility—for example in the mechanosensory feedback required to support normal ciliary motility. Notably, physiological evidence that both motile and non-motile cilia can support mechanosensation have been available for over 40 years (Bloodgood, 2010; Wiederhold, 1976). Our work in a representative eumetazoan (*C. elegans*) that lacks motile cilia supports this idea, where EFHC-1 has been adapted to function in a specific class of non-motile ciliated mechanosensory cells, the dopaminergic neurons (**Figure 3.16**). Consistent with previous work on motile cilia (Suzuki et al., 2009), we find that ciliary ultrastructure is unaffected in *efhc-1* mutants **(Figures 3.12 and 3.13)** but mechanosensory transduction is disrupted **(Figure 3.9)**.

Our findings suggest that EFHC1, by being an integral part of the ciliary axoneme and by potentially modulating TRP (or other types of) mechanosensitive calcium

channels, may have adapted its mechanosensation role from motile cilia to non-motile cilia. Interestingly, while known mechanosensory defects in these dopaminergic neurons result in decreased dopamine release (Kindt et al., 2007b), dopamine transmission is increased in *efhc-1* mutants **(Figures 3.6, 3.7 and 3.8)**. We find that EFHC-1 not only localises to non-motile cilia but also to synapses of dopaminergic neurons **(Figure 3.1)**, and it appears that the increased dopamine signalling phenotypes observed may be a result of increased synaptic activity **(Figure 3.15)**. Importantly, this role is also related to the modulation of a calcium channel, namely UNC-2, which is essential for dopamine neurotransmission. Together, our results show a role for EFHC-1 in fine-tuning neuronal excitation/transmission both at the cilium, the site sensory input (mechanosensation), and at the synapse, the site for sensory output that regulates the amount of neurotransmitter released.

How mutations in *EFHC1* contribute to epilepsy is poorly understood, largely due to the many neuronal/brain functions that have been attributed to EFHC1, including apoptosis, regulation of channels, cell division, neuronal migration and neurotransmitter release (de Nijs et al., 2006, 2009a; Rossetto et al., 2011; Suzuki et al., 2004). Furthermore, it remains controversial whether mutations in *EFHC1* are the primary cause of epilepsy, or instead increase susceptibility (depending on ancestral history/genetic background), considering that variants previously deemed pathogenic are found at a high frequency in individuals without epilepsy (Subaran et al., 2015). Given that EFHC1 is expressed in many brain regions that only harbour non-motile cilia (Conte et al., 2009a; Ikeda et al., 2005; Léon et al., 2010; Nijs et al., 2012; de Nijs et al., 2009b; Suzuki et al., 2004), it is possible that *EFHC1* mutations affect neuronal excitability and transmission in different subsets of neurons, including the dopaminergic neurons (**Figure 3.16**). Importantly, while dopamine receptors are known to localise to non-motile cilia in mammals (Domire et al., 2011), our study reveals a novel role for EFHC1 in modulating dopamine release. We propose that such alterations in neuronal excitability and dopamine release contribute to epilepsy in JME patients. Indeed, our work helps to strengthen the potential link between dopamine signalling and epilepsy (Bozzi and Borrelli, 2013). More generally, we suggest that our findings hint at a potentially novel mechanism by which a protein can modulate excitation thresholds in neurons through its action on ion channels at both cilia and the synapse. It will be of interest in probing

whether mammalian EFHC1—and potentially other ciliary proteins—plays such a general role in various neuronal cell types.

# Chapter 4. Conclusions and future directions

Although both motile and non-motile cilia are based on similar axonemal structures, ciliary motility requires motility-associated components that are arranged along the outer microtubule doublets at defined intervals thought to be dictated or anchored by the protofilament ribbon (pf-ribbon). Loss of pf-ribbon proteins impairs ciliary motility in several organisms, but non-motile ciliary functions for these proteins have not been previously uncovered. In this work, we wished to study the pf-ribbon-associated proteins, PCRG-1 and EFHC-1, in an organism (*C. elegans*) that lacks motile cilia to allow for the dissection of their potential sensory roles.

We find that both PCRG-1 and EFHC-1 localise to a small subset of non-motile ciliated neurons in *C. elegans.* PCRG-1 localises to ASE cilia that play important roles in the sensation of water-soluble attractants such as salt, while EFHC-1 localises to the mechanosensory dopaminergic neurons that are responsible for modulating behaviours based on food availability. Interestingly, both PCRG-1 and EFHC-1 also localise to mechanosensory OLQ neurons that influence foraging (side-to-side head movements) and responses to nose touch. The restricted localisation pattern of both PCRG-1 and EFHC-1 suggests that they have been adapted to mediate specific sensory/signalling functions, likely owing to the fact that they were both previously associated with the pf-ribbon that may play a specific role in anchoring/regulating motility-associated components in motile cilia or signalling proteins in non-motile cilia.

As expected, neither PCRG-1 nor EFHC-1 are implicated in general ciliary functions, and general ciliary structure is maintained in animals deficient in either protein. Additionally, *efhc-1* mutants show no obvious defects in axonemal structure of either OLQ or CEP cilia, yet are defective in one form of mechanosensation mediated by CEP cilia and dependent on mechanosensory TRP-4 channels. It remains unclear how mechanosensory channels such as TRP-4 open in response to mechanosensory stimuli.

One model that has been proposed is the tether model, in which mechanosensory channels are thought to be tethered to either intracellular structures such as microtubules and/or extracellular structures. In this model, the mechanical stimuli transmit force through the tethers to mediate channel gating (Orr et al., 2006). Recently, the ankyrin repeats in the *Drosophila* orthologue of TRP-4 (NOMPC) were found to form the microtubule-membrane connections observable through transmission electron microscopy, where they form a tether required for gating the channel (Zhang et al., 2015). While similar microtubule-membrane connections have been seen in *C. elegans* CEP cilia (Doroquez et al., 2014; Perkins et al., 1986), they were not readily observable/quantifiable in our imaging experiments. Therefore, although we did not see any differences between the ciliary axonemes of *efhc-1* mutants compared to wild-type animals, it is possible that in the absence of EFHC-1 these microtubule-membrane connections are disrupted, leading to the defective or inefficient TRP-4 mechanosensory gating. It is also possible that instead of directly gating TRP-4 channels in cooperation with microtubule-membrane connections, EFHC-1 functions to increase the sensitivity of TRP-4 channels to mechanosensory stimuli. This idea is consistent with our data showing that neuronal activation is less likely to occur in *efhc-1* mutants, but that when it does occur, responses are similar to wild-type responses.

Microtubule-membrane connections that could function as tethers for mechanosensory gating of channels have not been observed in OLQ neurons, yet the connections seen between microtubules in these cilia could be essential for mechanosensation. Subtle axonemal defects in OLQ cilia are seen in *pcrg-1* mutants, with a progressive loss of outer microtubules and associated connections, but these defects do not appear to disrupt OLQ-mediated mechanosensation or behaviours. Our data suggest that the microtubule-microtubule connections may not be essential for mechanosensation. Furthermore, the progressive loss of microtubules toward the distal end of OLQ cilia in *pcrg-1* mutants suggests that microtubules may not play a major role in OLQ-based mechanosensation. Alternatively, axonemal defects may not be present in all four OLQ cilia of individual animals, allowing for compensation during mechanosensation. Additionally, because OLQ is connected to other neurons that respond to mechanical stimuli at the nose via gap junctions (Chatzigeorgiou and Schafer, 2011), it is possible that other neurons compensate for defects in OLQ-based

mechanosensation in *pcrg-1* mutants. Given that this work has not uncovered a clear link between ciliary structure and mechanosensation, it is likely that both PCRG-1 and EFHC-1 play important roles in anchoring specific sensory/signalling molecules in the cilia they are found in.

In this work, we find that EFHC-1 localises to both cilia and synapses in CEP neurons, and our data provide insight into how it might function at both locations. Given that EFHC1 is known to interact with and regulate a TRP channel (TRPM2) in human cells (Katano et al., 2012), we hypothesised that *C. elegans* EFHC-1 may also interact with and regulate the mechanosensory TRP-4 channel at the cilium. While our data are consistent with this hypothesis, it cannot be ruled out that EFHC-1 functions downstream of ciliary mechanosensation. Specifically, the calcium transients (indicative of neuronal activation) were not measured at the cilium, but instead downstream at the cell body. Therefore, the lower probability of neuronal activation in response to the buzz stimulus in *efhc-1* mutants could be due to a role for EFHC-1 in modulating the channel properties of TRP-4 at the cilium to either increase its sensitivity or facilitate gating in response to mechanical stimuli. Alternatively, EFHC-1 could work to amplify the TRP-4 mechanonsensory response either at the cilium or further downstream, possibly through the interaction with other channels or signalling proteins. Despite these limitations, our data show that mechanosensory transduction in response to the mechanical buzz stimulus is reduced in *efhc-1* mutants upstream of the cell body/synapses.

The dopamine-related phenotypes observed in *efhc-1* mutants are indicative of increased dopamine signalling, and given that the mechanosensory response at the cell body is reduced in these mutants, EFHC-1 must function downstream of the cell body to increase dopamine signalling. Since EFHC1 is also known to interact with and regulate the R-type voltage-gated calcium channel (UNC-2 homologue) in human cells (Suzuki et al., 2004), we hypothesised that *C. elegans* EFHC-1 may also interact with and regulate the mechanosensory UNC-2 channel at the synapse. Our genetic data support a model in which UNC-2 functions downstream of EFHC-1, consistent with EFHC-1 modulating UNC-2 channels to alter the amount of calcium influx permitted. For example, EFHC-1 may prevent calcium influx in the absence of mechanosensory signals to prevent spontaneous dopamine release, possibly by decreasing the sensitivity of UNC-2

channels. It is also possible that EFHC-1 does not directly regulate UNC-2 function, but could instead regulate other channels or signalling molecules upstream of UNC-2 activation, or upstream of the synapse, to limit the influx of calcium through UNC-2 in the absence of mechanosensation. In future work, it would be informative to directly investigate synaptic dynamics in *efhc-1* mutants to determine if, as hypothesised, EFHC-1 limits the spontaneous release of dopamine.

Consistent with a role for PCRG-1 in ASE-based signalling functions, we find that PCRG-1 influences a learning behaviour known as gustatory plasticity, through interactions with a subset of G-proteins that localise to ciliated neurons also implicated in the regulation of gustatory plasticity. PCRG-1 also promotes longevity by acting upstream of the lifespan-promoting FOXO transcription factor DAF-16 and likely upstream of insulin/IGF signalling. Similarly, EFHC-1 promotes longevity, suggesting that both PCRG-1 and EFHC-1 share signalling functions in common that we have attributed to the actions of both proteins in OLQ neurons due to the overlapping localisation of both proteins to these neurons as well as the ability of OLQ disruption to increase longevity. Interestingly, no defects in OLQ-mediated mechanosensation or behaviours were observed in *pcrg-1* or *efhc-1* mutants, suggesting that more complex/subtle defects may exist, perhaps related to learning behaviours. Future work would be to investigate the mechanosensory responses of these mutants to repeated stimulation.

Our findings establish previously unrecognised sensory/signalling functions for both PACRG and EFHC1 and highlights the importance of exaptation (functional adaptation) of proteins associated with ciliary motility in non-motile sensory cilia. Although this work focuses on the roles of PACRG and EFHC1 in *C. elegans* non-motile cilia, these proteins also likely have specific sensory functions in the human brain due to their high abundance, and at least one, EFHC1, is important for neuronal communication. A better understanding of these proteins, in particular EFHC1, may provide important clues for understanding and ultimately providing novel avenues for intervention of disorders such as epilepsy.

# References

Alcedo, J., and Kenyon, C. (2004). Regulation of C. elegans Longevity by Specific Gustatory and Olfactory Neurons. Neuron *41*, 45–55.

Alkema, M.J., Hunter-Ensor, M., Ringstad, N., and Horvitz, H.R. (2005). Tyramine Functions Independently of Octopamine in the Caenorhabditis elegans Nervous System. Neuron *46*, 247–260.

Amos, L.A. (2008). The tektin family of microtubule-stabilizing proteins. Genome Biol. *9*, 229.

Apfeld, J., and Kenyon, C. (1999). Regulation of lifespan by sensory perception in Caenorhabditis elegans. Nature *402*, 804–809.

Apfeld, J., O'Connor, G., McDonagh, T., DiStefano, P.S., and Curtis, R. (2004). The AMP-activated protein kinase AAK-2 links energy levels and insulin-like signals to lifespan in C. elegans. Genes Dev. *18*, 3004–3009.

Avidor-Reiss, T., Maer, A.M., Koundakjian, E., Polyanovsky, A., Keil, T., Subramaniam, S., and Zuker, C.S. (2004). Decoding Cilia Function. Cell *117*, 527–539.

Bae, Y.-K., and Barr, M.M. (2008). Sensory roles of neuronal cilia: Cilia development, morphogenesis, and function in C. elegans. Front. Biosci. J. Virtual Libr. *13*, 5959–5974.

Bargmann, C.I., Thomas, J.H., and Horvitz, H.R. (1990). Chemosensory cell function in the behaviour and development of Caenorhabditis elegans. Cold Spring Harb. Symp. Quant. Biol. *55,* 529-538.

Bargmann, C.I. (2006). Chemosensation in C. elegans. WormBook Online Rev. C Elegans Biol. 1–29.

Bargmann, C.I., and Horvitz, H.R. (1991). Chemosensory neurons with overlapping functions direct chemotaxis to multiple chemicals in C. elegans. Neuron *7*, 729–742.

Bialas, N.J., Inglis, P.N., Li, C., Robinson, J.F., Parker, J.D.K., Healey, M.P., Davis, E.E., Inglis, C.D., Toivonen, T., Cottell, D.C., et al. (2009). Functional interactions between the ciliopathy-associated Meckel syndrome 1 (MKS1) protein and two novel MKS1-related (MKSR) proteins. J Cell Sci *122*, 611–624.

Blacque, O.E., Reardon, M.J., Li, C., McCarthy, J., Mahjoub, M.R., Ansley, S.J., Badano, J.L., Mah, A.K., Beales, P.L., Davidson, W.S., et al. (2004). Loss of C. elegans BBS-7 and BBS-8 protein function results in cilia defects and compromised intraflagellar transport. Genes Dev. *18*, 1630–1642.

Blacque, O.E., Li, C., Inglis, P.N., Esmail, M.A., Ou, G., Mah, A.K., Baillie, D.L., Scholey, J.M., and Leroux, M.R. (2006). The WD Repeat-containing Protein IFTA-1 Is Required for Retrograde Intraflagellar Transport. Mol. Biol. Cell *17*, 5053–5062.

Bloodgood, R.A. (2010). Sensory reception is an attribute of both primary cilia and motile cilia. J Cell Sci *123*, 505–509.

de Bono, M., Tobin, D.M., Davis, M.W., Avery, L., and Bargmann, C.I. (2002). Social feeding in Caenorhabditis elegans is induced by neurons that detect aversive stimuli. Nature *419*, 899–903.

Bozzi, Y., and Borrelli, E. (2013). The role of dopamine signaling in epileptogenesis. Front. Cell. Neurosci. *7*.

Brody, K.M., Taylor, J.M., Wilson, G.R., Delatycki, M.B., and Lockhart, P.J. (2008). Regional and cellular localisation of Parkin co-regulated gene in developing and adult mouse brain. Brain Res. *1201*, 177–186.

Catterall, W.A. (2000). Structure and Regulation of Voltage-Gated Ca2+ Channels. Annu. Rev. Cell Dev. Biol. *16*, 521–555.

Chase, D.L., Pepper, J.S., and Koelle, M.R. (2004). Mechanism of extrasynaptic dopamine signalling in Caenorhabditis elegans. Nat. Neurosci. *7,* 1096-1103.

Chatzigeorgiou, M., Schafer, W.R. (2011). Lateral facilitation between primary mechanosensory neurons controls nose touch perception in C. elegans. Neuron *70,* 299-309.

Conte, F.F., Ribeiro, P.A.O., Marchesini, R.B., Pascoal, V.D.B., Silva, J.M., Oliveira, A.R., Gilioli, R., Sbragia, L., Bittencourt, J.C., and Lopes-Cendes, I. (2009a). Expression Profile and Distribution of Efhc1 Gene Transcript During Rodent Brain Development. J. Mol. Neurosci. *39*, 69–77.

Conte, F.F., Ribeiro, P.A.O., Marchesini, R.B., Pascoal, V.D.B., Silva, J.M., Oliveira, A.R., Gilioli, R., Sbragia, L., Bittencourt, J.C., and Lopes-Cendes, I. (2009b). Expression profile and distribution of Efhc1 gene transcript during rodent brain development. J. Mol. Neurosci. MN *39*, 69–77.

Correa, P., LeBoeuf, B., and García, L.R. (2012). C. elegans Dopaminergic D2-Like Receptors Delimit Recurrent Cholinergic-Mediated Motor Programs during a Goal-Oriented Behavior. PLOS Genet *8*, e1003015.

Dawe, H.R., Farr, H., Portman, N., Shaw, M.K., and Gull, K. (2005). The Parkin co-regulated gene product, PACRG, is an evolutionarily conserved axonemal protein that functions in outer-doublet microtubule morphogenesis. J. Cell Sci. *118*, 5421–5430.

Delgado-Escueta, A.V. (2007). Advances in Genetics of Juvenile Myoclonic Epilepsies. Epilepsy Curr. *7*, 61–67.

Delgado-Escueta, A.V., and Enrile-Bacsal, F. (1984). Juvenile myoclonic epilepsy of Janz. Neurology *34*, 285–294.

Deng, H., Le, W.-D., Xie, W.-J., Pan, T.-H., Zhang, X., and Jankovic, J. (2005). Genetic analysis of parkin co-regulated gene (PACRG) in patients with early-onset parkinsonism. Neurosci. Lett. *382*, 297–299.

Domire, J.S., Green, J.A., Lee, K.G., Johnson, A.D., Askwith, C.C., and Mykytyn, K. (2011). Dopamine Receptor 1 Localizes to Neuronal Cilia in a Dynamic Process that Requires the Bardet-Biedl Syndrome Proteins. Cell. Mol. Life Sci. *68*, 2951–2960.

Doroquez, D.B., Berciu, C., Anderson, J.R., Sengupta, P., and Nicastro, D. (2014). A high-resolution morphological and ultrastructural map of anterior sensory cilia and glia in Caenorhabditis elegans. eLife *3*, e01948.

Efimenko, E., Bubb, K., Mak, H.Y., Holzman, T., Leroux, M.R., Ruvkun, G., Thomas, J.H., and Swoboda, P. (2005). Analysis of xbx genes in C. elegans. Development *132*, 1923–1934.

Ewbank, J.J., Barnes, T.M., Lakowski, B., Lussier, M., Bussey, H., and Hekimi, S. (1997). Structural and functional conservation of the Caenorhabditis elegans timing gene clk-1. Science *275*, 980–983.

Ezcurra, M., Tanizawa, Y., Swoboda, P., and Schafer, W.R. (2011). Food sensitizes C. elegans avoidance behaviours through acute dopamine signalling. EMBO J. *30*, 1110–1122.

Fujiwara, M., Sengupta, P., and McIntire, S.L. (2002). Regulation of Body Size and Behavioral State of C. elegans by Sensory Perception and the EGL-4 cGMP-Dependent Protein Kinase. Neuron *36*, 1091–1102.

Hart, A.C., Sims, S., and Kaplan, J.M. (1995). Synaptic code for sensory modalities revealed by C. elegans GLR-1 glutamate receptor. Nature *378*, 82–85.

Hills, T., Brockie, P.J., and Maricq, A.V. (2004). Dopamine and Glutamate Control Area-Restricted Search Behavior in Caenorhabditis elegans. J. Neurosci. *24*, 1217–1225.

Hukema, R.K., Rademakers, S., Dekkers, M.P.J., Burghoorn, J., and Jansen, G. (2006). Antagonistic sensory cues generate gustatory plasticity in Caenorhabditis elegans. EMBO J. *25*, 312–322.

Hukema, R.K., Rademakers, S., and Jansen, G. (2008). Gustatory plasticity in C. elegans involves integration of negative cues and NaCl taste mediated by serotonin, dopamine, and glutamate. Learn. Mem. *15*, 829–836.

Ikeda, T. (2008). Parkin-co-regulated gene (PACRG) product interacts with tubulin and microtubules. FEBS Lett. *582*, 1413–1418.

Ikeda, K., Brown, J.A., Yagi, T., Norrander, J.M., Hirono, M., Eccleston, E., Kamiya, R., and Linck, R.W. (2003). Rib72, a Conserved Protein Associated with the Ribbon Compartment of Flagellar A-microtubules and Potentially Involved in the Linkage between Outer Doublet Microtubules. J. Biol. Chem. *278*, 7725–7734.

Ikeda, K., Ikeda, T., Morikawa, K., and Kamiya, R. (2007). Axonemal localization of Chlamydomonas PACRG, a homologue of the human Parkin-coregulated gene product. Cell Motil. Cytoskeleton *64*, 814–821.

Ikeda, T., Ikeda, K., Enomoto, M., Park, M.K., Hirono, M., and Kamiya, R. (2005). The mouse ortholog of EFHC1 implicated in juvenile myoclonic epilepsy is an axonemal protein widely conserved among organisms with motile cilia and flagella. FEBS Lett. *579*, 819–822.

Imai, Y., Soda, M., Murakami, T., Shoji, M., Abe, K., and Takahashi, R. (2003). A product of the human gene adjacent to parkin is a component of Lewy bodies and suppresses Pael receptor-induced cell death. J. Biol. Chem. *278*, 51901–51910.

Inglis, P.N., Ou, G., Leroux, M.R., and Scholey, J.M. (2007). The sensory cilia of Caenorhabditis elegans. WormBook Online Rev. C Elegans Biol. 1–22.

Ito, E., Xie, G., Maruyama, K., and Palmer, P.P. (2000). A core-promoter region functions bi-directionally for human opioid-receptor-like gene ORL1 and its 5'-adjacent gene GAIP. J. Mol. Biol. *304*, 259–270.

Jansen, G. (2002). The G-protein gamma subunit gpc-1 of the nematode C.elegans is involved in taste adaptation. EMBO J. *21*, 986–994.

Jansen, G., Thijssen, K.L., Werner, P., van der Horst, M., Hazendonk, E., and Plasterk, R.H. (1999). The complete family of genes encoding G proteins of Caenorhabditis elegans. Nat. Genet. *21*, 414–419.

Kang, L., Gao, J., Schafer, W.R., Xie, Z., and Xu, X.Z.S. (2010). C. elegans TRP Family Protein TRP-4 Is a Pore-Forming Subunit of a Native Mechanotransduction Channel. Neuron *67*, 381–391.

Kaplan, J.M., and Horvitz, H.R. (1993). A dual mechanosensory and chemosensory neuron in Caenorhabditis elegans. Proc. Natl. Acad. Sci. U. S. A. *90*, 2227–2231.

Katano, M., Numata, T., Aguan, K., Hara, Y., Kiyonaka, S., Yamamoto, S., Miki, T., Sawamura, S., Suzuki, T., Yamakawa, K., et al. (2012). The juvenile myoclonic epilepsy-related protein EFHC1 interacts with the redox-sensitive TRPM2 channel linked to cell death. Cell Calcium *51*, 179–185.

Keller, L.C., Romijn, E.P., Zamora, I., Yates, J.R., and Marshall, W.F. (2005). Proteomic Analysis of Isolated Chlamydomonas Centrioles Reveals Orthologs of Ciliary-Disease Genes. Curr. Biol. *15*, 1090–1098.

Kenyon, C.J. (2010). The genetics of ageing. Nature *464*, 504–512.

Kenyon, C., Chang, J., Gensch, E., Rudner, A., and Tabtiang, R. (1993). A C. elegans mutant that lives twice as long as wild type. Nature *366*, 461–464.

Kindt, K.S., Viswanath, V., Macpherson, L., Quast, K., Hu, H., Patapoutian, A., and Schafer, W.R. (2007a). Caenorhabditis elegans TRPA-1 functions in mechanosensation. Nat. Neurosci. *10*, 568–577.

Kindt, K.S., Quast, K.B., Giles, A.C., De, S., Hendrey, D., Nicastro, I., Rankin, C.H., and Schafer, W.R. (2007b). Dopamine Mediates Context-Dependent Modulation of Sensory Plasticity in C. elegans. Neuron *55*, 662–676.

Klass, M.R. (1977). Aging in the nematode Caenorhabditis elegans: major biological and environmental factors influencing life span. Mech. Ageing Dev. *6*, 413–429.

Lans, H., and Jansen, G. (2007). Multiple sensory G proteins in the olfactory, gustatory and nociceptive neurons modulate longevity in Caenorhabditis elegans. Dev. Biol. *303*, 474–482.

Lee, L. (2011). Mechanisms of mammalian ciliary motility: Insights from primary ciliary dyskinesia genetics. Gene *473*, 57–66.

Lee, R.Y.N., Hench, J., and Ruvkun, G. (2001). Regulation of C. elegans DAF-16 and its human ortholog FKHRL1 by the daf-2 insulin-like signaling pathway. Curr. Biol. *11*, 1950–1957.

Lennard, A., Gaston, K., and Fried, M. (1994). The Surf-1 and Surf-2 genes and their essential bidirectional promoter elements are conserved between mouse and human. DNA Cell Biol. *13*, 1117–1126.

Léon, C., de Nijs, L., Chanas, G., Delgado-Escueta, A.V., Grisar, T., and Lakaye, B. (2010). Distribution of EFHC1 or Myoclonin 1 in mouse neural structures. Epilepsy Res. *88*, 196–207.

Li, J.B., Gerdes, J.M., Haycraft, C.J., Fan, Y., Teslovich, T.M., May-Simera, H., Li, H., Blacque, O.E., Li, L., Leitch, C.C., et al. (2004). Comparative Genomics Identifies a Flagellar and Basal Body Proteome that Includes the BBS5 Human Disease Gene. Cell *117*, 541–552.

Li, W., Feng, Z., Sternber, P.W., and Xu, X.Z. (2006). A C. elegans stretch receptor neuron revealed by a mechanosensative TRP channel homologue. Nature *440,* 684-687.

Linck, R.W., and Norrander, J.M. (2003). Protofilament ribbon compartments of ciliary and flagellar microtubules. Protist *154*, 299–311.

Linck, R.W., and Stephens, R.E. (2007). Functional protofilament numbering of ciliary, flagellar, and centriolar microtubules. Cell Motil. Cytoskeleton *64*, 489–495.

Lorenzetti, D., Bishop, C.E., and Justice, M.J. (2004). Deletion of the Parkin coregulated gene causes male sterility in the quakingviable mouse mutant. Proc. Natl. Acad. Sci. U. S. A. *101*, 8402–8407.

Loucks, C.M., Bialas, N.J., Dekkers, M.P., Walker, D.S., Grundy, L.J., Li, C., Inglis, P.N., Kida, K., Schafer, W.R., Blacque, O.E., Jansen G., and Leroux, M.R. (2016). PACRG, a protein linked to ciliary motility, mediates cellular signaling. Mol. Biol. Cell. *27,* 2133-2144.

McDonald, P.W., Hardie, S.L., Jessen, T.N., Carvelli, L., Matthies, D.S., and Blakely, R.D. (2007). Vigorous Motor Activity in Caenorhabditis elegans Requires Efficient Clearance of Dopamine Mediated by Synaptic Localization of the Dopamine Transporter DAT-1. J. Neurosci. *27*, 14216–14227.

Naitoh, Y., and Eckert, R. (1969). Ionic mechanisms controlling behavioral responses of paramecium to mechanical stimulation. Science *164*, 963–965.

Nijs, L. de, Wolkoff, N., Coumans, B., Delgado-Escueta, A.V., Grisar, T., and Lakaye, B. (2012). Mutations of EFHC1, linked to juvenile myoclonic epilepsy, disrupt radial and tangential migrations during brain development. Hum. Mol. Genet. *21*, 5106–5117.

de Nijs, L., Lakaye, B., Coumans, B., Léon, C., Ikeda, T., Delgado-Escueta, A.V., Grisar, T., and Chanas, G. (2006). EFHC1, a protein mutated in juvenile myoclonic epilepsy, associates with the mitotic spindle through its N-terminus. Exp. Cell Res. *312*, 2872–2879.

de Nijs, L., Léon, C., Nguyen, L., LoTurco, J.J., Delgado-Escueta, A.V., Grisar, T., and Lakaye, B. (2009a). EFHC1 interacts with microtubules to regulate cell division and cortical development. Nat. Neurosci. *12*, 1266–1274.

de Nijs, L., Léon, C., Nguyen, L., Loturco, J.J., Delgado-Escueta, A.V., Grisar, T., and Lakaye, B. (2009b). EFHC1 interacts with microtubules to regulate cell division and cortical development. Nat. Neurosci. *12*, 1266–1274.

Norrander, J., Larsson, M., Ståhl, S., Höög, C., and Linck, R. (1998). Expression of ciliary tektins in brain and sensory development. J. Neurosci. Off. J. Soc. Neurosci. *18*, 8912–8918.

Norrander, J.M., Perrone, C.A., Amos, L.A., and Linck, R.W. (1996). Structural comparison of tektins and evidence for their determination of complex spacings in flagellar microtubules. J. Mol. Biol. *257*, 385–397.

Ogura, A., and Takahashi, K. (1976). Artificial deciliation causes loss of calcium-dependent responses in Paramecium. Nature *264*, 170–172.

Orii, K.E., Orii, K.O., Souri, M., Orii, T., Kondo, N., Hashimoto, T., and Aoyama, T. (1999). Genes for the human mitochondrial trifunctional protein alpha- and beta-subunits are divergently transcribed from a common promoter region. J. Biol. Chem. *274*, 8077–8084.

Orr, A.W., Helmke, B.P., Blackman, B.R., and Schwartz, M.A. (2006). Mechanisms of mechanotransduction. Dev. Cell *10*, 11–20.

Ostrowski, L.E., Blackburn, K., Radde, K.M., Moyer, M.B., Schlatzer, D.M., Moseley, A., and Boucher, R.C. (2002). A Proteomic Analysis of Human Cilia Identification of Novel Components. Mol. Cell. Proteomics *1*, 451–465.

Ou, G., Blacque, O.E., Snow, J.J., Leroux, M.R., and Scholey, J.M. (2005). Functional coordination of intraflagellar transport motors. Nature *436*, 583–587.

Patel-King, R.S., Benashski, S.E., and King, S.M. (2002). A Bipartite Ca2+-regulated Nucleoside-diphosphate Kinase System within theChlamydomonas Flagellum THE REGULATORY SUBUNIT p72. J. Biol. Chem. *277*, 34271–34279.

Pazour, G.J., Agrin, N., Leszyk, J., and Witman, G.B. (2005). Proteomic analysis of a eukaryotic cilium. J. Cell Biol. *170*, 103–113.

Perkins, L.A., Hedgecock, E.M., Thomson, J.N., and Culotti, J.G. (1986). Mutant sensory cilia in the nematode Caenorhabditis elegans. Dev. Biol. *117*, 456–487.

Pirner, M.A., and Linck, R.W. (1994). Tektins are heterodimeric polymers in flagellar microtubules with axial periodicities matching the tubulin lattice. J. Biol. Chem. *269*, 31800–31806.

Polymeropoulos, M.H., Lavedan, C., Leroy, E., Ide, S.E., Dehejia, A., Dutra, A., Pike, B., Root, H., Rubenstein, J., Boyer, R., et al. (1997). Mutation in the alpha-synuclein gene identified in families with Parkinson's disease. Science *276*, 2045–2047.

Rankin, C.H., and Broster, B.S. (1992). Factors affecting habituation and recovery from habituation in the nematode Caenorhabditis elegans.. Behav. Neurosci. *106*, 239–249.

Rankin, C.H., Beck, C.D.O., and Chiba, C.M. (1990). Caenorhabditis elegans: A new model system for the study of learning and memory. Behav. Brain Res. *37*, 89–92.

Richmond, J.E., Weimer, R.M., and Jorgensen, E.M. (2001). An open form of syntaxin bypasses the requirement for UNC-13 in vesicle priming. Nature *412*, 338–341.

Roayaie, K., Crump, J.G., Sagasti, A., and Bargmann, C.I. (1998). The Gα Protein ODR-3 Mediates Olfactory and Nociceptive Function and Controls Cilium Morphogenesis in C. elegans Olfactory Neurons. Neuron *20*, 55–67.

Rossetto, M.G., Zanarella, E., Orso, G., Scorzeto, M., Megighian, A., Kumar, V., Delgado-Escueta, A.V., and Daga, A. (2011). Defhc1.1, a homologue of the juvenile myoclonic gene EFHC1, modulates architecture and basal activity of the neuromuscular junction in Drosophila. Hum. Mol. Genet. *20*, 4248–4257.

Sanyal, S., Wintle, R.F., Kindt, K.S., Nuttley, W.M., Arvan, R., Fitzmaurice, P., Bigras, E., Merz, D.C., Hébert, T.E., van der Kooy, D., et al. (2004). Dopamine modulates the plasticity of mechanosensory responses in Caenorhabditis elegans. EMBO J. *23*, 473–482.

Sawin, E.R., Ranganathan, R., and Horvitz, H.R. (2000). C. elegans Locomotory Rate Is Modulated by the Environment through a Dopaminergic Pathway and by Experience through a Serotonergic Pathway. Neuron *26*, 619–631.

Schafer, W.R., and Kenyon, C.J. (1995). A calcium-channel homologue required for adaptation to dopamine and serotonin in Caenorhabditis elegans. Nature *375*, 73–78.

Schafer, J.C., Winkelbauer, M.E., Williams, C.L., Haycraft, C.J., Desmond, R.A., and Yoder, B.K. (2006). IFTA-2 is a conserved cilia protein involved in pathways regulating longevity and dauer formation in Caenorhabditis elegans. J. Cell Sci. *119*, 4088–4100.

Setter, P.W., Malvey-Dorn, E., Steffen, W., Stephens, R.E., and Linck, R.W. (2006). Tektin interactions and a model for molecular functions. Exp. Cell Res. *312*, 2880–2896.

Shah, A.S., Ben-Shahar, Y., Moninger, T.O., Kline, J.N., and Welsh, M.J. (2009). Motile Cilia of Human Airway Epithelia Are Chemosensory. Science *325*, 1131–1134.

Silverman, M.A., and Leroux, M.R. (2009). Intraflagellar transport and the generation of dynamic, structurally and functionally diverse cilia. Trends Cell Biol. *19*, 306–316.

Smith, J.C., Northey, J.G.B., Garg, J., Pearlman, R.E., and Siu, K.W.M. (2005). Robust method for proteome analysis by MS/MS using an entire translated genome: demonstration on the ciliome of Tetrahymena thermophila. J. Proteome Res. *4*, 909–919.

Snow, J.J., Ou, G., Gunnarson, A.L., Walker, M.R.S., Zhou, H.M., Brust-Mascher, I., and Scholey, J.M. (2004). Two anterograde intraflagellar transport motors cooperate to build sensory cilia on C. elegans neurons. Nat. Cell Biol. *6*, 1109–1113.

Stolc, V., Samanta, M.P., Tongprasit, W., and Marshall, W.F. (2005). Genome-wide transcriptional analysis of flagellar regeneration in Chlamydomonas reinhardtii identifies orthologs of ciliary disease genes. Proc. Natl. Acad. Sci. U. S. A. *102*, 3703–3707.

Subaran, R.L., Conte, J.M., Stewart, W.C.L., and Greenberg, D.A. (2015). Pathogenic EFHC1 mutations are tolerated in healthy individuals dependent on reported ancestry. Epilepsia *56*, 188–194.

Sulston, J., Dew, M., and Brenner, S. (1975). Dopaminergic neurons in the nematode Caenorhabditis elegans. J. Comp. Neurol. *163*, 215–226.

Suzuki, T., Delgado-Escueta, A.V., Aguan, K., Alonso, M.E., Shi, J., Hara, Y., Nishida, M., Numata, T., Medina, M.T., Takeuchi, T., et al. (2004). Mutations in EFHC1 cause juvenile myoclonic epilepsy. Nat. Genet. *36*, 842–849.

Suzuki, T., Inoue, I., Yamagata, T., Morita, N., Furuichi, T., and Yamakawa, K. (2008). Sequential expression of Efhc1/myoclonin1 in choroid plexus and ependymal cell cilia. Biochem. Biophys. Res. Commun. *367*, 226–233.

Suzuki, T., Miyamoto, H., Nakahari, T., Inoue, I., Suemoto, T., Jiang, B., Hirota, Y., Itohara, S., Saido, T.C., Tsumoto, T., et al. (2009). Efhc1 deficiency causes spontaneous myoclonus and increased seizure susceptibility. Hum. Mol. Genet. *18*, 1099–1109.

Swierczek, N.A., Giles, A.C., Rankin, C.H., and Kerr, R.A. (2011). High-throughput behavioral analysis in C. elegans. Nat. Methods *8*, 592–598.

Swoboda, P., Adler, H.T., and Thomas, J.H. (2000). The RFX-Type Transcription Factor DAF-19 Regulates Sensory Neuron Cilium Formation in C. elegans. Mol. Cell *5*, 411–421.

Takeda, S., and Narita, K. (2012). Structure and function of vertebrate cilia, towards a new taxonomy. Differ. Res. Biol. Divers. *83*, S4–S11.

Tanaka, H., Iguchi, N., Toyama, Y., Kitamura, K., Takahashi, T., Kaseda, K., Maekawa, M., and Nishimune, Y. (2004). Mice Deficient in the Axonemal Protein Tektin-t Exhibit Male Infertility and Immotile-Cilium Syndrome Due to Impaired Inner Arm Dynein Function. Mol. Cell. Biol. *24*, 7958–7964.

Taylor, J.M., Brody, K.M., and Lockhart, P.J. (2012). Parkin co-regulated gene is involved in aggresome formation and autophagy in response to proteasomal impairment. Exp. Cell Res. *318*, 2059–2070.

Tobin, D.M., Madsen, D.M., Kahn-Kirby, A., Peckol, E.L., Moulder, G., Barstead, R., Maricq, A.V., and Bargmann, C.I. (2002). Combinatorial Expression of TRPV Channel Proteins Defines Their Sensory Functions and Subcellular Localization in C. elegans Neurons. Neuron *35*, 307–318.

Waters, A.M., and Beales, P.L. (2011). Ciliopathies: an expanding disease spectrum. Pediatr. Nephrol. Berl. Ger. *26*, 1039–1056.

West, A.B., Lockhart, P.J., O'Farell, C., and Farrer, M.J. (2003). Identification of a novel gene linked to parkin via a bi-directional promoter. J. Mol. Biol. *326*, 11–19.

White, J.G., Southgate, E., Thomson, J.N., and Brenner, S. (1986). The Structure of the Nervous System of the Nematode Caenorhabditis elegans. Philos. Trans. R. Soc. Lond. B. Biol. Sci. *314*, 1–340.

Wicks, S.R., de Vries, C.J., van Luenen, H.G.A.M., and Plasterk, R.H.A. (2000). CHE-3, a Cytosolic Dynein Heavy Chain, Is Required for Sensory Cilia Structure and Function in Caenorhabditis elegans. Dev. Biol. *221*, 295–307.

Wiederhold, M.L. (1976). Mechanosensory transduction in "sensory" and "motile" cilia. Annu. Rev. Biophys. Bioeng. *5*, 39–62.

Wilson, G.R., Wang, H.X., Egan, G.F., Robinson, P.J., Delatycki, M.B., O'Bryan, M.K., and Lockhart, P.J. (2010). Deletion of the Parkin co-regulated gene causes defects in ependymal ciliary motility and hydrocephalus in the quakingviable mutant mouse. Hum. Mol. Genet. *19*, 1593–1602.

Winkelbauer, M.E., Schafer, J.C., Haycraft, C.J., Swoboda, P., and Yoder, B.K. (2005). The C. elegans homologs of nephrocystin-1 and nephrocystin-4 are cilia transition zone proteins involved in chemosensory perception. J. Cell Sci. *118*, 5575–5587.

Wolf, M.T.F., Lee, J., Panther, F., Otto, E.A., Guan, K.-L., and Hildebrandt, F. (2005). Expression and Phenotype Analysis of the Nephrocystin-1 and Nephrocystin-4 Homologs in Caenorhabditis elegans. J. Am. Soc. Nephrol. *16*, 676–687.

Yanagisawa, H., and Kamiya, R. (2004). A tektin homologue is decreased in chlamydomonas mutants lacking an axonemal inner-arm dynein. Mol. Biol. Cell *15*, 2105–2115.

Yeh, C., Li, A., Chuang, J.-Z., Saito, M., Cáceres, A., and Sung, C.-H. (2013). IGF-1 activates a cilium-localized non-canonical Gβγ signaling pathway that regulates cell cycle progression. Dev. Cell *26*, 358–368.

Yemini, E., Jucikas, T., Grundy, L.J., Brown, A.E.X., and Schafer, W.R. (2013). A database of C. elegans behavioral phenotypes. Nat. Methods *10*, 877–879.

Zhang, W., Cheng, L.E., Kittelmann, M., Li, J., Petkovic, M., Cheng, T., Jin, P., Guo, Z., Göpfert, M.C., Jan, L.Y., and Jan, Y.N. (2015). Ankyrin Repeats Convey Force to Gate the NOMPC Mechanotransduction Channel. Cell *162,* 1391-1403.

Zhao, Y., Shi, J., Winey, M., and Klymkowsky, M.W. (2016). Identifying domains of EFHC1 involved in ciliary localization, ciliogenesis, and the regulation of Wnt signaling. Dev. Biol. *411*, 257–265.

Zhu, D., Shi, S., Wang, H., and Liao, K. (2009). Growth arrest induces primary-cilium formation and sensitizes IGF-1-receptor signaling during differentiation induction of 3T3-L1 preadipocytes. J. Cell Sci. *122*, 2760–2768.

Zwaal, R.R., Ahringer, J., Luenen, H.G.A.M. van, Rushforth, A., Anderson, P., and Plasterk, R.H.A. (1996). G Proteins Are Required for Spatial Orientation of Early Cell Cleavages in C. elegans Embryos. Cell *86*, 619–629.

# Appendix.

# Statistical analysis of all lifespan experiments in Chapter 2

**Table A.1 Statistical analysis of all lifespan experiments in Chapter 2.**

| Figure | Strain | Mean Lifespan (days) | n | p-value (vs.) |
|---|---|---|---|---|
| **2.4A** | wild-type | 19.83 +/- 0.37 | 81 | n/a (wild-type) |
| | *pcrg-1(gk480)* | 13.86 +/- 0.28 | 84 | <0.0001 (wild-type) |
| | *pcrg-1(tm2597)* | 14.53 +/- 0.35 | 60 | <0.0001 (wild-type) |
| **2.4B** | wild-type | 19.46 +/- 0.42 | 71 | n/a (wild-type) |
| | *pcrg-1(gk480)* | 14.79 +/- 0.36 | 68 | <0.0001 (wild-type) |
| | *pcrg-1(gk480);* PCRG-1::GFP (construct A) | 19.29 +/- 0.41 | 68 | 0.7865 (wild-type) |
| **2.4C** | wild-type | 20.87 +/- 0.43 | 87 | n/a (wild-type) |
| | *pcrg-1(tm2597)* | 14.93 +/- 0.32 | 82 | <0.0001 (wild-type) |
| | *pcrg-1(tm2597);* PCRG-1::GFP (construct B) | 20.05 +/- 0.52 | 76 | 0.441 (wild-type) |
| **2.4A** | wild-type | 20.87 +/- 0.43 | 87 | n/a (wild-type) |
| | *pcrg-1(tm2597)* | 14.93 +/- 0.32 | 82 | <0.0001 (wild-type) |
| | wild-type; PCRG-1::GFP (construct B) | 21.47 +/- 0.50 | 83 | 0.18 (wild-type) |
| **2.5A** | wild-type | 18.60 +/- 0.53 | 67 | <0.0001 (*gpc-1*), n/a (wild-type), <0.0001 (*pcrg-1)* |
| | *pcrg-1(tm2597)* | 13.45 +/- 0.45 | 62 | <0.0001 (*gpc-1*), <0.0001 (wild-type), n/a (*pcrg-1*) |

| Figure | Strain | Mean Lifespan (days) | n | p-value (vs.) |
|---|---|---|---|---|
| | *gpc-1(pk298)* | 22.17 +/- 0.50 | 69 | n/a (*gpc-1*), <0.0001 (wild-type), <0.0001 (*pcrg-1*) |
| | *pcrg-1(tm2597); gpc-1(pk298)* | 21.38 +/- 0.45 | 64 | 0.1231 (*gpc-1*), 0.0012* (wild-type), <0.0001 (*pcrg-1*) |
| **2.5B** | wild-type | 18.60 +/- 0.53 | 67 | <0.0001 (*gpa-1*), n/a (wild-type), <0.0001 (*pcrg-1)* |
| | *pcrg-1(tm2597)* | 13.45 +/- 0.45 | 62 | <0.0001 (*gpa-1*), <0.0001 (wild-type), n/a (*pcrg-1*) |
| | *gpa-1(pk15)* | 21.82 +/- 0.61 | 67 | n/a (*gpa-1*), <0.0001 (wild-type), <0.0001 (*pcrg-1*) |
| | *pcrg-1(tm2597); gpa-1(pk15)* | 19.97 +/- 0.62 | 65 | 0.0825 (*gpa-1*), 0.0827 (wild-type), <0.0001 (*pcrg-1*) |
| **2.5C** | wild-type | 18.60 +/- 0.53 | 67 | 0.4275 (*gpa-11*), n/a (wild-type), <0.0001 (*pcrg-1)* |
| | *pcrg-1(tm2597)* | 13.45 +/- 0.45 | 62 | <0.0001 (*gpa-11*), <0.0001 (wild-type), n/a (*pcrg-1*) |
| | *gpa-11(pk349)* | 18.33 +/- 0.43 | 72 | n/a (*gpa-11*), 0.4275 (wild-type), <0.0001 (*pcrg-1*) |
| | *pcrg-1(tm2597); gpa-11(pk349)* | 15.49 +/- 0.40 | 67 | <0.0001 (*gpa-11*), <0.0001 (wild-type), 0.0060* (*pcrg-1*) |
| **2.5D** | wild-type | 18.60 +/- 0.53 | 67 | <0.0001 (*gpa-11XS),* n/a (wild-type), <0.0001 (*pcrg-1)* |
| | *pcrg-1(tm2597)* | 13.45 +/- 0.45 | 62 | <0.0001 (*gpa-11XS),* <0.0001 (wild-type), n/a (*pcrg-1*) |
| | *gpa-11XS* | 25.68 +/- 0.79 | 75 | n/a (*gpa-11XS),* <0.0001 (wild-type), <0.0001 (*pcrg-1)* |
| | *pcrg-1(tm2597); gpa-11XS* | 22.39 +/- 0.82 | 82 | 0.0161* (*gpa-11XS),* <0.0001 (wild-type), <0.0001 (*pcrg-1)* |
| **2.5E** | wild-type | 18.60 +/- 0.53 | 67 | <0.0001 (*odr-3*), n/a (wild-type), <0.0001 (*pcrg-1)* |

| Figure | Strain | Mean Lifespan (days) | n | p-value (vs.) |
|---|---|---|---|---|
| | *pcrg-1(tm2597)* | 13.45 +/- 0.45 | 62 | <0.0001 (*odr-3*), <0.0001 (wild-type), n/a (*pcrg-1*) |
| | *odr-3(n1605)* | 22.52 +/- 0.58 | 85 | n/a (*odr-3*), <0.0001 (wild-type), <0.0001 (*pcrg-1)* |
| | *pcrg-1(tm2597); odr-3(n1605)* | 15.80 +/- 0.39 | 61 | <0.0001 (*odr-3*), <0.0001 (wild-type), 0.0025* (*pcrg-1)* |
| **2.5F** | wild-type | 18.60 +/- 0.53 | 67 | <0.0001 (*odr-3;gpa-11XS*), n/a (wild-type), <0.0001 (*pcrg-1)* |
| | *pcrg-1(tm2597)* | 13.45 +/- 0.45 | 62 | <0.0001 (*odr-3;gpa-11XS*), <0.0001 (wild-type), n/a (*pcrg-1*) |
| | *odr-3(n1605); gpa-11XS* | 27.31 +/- 0.91 | 67 | n/a (*odr-3;gpa-11XS*), <0.0001 (wild-type), <0.0001 (*pcrg-1)* |
| | *pcrg-1(tm2597); odr-3(n1605); gpa-11XS* | 27.96 +/- 1.10 | 53 | 0.6048 (*odr-3;gpa-11XS*), <0.0001 (wild-type), 0.0025* (*pcrg-1)* |
| **2.6A** | wild-type | 18.45 +/- 0.53 | 85 | <0.0001 (*osm-5*), n/a (wild-type), <0.0001 (*pcrg-1)* |
| | *pcrg-1(tm2597)* | 13.22 +/- 0.33 | 74 | <0.0001 (*osm-5*), <0.0001 (wild-type), n/a (*pcrg-1)* |
| | *osm-5(p813)* | 35.57 +/- 0.90 | 84 | n/a (*osm-5*), <0.0001 (wild-type), <0.0001 (*pcrg-1)* |
| | *pcrg-1(tm2597); osm-5(p813)* | 28.14 +/- 0.53 | 71 | <0.0001 (*osm-5*), <0.0001 (wild-type), <0.0001 (*pcrg-1)* |
| **2.6B** | wild-type | 18.45 +/- 0.53 | 85 | <0.0001 (*che-11*), n/a (wild-type), <0.0001 (*pcrg-1)* |
| | *pcrg-1(tm2597)* | 13.22 +/- 0.33 | 74 | <0.0001 (*che-11*), <0.0001 (wild-type), n/a (*pcrg-1)* |
| | *che-11(e1810)* | 27.16 +/- 0.86 | 71 | n/a (*che-11*), <0.0001 (wild-type), <0.0001 (*pcrg-1)* |

| Figure | Strain | Mean Lifespan (days) | n | p-value (vs.) |
|---|---|---|---|---|
| | *pcrg-1(tm2597); che-11(e1810)* | 20.02 +/- 0.53 | 74 | <0.0001 (*che-11*), 0.061 (wild-type), <0.0001 (*pcrg-1)* |
| **2.6C** | wild-type | 18.57 +/- 0.51 | 76 | <0.0001 (*nphp-1*), n/a (wild-type), <0.0001 (*pcrg-1)* |
| | *pcrg-1(tm2597)* | 12.19 +/- 0.28 | 93 | <0.0001 (*nphp-1*), <0.0001 (wild-type), n/a (*pcrg-1)* |
| | *nphp-1(ok500)* | 23.29 +/- 0.44 | 87 | n/a (*nphp-1*), <0.0001 (wild-type), <0.0001 (*pcrg-1)* |
| | *pcrg-1(tm2597); nphp-1(ok500)* | 16.25 +/- 0.39 | 73 | <0.0001 (*nphp-1*), 0.061 (wild-type), <0.0001 (*pcrg-1)* |
| **2.6D** | wild-type | 19.77 +/- 0.54 | 71 | <0.0001 (*nphp-4*), n/a (wild-type), <0.0001 (*pcrg-1)* |
| | *pcrg-1(tm2597)* | 13.97 +/- 0.37 | 71 | <0.0001 (*nphp-4*), <0.0001 (wild-type), n/a (*pcrg-1)* |
| | *nphp-4(tm925)* | 26.98 +/- 0.60 | 84 | n/a (*nphp-4*), <0.0001 (wild-type), <0.0001 (*pcrg-1)* |
| | *pcrg-1(tm2597); nphp-4(tm925)* | 17.09 +/- 0.56 | 77 | <0.0001 (*nphp-4*), 0.0044* (wild-type), <0.0001 (*pcrg-1)* |
| **2.7A** | wild-type | 22.37 +/- 0.55 | 71 | <0.0001 (*osm-5*), n/a (wild-type), <0.0001 (*pcrg-1)* |
| | *pcrg-1(gk480)* | 13.00 +/- 0.46 | 72 | <0.0001 (*osm-5*), <0.0001 (wild-type), n/a (*pcrg-1)* |
| | *osm-5(p813)* | 35.61 +/- 0.69 | 71 | n/a (*osm-5*), <0.0001 (wild-type), <0.0001 (*pcrg-1)* |
| | *pcrg-1(gk480); osm-5(p813)* | 31.55 +/- 0.71 | 58 | <0.0001 (*osm-5*), <0.0001 (wild-type), <0.0001 (*pcrg-1)* |
| **2.7B** | wild-type | 22.37 +/- 0.55 | 71 | <0.0001 (*che-11*), n/a (wild-type), <0.0001 (*pcrg-1)* |

| Figure | Strain | Mean Lifespan (days) | n | p-value (vs.) |
|---|---|---|---|---|
| | *pcrg-1(gk480)* | 13.00 +/- 0.46 | 72 | <0.0001 (*che-11*), <0.0001 (wild-type), n/a (*pcrg-1)* |
| | *che-11(e1810)* | 28.58 +/- 0.65 | 79 | n/a (*che-11*), <0.0001 (wild-type), <0.0001 (*pcrg-1)* |
| | *pcrg-1(gk480); che-11(e1810)* | 23.51 +/- 0.64 | 74 | <0.0001 (*che-11*), 0.1241 (wild-type), <0.0001 (*pcrg-1)* |
| **2.7C** | wild-type | 19.83 +/- 0.37 | 81 | <0.0001 (*nphp-1*), n/a (wild-type), <0.0001 (*pcrg-1)* |
| | *pcrg-1(gk480)* | 13.86 +/- 0.28 | 84 | <0.0001 (*nphp-1*), <0.0001 (wild-type), n/a (*pcrg-1)* |
| | *nphp-1(ok500)* | 23.45 +/- 0.56 | 83 | n/a (*nphp-1*), <0.0001 (wild-type), <0.0001 (*pcrg-1)* |
| | *pcrg-1(gk480); nphp-1(ok500)* | 18.25 +/- 0.66 | 64 | <0.0001 (*nphp-1*), 0.2159 (wild-type), <0.0001 (*pcrg-1)* |
| **2.7D** | wild-type | 19.83 +/- 0.37 | 81 | <0.0001 (*nphp-4*), n/a (wild-type), <0.0001 (*pcrg-1)* |
| | *pcrg-1(gk480)* | 13.86 +/- 0.28 | 84 | <0.0001 (*nphp-4*), <0.0001 (wild-type), n/a (*pcrg-1)* |
| | *nphp-4(tm925)* | 25.97 +/- 0.62 | 75 | n/a (*nphp-4*), <0.0001 (wild-type), <0.0001 (*pcrg-1)* |
| | *pcrg-1(gk480); nphp-4(tm925)* | 19.65 +/- 0.35 | 69 | <0.0001 (*nphp-4*), 0.6937 (wild-type), <0.0001 (*pcrg-1)* |
| **2.8A** | wild-type | 19.92 +/- 0.48 | 74 | <0.0001 (*daf-16*), n/a (wild-type), <0.0001 (*pcrg-1*) |
| | *pcrg-1(tm2597)* | 12.46 +/- 0.37 | 69 | 0.26 (*daf-16*), <0.0001 (wild-type), n/a (*pcrg-1*) |
| | *daf-16(mu86)* | 13.08 +/- 0.30 | 89 | n/a (*daf-16*), <0.0001 (wild-type), <0.0001 (*pcrg-1*) |
| | *pcrg-1(tm2597), daf-16(mu86)* | 12.68 +/- 0.27 | 68 | 0.19 (*daf-16*), <0.0001 (wild-type), <0.0001 (*pcrg-1*) |

| Figure | Strain | Mean Lifespan (days) | n | p-value (vs.) |
|---|---|---|---|---|
| **2.8B** | wild-type | 18.05 +/- 0.29 | 86 | <0.0001 (*daf-2*), n/a (wild-type), <0.0001 (*pcrg-1*) |
| | *pcrg-1(tm2597)* | 11.76 +/- 0.23 | 90 | <0.0001 (*daf-2*), <0.0001 (wild-type), n/a (*pcrg-1*) |
| | *daf-2(e1370)* | 34.07 +/- 1.01 | 83 | n/a (*daf-2*), <0.0001 (wild-type), <0.0001 (*pcrg-1*) |
| | *pcrg-1(tm2597);daf-2(e1370)* | 33.43 +/- 0.89 | 74 | 0.33 (*daf-2*), <0.0001 (wild-type), <0.0001 (*pcrg-1*) |
| **2.8C** | wild-type | 18.07 +/- 0.30 | 86 | <0.0001 (*eat-2*), n/a (wild-type), <0.0001 (*pcrg-1)* |
| | *pcrg-1(tm2597)* | 12.75 +/- 0.35 | 80 | <0.0001 (*eat-2*), <0.0001 (wild-type), n/a (*pcrg-1)* |
| | *eat-2(ad465)* | 22.76 +/- 0.45 | 84 | n/a (*eat-2*), <0.0001 (wild-type), <0.0001 (*pcrg-1)* |
| | *pcrg-1(tm2597);eat-2(ad465)* | 17.05 +/- 0.36 | 91 | <0.0001 (*eat-2*), 0.175 (wild-type), <0.0001 (*pcrg-1)* |
| **2.8D** | wild-type | 19.09 +/- 0.47 | 68 | <0.0001 (*clk-1*), n/a (wild-type), <0.0001 (*pcrg-1)* |
| | *pcrg-1(tm2597)* | 13.36 +/- 0.42 | 69 | <0.0001 (*clk-1*), <0.0001 (wild-type), n/a (*pcrg-1)* |
| | *clk-1(e2519)* | 21.97 +/- 0.46 | 74 | n/a (*clk-1*), <0.0001 (wild-type), <0.0001 (*pcrg-1)* |
| | *pcrg-1;clk-1* | 17.95 +/- 0.54 | 83 | <0.0001 (*clk-1*), 0.3840 (wild-type), <0.0001 (*pcrg-1)* |
| **2.9C** | wild-type | 18.18 +/- 0.36 | 135 | <0.0001 (*efhc-1(gk424336)*), n/a (wild-type), <0.0001 (*efhc-1(tm6235)*) |
| | *efhc-1(gk424336)* | 13.97 +/- 0.14 | 150 | n/a (*efhc-1(gk424336)*), <0.0001 (wild-type), 0.0135* (*efhc-* |

| Figure | Strain | Mean Lifespan (days) | n | p-value (vs.) |
|---|---|---|---|---|
| | | | | *1(tm6235)*) |
| | *efhc-1(tm6235)* | 14.51 +/- 0.17 | 145 | 0.0135* (*efhc-1(gk424336)*), <0.0001 (wild-type), n/a (*efhc-1(tm6235)*) |
| **2.9D** | wild-type | 19.08 +/- 1.08 | 110 | <0.0001 (*efhc-1*), n/a (wild-type), <0.0001 (*pcrg-1*), <0.0001 (*pcrg-1;efhc-1*) |
| | *pcrg-1(tm2597)* | 13.04 +/- 0.64 | 149 | 0.6138 (*efhc-1*), <0.0001 (wild-type), n/a (*pcrg-1*), 0.9508 (*pcrg-1;efhc-1*) |
| | *efhc-1(gk424336)* | 13.49 +/- 0.42 | 136 | n/a (*efhc-1*), <0.0001 (wild-type), 0.9508 (*pcrg-1*), 0.1627 (*pcrg-1;efhc-1*) |
| | *pcrg-1(tm2597); efhc-1(gk424336)* | 12.35 +/- 0.49 | 154 | 0.1627 (*efhc-1*), <0.0001 (wild-type), 0.9508 (*pcrg-1*), n/a (*pcrg-1;efhc-1*) |
| **2.11B** | wild-type | 18.01 +/- 0.47 | 95 | <0.0001 (*pocr-4::egl-1* (1)), <0.0001 (*pocr-4::egl-1* (2)) |
| | *pocr-4::egl-1* (1) | 23.58 +/- 0.51 | 100 | <0.0001 (*pocr-4::egl-1* (2)), <0.0001 (wild-type) |
| | *pocr-4::egl-1* (2) | 22.98 +/- 0.68 | 86 | <0.0001 (*pocr-4::egl-1* (1)), <0.0001 (wild-type) |
| **2.11C** | *pcrg-1(tm2597)* | 17.22 +/- 0.45 | 99 | <0.0001 (*pocr-4::PCRG::GFP*) |
| | *pocr-4::PCRG::GFP* | 20.43 +/- 0.55 | 99 | <0.0001 (*pcrg-1*) |
| **Supp. 2A** | wild-type | 22.37 +/- 0.55 | 71 | <0.0001 (*osm-5*), n/a (wild-type), <0.0001 (*pcrg-1)* |
| | *pcrg-1(gk480)* | 13.00 +/- 0.46 | 72 | <0.0001 (*osm-5*), <0.0001 (wild-type), n/a (*pcrg-1)* |

| Figure | Strain | Mean Lifespan (days) | n | p-value (vs.) |
|---|---|---|---|---|
| | *osm-5(p813)* | 35.61 +/- 0.69 | 71 | n/a (*osm-5*), <0.0001 (wild-type), <0.0001 (*pcrg-1)* |
| | *pcrg-1(gk480); osm-5(p813)* | 31.55 +/- 0.71 | 58 | <0.0001 (*osm-5*), <0.0001 (wild-type), <0.0001 (*pcrg-1)* |
| **Supp. 2B** | wild-type | 22.37 +/- 0.55 | 71 | <0.0001 (*che-11*), n/a (wild-type), <0.0001 (*pcrg-1)* |
| | *pcrg-1(gk480)* | 13.00 +/- 0.46 | 72 | <0.0001 (*che-11*), <0.0001 (wild-type), n/a (*pcrg-1)* |
| | *che-11(e1810)* | 28.58 +/- 0.65 | 79 | n/a (*che-11*), <0.0001 (wild-type), <0.0001 (*pcrg-1)* |
| | *pcrg-1(gk480); che-11(e1810)* | 23.51 +/- 0.64 | 74 | <0.0001 (*che-11*), 0.1241 (wild-type), <0.0001 (*pcrg-1)* |
| **Supp. 2C** | wild-type | 19.83 +/- 0.37 | 81 | <0.0001 (*nphp-1*), n/a (wild-type), <0.0001 (*pcrg-1)* |
| | *pcrg-1(gk480)* | 13.86 +/- 0.28 | 84 | <0.0001 (*nphp-1*), <0.0001 (wild-type), n/a (*pcrg-1)* |
| | *nphp-1(ok500)* | 23.45 +/- 0.56 | 83 | n/a (*nphp-1*), <0.0001 (wild-type), <0.0001 (*pcrg-1)* |
| | *pcrg-1(gk480); nphp-1(ok500)* | 18.25 +/- 0.66 | 64 | <0.0001 (*nphp-1*), 0.2159 (wild-type), <0.0001 (*pcrg-1)* |
| **Supp. 2D** | wild-type | 19.83 +/- 0.37 | 81 | <0.0001 (*nphp-4*), n/a (wild-type), <0.0001 (*pcrg-1)* |
| | *pcrg-1(gk480)* | 13.86 +/- 0.28 | 84 | <0.0001 (*nphp-4*), <0.0001 (wild-type), n/a (*pcrg-1)* |
| | *nphp-4(tm925)* | 25.97 +/- 0.62 | 75 | n/a (*nphp-4*), <0.0001 (wild-type), <0.0001 (*pcrg-1)* |
| | *pcrg-1(gk480); nphp-4(tm925)* | 19.65 +/- 0.35 | 69 | <0.0001 (*nphp-4*), 0.6937 (wild-type), <0.0001 (*pcrg-1)* |